FEBRUARY, 1986

ENVIRONMENTAL PROGRESS

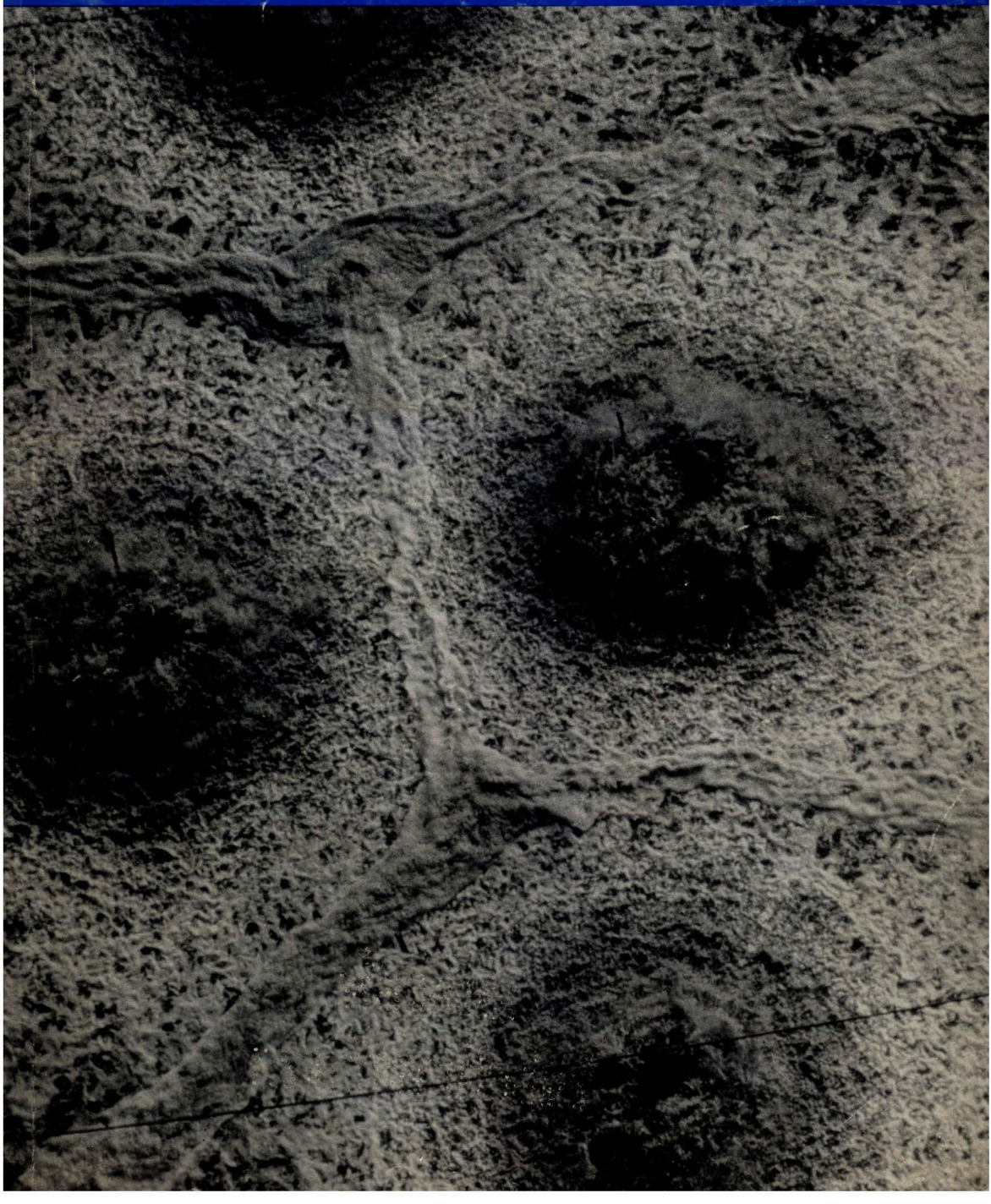

Are you looking for the latest information on

• toxic air issues
• hazardous waste management
• indoor air quality
• criteria air pollutants

Come to

APCA '86

The only such technical and educational conference annually held in North America for and by professionals

• 90 technical sessions
• 4,000 environmental experts
• 150 international suppliers

by the Air Pollution Control Association (APCA)
June 22-27, 1986
Minneapolis, Minnesota

Complete and mail this coupon for your program and registration forms. Or phone 412-232-3444.

- ☐ Yes, I want to come to APCA '86. Send me a registration form.
- ☐ I'd like more details. Send me a preliminary program.
- ☐ Send me information about membership in APCA.

Name _____

Title _____

Company _____

Address _____

_____

(Note: APCA members automatically receive a preliminary program and registration forms and should not respond to this ad.)

ENVIRONMENTAL PROGRESS

Environmental Progress is a publication of the American Institute of Chemical Engineers. It will deal with multi-faceted aspects of the pollution problem. It will provide thorough coverage of abatement, control, and containment of effluents and emissions within compliance standards. Papers will cover all aspects including water, air, liquid and solid wastes. Progress and technological advances vital to the environmental engineer will be reported.

Publication Office, 215 Canal Street, Manchester, N.H. Published quarterly by the American Institute of Chemical Engineers, 345 East 47 St., New York, N.Y. 10017. (ISSN 0278-4491). Manuscripts should be submitted to the Manuscript Center, American Institute of Chemical Engineers, 345 East 47 St., New York, N.Y. 10017. Statements and opinions in *Environmental Progress* are those of the contributors, and the American Institute of Chemical Engineers assumes no responsibility for them. Subscription price per year: $50. Outside the U.S. please add $5 per subscription for postage and handling. Single copies $18. Outside the U.S. please add $2 for postage and handling. Payment must be made in U.S. dollars. Second-class postage paid at New York, N.Y. and additional mailing offices. Copyright 1986 by the American Institute of Chemical Engineers.

Volume 5 **Contents** Number 1

Cover: Aerial view of wastewater treatment pond at Monsanto Plant. Photo courtesy Monsanto Inc.

Environmental Progress fee code: 0278-4491/86 $2.00. Postmaster: Please send change of addresses to *Environmental Progress*, AIChE, 345 East 47 Street, New York, N.Y. 10017.

Bhopal Plus One: A Chemical Engineer's Watershed

by
Peter B. Lederman

Much has been written on the anniversary of the Bhopal Tragedy and its aftermath. It sensitized the public as never before to activities and operations within the "Black Box" of the chemical plant within the fence. More often than not in the past, emissions and even small fires were overlooked. Even major fires and explosions were soon forgotten. The chemical industry and the chemical engineer were the "good guys" in producing materials that made life easier. Bhopal, as no other incident, has changed that. The chemical industry has become "suspect" at best, and the professionals who built and managed those operations are being critically evaluated by the general public.

The challenge presented by Bhopal is a multi-faceted one in that it is being approached on many levels and needs to be approached on additional ones. Bhopal, followed by Institute, West Virginia, and other less publicized incidents, has created tremendous pressures on the legislative and regulatory communities. Numerous pieces of legislation are being submitted for consideration in the Congress, while state and local municipalities have enacted a number of laws. Action is also taking place in the legislatures of foreign countries and in the international technical community. This legislative pressure has produced and continues to produce significant regulatory initiatives. Both the legislative and regulatory initiatives will mean that "proprietary" or "trade secret" claims will be much more difficult to sell and utilize to protect the innovations which have kept the chemical industry in the forefront. The industry and our profession are in the spotlight, possibly even more so than the nuclear industry. This means that we as chemical professionals will have to adapt a different style of operation, a style which will require significantly more communication with the public.

The public now expects to know what is going on inside the fence. What are the plans, what are the risks and what are the benefits? We will no longer be able to hide behind "it is too complicated" or "its safe and we're making something which will make your life better." The public is "from Missouri" and it will be our job to prove to the public that what we are planning, building and operating is indeed safe and desirable. This places an added dimension on our industry and on us as professionals. It is a dimension that we have approached slowly as a result of environmental pressures, one that we must now face and meet head-on and requires our very best efforts.

The American Institute of Chemical Engineers has taken a lead position in establishing the Center for Chemical Process Safety. The Center has focused on development of guidelines for evaluating risks and hazards in process operations. The Chemical Manufacturer's Association has responded with programs to help communities become more aware and develop emergency response plans. The Environmental Protection Agency has just announced a program to assist communities in developing emergency response plans. Similar activities are going on throughout the world. It is a critical activity and will provide some of the tools that are necessary to respond to the concern, even fear, that the Bhopal Incident has engendered in the public.

Risk Assessment, Community Awareness and Emergency Response Planning are all important but must be complemented with superior operation, superior design and attention to detail and corrective actions pointed out by the risk and operational analyses. The operational design and corrective actions we take now will be critical to the future of our profession and industry. The dollars expended now will be inconsequential compared to the dollars that could be spent later if we have an incident.

The chemical industry has always prided itself on being a good neighbor. That image is now tarnished. It will take our energies and creative talent to make that image shine again. We have always prided ourselves as an industry that provides a good place to work and has a superior safety record. We must work to make that safety record even better. It will be difficult enough for major firms in the chemical process industry who have significant technical and financial resources. It will be especially difficult for the medium and small-sized companies who have neither the in-house technical talent nor the financial resources to undertake some of these very complex studies. If we as an industry are to survive, these studies must be undertaken and the changes suggested by these studies made.

In the past as a profession, we have been reticent to enter the public arena. We have prided ourselves on our technical know-how and judgment and let those attributes speak for themselves. This is no longer enough. Risk Analysis, Operational Improvements and Design Changes are also only a foundation. We must educate ourselves to become better communicators with the public. Public acceptance of our work and confidence in it are the keys to our future. It is important, therefore, that we as a profession become actively involved in our communities and in the community at large and that we establish a personal creditability which will be the foundation for establishing the public's confidence in our work and in our findings. On that creditability we will build the future of our profession and our industry. Even if the leaders in our profession and industry provide a positive, high level of visibility, each and every one of us must contribute at whatever strata we operate so a personal identification at a grass roots level is developed with the benefits we have and continue to provide.

Peter B. Lederman *has been working in the Hazardous Material Management Field for the past 15 years. During that time, he headed the Environmental Protection Agency's Hazardous Spill Research and Development Activity and for the last six years has been Vice President of F. Weston, Inc. Being Chairman of the New Jersey AIChE Section in the early 70's, he is well known to many in the New Jersey/North Jersey Sections. He has also served as Chairman of the Professional Development Committee of AIChE and is a Fellow of the Institute.*

Before joining the Weston staff, he worked for Exxon, and was a Professor at the Brooklyn Polytechnic Institute. He also worked with the United States EPA before he returned to private industry as Manager of Technical Development for Research-Cottrell.

He earned his B.S., M.S., and Ph.D. at the University of Michigan and is a Registered Professional Engineer, a Registered Professional Planner and a Certified Hazardous Material Manager.

He also serves on the advisory board of Environmental Progress *and has over 75 publications to his credit, mostly in the area of Hazardous Materials.*

Washington Environmental NEWSLETTER

AIChE Members Encouraged to Participate in Community Emergency Response Planning

As reported earlier, AIChE's Washington office has been working closely with EPA on its "Guidelines for Community Emergency Response." A key feature of the guidelines will be the identification and use of sources of technical advance within the community to serve as a resource in planning for emergencies involving hazardous materials. Since the technical expertise of chemical engineers is viewed as an integral part of this planning, AIChE members have an opportunity to provide a significant service to the communities in which they live and work.

AIChE's Government Programs Steering Committee (GPSC) has assumed responsibility to implement a pilot program for a limited number of AIChE local sections. This effort will be led by Ed McDowell (Vice Chairman of GPSC) and Gary Leach, and will be coordinated through AIChE's Washington office.

Role of Local Sections and Government Interaction Committees (GICs)

Local sections, through their GICs, would be the logical group to initiate and carry out this function, using the GPSC guidelines. Appropriate local section members can volunteer to make their expertise available to the community in its planning effort. It is anticipated that they would be part of a community team made up of plant managers, fire, police, local health officials and other interested parties.

Since the Chemical Manufacturers Association (CMA) has already prepared a Community Awareness and Emergency Response (CAER) program which suggests that local plant managers communicate with community leaders to prepare an emergency plan, the AIChE program will be complimentary to the CAER program by providing constructive, technical expertise from an independent, professional source.

Local sections are in the best position to identify those members who have the knowledge, experience, maturity and dedication to make a meaningful contribution as either a volunteer or in some cases as a consultant to the local planning group. Several communities which have already worked out emergency plans have had significant input from chemical engineers.

Retired Engineers as a Resource

Because of the possibility of an ongoing commitment, retired members of the local section can do an excellent job and should be contacted as potential participants in this effort. These individuals who may be retired (but not tired) can bring their years of experience and skills to bear on a worthwhile project that will also enhance the professional image of the chemical engineer in the community.

Local section chairmen will be contacted in the near future with GPSC guidelines and planning and implementation procedures.

Your comments are welcome. Please write, or call, Dr. Martin Siegel, Staff Director Government Relations, at the Washington office.

This material was prepared by AIChE's Washington Representative, Siegel • Houston & Associates, Inc. Suite 804, 1901 L Street, N.W., Washington, D.C. 20036. Tel. (202) 223-0650

Environmental Shorts

PPM Receives Permit Amendment For PCB Chemical Destruction Process

The U.S. Environmental Protection Agency has expanded PPM, Inc.'s existing mobile permit to destroy PCB-contaminated materials throughout the United States.

PPM's initial permit allowed the level of contamination for chemically destroying PCB materials could not exceed 4,100 ppm. With this new permit, PPM now can treat chemically PCB materials in concentrations up to 10,700 ppm. "The new level will allow a significant amount of contaminated oil, which is now being incinerated, to be reclaimed with the process," Dennis Tapaak, president of PPM said. "The new limit is an important step in PPM's efforts to provide the most environmentally acceptable disposal option for hazardous waste generators."

Chemical Hazards Database Acquired by VIS

The Chemtox Database, which contains information on more than 3,200 chemical substances that are hazardous and are common in the environment due to their economic importance, has been acquired by Van Nostrand Reinhold Information Services (VIS) from Resource Consultants, Inc.

Data within the Chemtox Database consists of identifiers, such as name, number, synonyms, chemical class, and DOT I.D. number; physical and chemical properties such as specific gravity, boiling point, flash point, and explosive limits; toxicological data such as carcinogenicity, target organs, short-term toxicity, and Regulatory Data such as Hazard Communication Standard requirements and EPA hazardous waste listings.

In all, more than 80 different data items are supported within the Chemtox Database record structure. Quarterly updates, delivered on floppy disks, will continue to update and expand this list in the future.

"Dealing with chemical data once with the exclusive province of the chemist or toxicologist," Richard Pohanish, VIS president, says. "Today, more and more managers possess less formal training are being asked to make critical decisions relating to the management of hazardous substances. Chemtox provides them with the necessary data to make informed decisions and offers superior assistance to all 'need-to-know' managers."

Reducing Nitrogen Oxide Emissions

The Environmental Protection Agency has proposed standards to limit nitrogen oxide emissions from new industrial boilers. At present, such boilers are not regulated by the agency, and there has been little incentive to develop control technologies for them. Nitrogen oxide emissions contribute to major air quality problems such as acid rain and ozone formation, and coal-fired industrial boilers are an important source of these emissions.

In response to this problem, the Environmental Protection Agency's (EPA) Air and Engineering Research Laboratory in Research Triangle Park, North Carolina, has developed a new method for destroying nitrogen oxide formed during combustion. Called reburning, or fuel staging, the technique uses an altered boiler design which expands the combustion zone within a boiler. A secondary zone above the main combustion zone burns a mixture of natural gas and ambient air diverted form the primary zone. Hydrocarbon radicals in this secondary burn destroy the nitrogen oxide formed during primary combustion. Compared with conventional pre- and post-combustion technologies, in-furnace reburning is inexpensive and appears capable of reducing nitrogen oxide emissions by 50 percent.

Report Criticizes Third World Pesticide Subsidies

By subsidizing pesticide production and sales, many Third World governments are encouraging farmers to use chemicals with serious environmental and safety side effects, and diverting hundreds of millions of dollars annually that could be used to promote safety and better methods of pest control, a new World Resources Institute research report charges.

Titled, "Paying the Price: Pesticide Subsidies in Developing Countries" finds that pesticide subsidies range from 15 per cent to as high as 90 per cent of full cost in China, Colombia, Ecuador, Egypt, Ghana, Honduras, Indonesia, Pakistan, and Senegal.

The Report charges that the "subsidies encourage farmers to use more chemicals than they would if they had to pay the full cost. Subsidies mainly benefit farmers who are better off than the people who bear the costs. The beneficiaries of pesticides subsidies are likely to be a different group that those who bear the costs and the environmental losses from increased chemical use, both human poisonings and destruction of beneficial animal species."

According to the Report, of the countries surveyed, only Pakistan, which discontinued subsidies in 1980, had analyzed the effects of its subsidies and the possible preferability of alternative ways of promoting pest management. Withdrawal of the subsidy, the report claims, "has made the Pakistani farmers more judicious in the choice and use of pesticides. Only effective and less expensive chemicals are finding favor with them. Wastage has been considerably reduced."

ENVIRONMENTAL INSTITUTE FOR WASTE MANAGEMENT STUDIES

The Environmental Institute for Waste Management Studies was established at the University of Alabama, Tuscaloosa, Alabama in January 1984 with a purpose to study and inform the public, the media and government of the major technical issues involving the safe management of hazardous and toxic waste. In the first two years, the Institute focussed on a strategy for the management of spent solvents and solvent-contaminated wastes.

The reports listed below are from these studies. Each is available for $10 or $20 depending on their length from the: Institute of Environmental Studies, P.O. Box 2310 Tuscaloosa, AL 35403

Published Reports of the Institute

- Disposal of Solvents and Solvent-Contaminated Wastes to Land—A Position Paper—Institute members and staff.
- Fate of Solvents in a Landfill—Gary F. Bennett.
- Interaction of Organic Solvents with Saturated Soil-Water Systems—R. A. Griffin and W. R. Roy.
- Toxicity Profiles of Selected Organic Solvents—William J. George, Laura A. Martin, and LuAnn E. White.
- Containment Barriers for Land Disposed Solvent-Bearing Hazardous Wastes—James K. Mitchell and Thomas L. Brandon.
- A Survey of Current Waste Management Technologies—Methods of Recovery, Treatment, Disposal, and Storage of Hazardous Wastes—T. H. Hughes, B. W. Norris, K. E. Brooks, B. M. Wilson, and B. N. Roche.
- A Descriptive Survey of Selected Organic Solvents—T. H. Hughes, K. E. Brooks, B. W. Norris, B. M. Wilson, and B. N. Roche.

Reports of the Institute In-Press

- Statistical Approaches to Groundwater Monitoring—Carl A. Silver.
- Hazardous Waste Incineration—James V. Walters.
- Risk Assessment and Selected Socio-Economic Considerations for Organic Solvents—Rae Zimmerman.
- Mathematical Models of Contaminant Transport in Groundwater—Yaron M. Sternberg.

Books

Handbook of Hazard Communications and OSHA Requirements, George G. Lowry and Robert C. Lowry, Lewis Publishers Inc., 121 S. Main St., Chelsea, MI 48118 (1985) 148 pp., $34.95, hardcover.

Mathematical Models and Design Methods in Solid-Liquid Separation, edited by A. Rushton, Martinus Nijhof, Spuiboulevard 50, 3300 AZ Dordrecht, The Netherlands (1985) 399 pp., hardcover $49.50.

Handbook of Laboratory Waste Disposal, by Martin J. Pitt and Eva Pitt, Halstead Press/John Wiley & Sons, New York (1985) 360 pp., hardcover $87.95.

Separation of Heavy Metals and Other Trace Contaminants, No. 243, Vol. 81, edited by Robert William Peters and M. Bo Kim, American Institute of Chemical Engineers (1985) 203 pp., AIChE members $20; others $40.

Reliability of Adhesive Bonds Under Severe Environments, National Materials Advisory Board, Commission on Engineering and Technical Systems, National Research Council. Order from: Defense Technical Information Center, Cameron Station, Alexandria, VA 22312 (1984) 52 pp. paper.

Agricultural Chemistry, Vols. 1, 2, by Y. A. Yagodin, MIR Publishers, Moscow. Order from Imported Publications, 320 W. Ohio St., Chicago, IL 60610 (1984) 758 pp., hardcover $16.95.

Stream, Lake, Estuary, and Ocean Pollution, by Nelson L. Nemerow, Van Nostrand Reinhold, New York (1985) 444 pp., $46.95 hardcover.

Computer Models in Environmental Planning, by Steven I. Gordon, Van Nostrand Reinhold, New York (1985) 222 pp., $34.50 hardcover.

Water Resources Planning, by Neil S. Grigg, McGraw-Hill Book Co., New York (1985) 328 pp., $39.95, hardcover.

CALL FOR PAPERS

The 6th International Conference on Chemistry for Protection of The Environment will be held in Turin, Italy, September 15-18 1987. Theme topics include physiochemical processes, and aspects of chemistry and chemical engineering in the treatment and monitoring of air, water and solid wastes.

Interested persons are requested to send their name, job title, affiliation and a general title of their papers to:

Dr. William J. Lacy
9114 Cherrytree Drive
Alexandria, VA 22309

The Dow Stretford Chemical Recovery Process

The Dow patented Stretford Chemical Recovery Process reclaims the two key chemicals while purging undesirable by-products from Stretford gas sweetening plants. Recovery of these chemicals can reduce costs in terms of chemical loss and solution disposal. The process involves filtration, charcoal adsorption and ion exchange.

C. Alan Hammond, Gas/Spec Technology, Dow Chemical USA, Freeport, TX 77541

STRETFORD PROCESS DESCRIPTION

The Stretford process is used for the removal of hydrogen sulfide from tail gas streams from various origins. In the United States these are principally from Claus units in refineries. The hydrogen sulfide is contacted with the Stretford solution in an absorber and reacts with sodium carbonate to form sodium hydrosulfide.

$$H_2S + Na_2CO_3 \rightarrow NaHS + NaHCO_3$$

The dissolved hydrosulfide ions then react with sodium vanadate in an oxidation-reduction reaction which produces elemental sulfur and a reduced vanadium salt.

$$2NaHS + 4NaVO_3 + 4NaHCO_3 \rightarrow 2S + Na_2V_4O_9 + 4Na_2CO_3 + 3H_2O$$

Also present in the solution is the disodium salt of anthraquinone disulphonic acid (ADA) which catalyzes the reoxidation of the vanadium.

$$Na_2V_4O_9 + O_2 + H_2O + 2Na_2CO_3 \xrightarrow{ADA} 4NaVO_3 + 2NaHCO_3$$

After the solution has been contacted with hydrogen sulfide to produce sulfur, the sulfur is separated from the solution by flotation and a melter-decanter. Filters or centrifuges can be used in place of the melter-decanter. The vanadium oxidation and the sulfur flotation both occur in the oxidizers where air is blown into the solution. The Stretford solution is then recycled back to the absorber.

In addition to the above reactions, several side reactions take place which produce sodium thiosulfate and sodium sulfate. Oxygen in the feed gas and in the oxidizers reacts with sodium carbonate and sulfur to form sodium thiosulfate.

$$Na_2CO_3 + 2S + O_2 \rightarrow Na_2S_2O_3 + CO_2$$

Feed gas oxygen also reacts with the sodium hydrosulfide in the absorber to form sodium thiosulfate.

$$2NaHS + 2O_2 \rightarrow Na_2S_2O_3 + H_2O$$

Sodium thiosulfate will also be formed in the absorber if sulfur dioxide is in the feed gas.

$$SO_2 + Na_2CO_3 + S \rightarrow Na_2S_2O_3 + CO_2$$

Another source of sulfur dioxide is the reverse Claus reaction which occurs in the autoclave.

$$3S + 2H_2O \rightarrow 2H_2S + SO_2$$

Some of the sodium thiosulfate will then be biologically oxidized to form sodium sulfate.

$$Na_2S_2O_3 + Na_2CO_3 + 2O_2 \rightarrow 2Na_2SO_4 + CO_2$$

The concentrations of sodium thiosulfate and sodium sulfate must be kept low enough so that these salts do not fall out of solution. Control of these concentrations has traditionally been accomplished by either purging a stream and adding make-up chemicals, or by changing out the entire system solution when the salt levels get too high.

In either case the chemical costs are high due to the prices of ADA and vanadium; and in some cases, the waste disposal costs are also very high. Figure 1 shows the calculated vanadium and ADA costs if a purge stream is used to maintain a thiosulfate concentration of 160 grams per liter.

CHEMICAL RECOVERY PROCESS

The Dow Stretford Chemical Recovery Process is a patented process which was developed as a method of purging the thiosulfate while recovering the ADA and vanadium to recycle back to the Stretford unit. This function is shown in Figure 2. The process consists of three

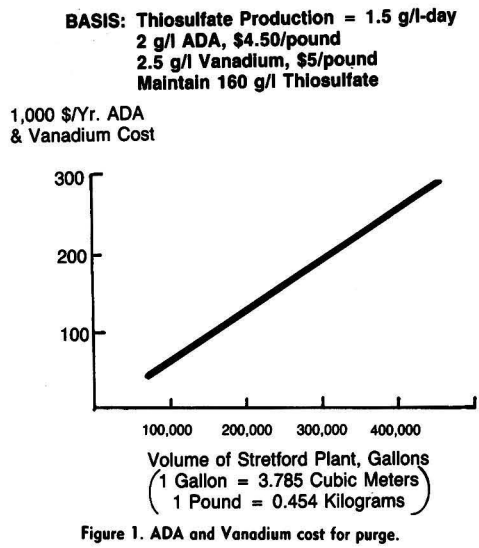

Figure 1. ADA and Vanadium cost for purge.

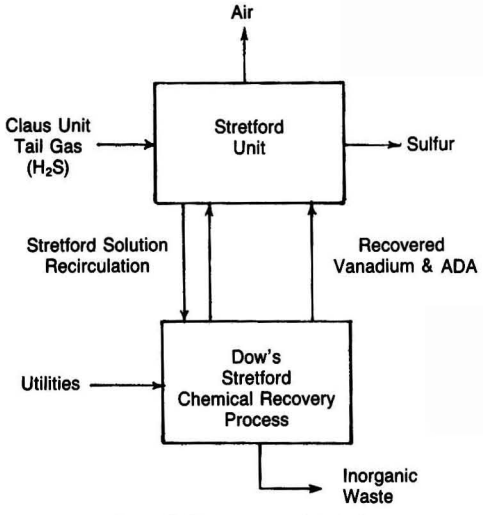

Figure 2. The process-implemented.

unit operations: filtration, charcoal adsorption, and ion exchange operating on a semi-batch cycle. The filtration section provides a stream that contains no sulfur particles that would interfere with performance of the activated charcoal or the ion exchange resin. The charcoal removes the ADA from the purge stream while the ion exchange resin removes the vanadium. This "loading step" in which the chemicals are loaded into the recovery beds, is shown in Figure 3. After the charcoal and ion exchange beds are fully loaded, they are simultaneously regenerated, thus recovering the ADA and vanadium. This "regeneration step" is shown in Figure 4. Four percent caustic is used to remove the vanadium from the ion exchange resin. The effluent from the resin bed is then heated and used to strip the ADA from the charcoal. A system flush follows to lower the pH in the resin bed and to cool the charcoal. The recovery beds are then ready to be loaded again.

LABORATORY WORK

The first stage of this project was a laboratory evaluation of the process using solution samples taken from nine different Stretford plants. Process variables were studied and comparisons were made using different ion exchange resins and charcoals.

After the optimum operating conditions were found, the

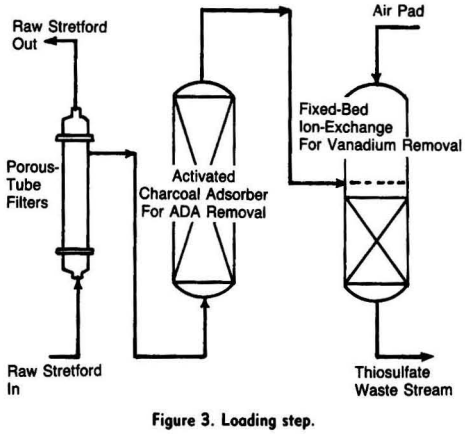

Figure 3. Loading step.

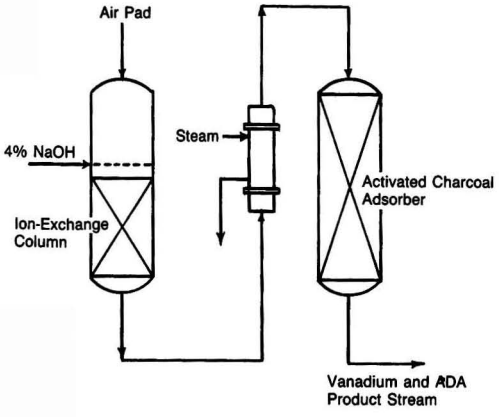

Figure 4. Regeneration step.

ADA recovery was greater than 95% in most cases. The vanadium recovery, however, was not consistent, and in most cases ranged from 70 to 95%. As the thiosulfate concentration increased, the vanadium recovery tended to decrease; but in general, the selectivity of the resin was favorable. Besides competition between the vanadium and thiosulfate, other conditions exist which are believed to be a factor in this correlation. For instance, reduced vanadium forms will not be recovered as well as the oxidized forms. There are also several oxidized forms of vanadium which will be recovered to different degrees, and the equilibrium between these species appears to be affected by the pH and the thiosulfate concentration.

The thiosulfate removal efficiency is consistently about 90%, that is, 10% is retained in the ion exchange column and is recycled with the ADA and vanadium product stream. Any inefficiency in the thiosulfate removal will affect the amount of solution that has to be processed in order to purge a given amount of thiosulfate.

PILOT PLANT

Since the component recoveries were acceptable, the second stage was to build a larger demonstration plant. This plant was used to confirm the laboratory results, evaluate the mechanical aspects of such a process, optimize the recovery cycle, and to process solution trucked in from nearby Stretford plants. The first truckload of solution was used to verify the lab results and to optimize the process. Twenty-three cycles were run with this solution, and the vanadium and ADA recoveries were 85% and 82% respectively.

Two more truckloads of solution were received from a different source and was primarily used to evaluate the mechanical dependability of the process. In these runs, the ADA and vanadium recoveries were 99% and 85% respectively. In the first five-day continuous run, no major mechanical problems were encountered. The actuated values needed attention at start-up but were not a problem once the unit was running and the valves operated routinely. The major area of concern was a decrease in filter capacity towards the end of the five-day run.

The filters used in this process resemble a shell and tube heat exchanger in which the tubes are constructed of a porous material. The Stretford solution containing solid sulfur is pumped through the inside of the tubes at a high velocity and at a pressure higher than the shell side pressure. A filtrate bleeds through the tube walls due to the pressure differential while most of the solution carries the sulfur back to the Stretford plant. A flow rate of 100 gpm through one filter module will produce a little less than 1 gpm of filtrate when the temperature is kept above 95°F.

Theoretically a solid free boundary layer develops on the inside of the tube wall, and the high velocity minimizes movement of solid particles into this boundary layer. However, eventually enough sulfur gets into the filter membrane to lower its capacity. To keep this sulfur from completely plugging the filters, a pressure back pulse is used. This is achieved by periodically increasing the shell side pressure enough to reverse the flow through the membrane, thus pushing the sulfur back into the main flow to be carried back to the Stretford plant.

It was found that by increasing the frequency and decreasing the duration of these back pulses, an acceptable steady state filter capacity was reached. On the next five-day continuous run, there was no significant loss in filter capacity.

FIELD TRIAL

After operating the plant successfully in Freeport, the third and final stage of development was to conduct a field trial in which the plant would process solution from an operating Stretford plant. The recovery unit was installed so the recirculation pumps on the balance tank would pump 100 gpm of Stretford solution through the filters.

The component recoveries are plotted in Figure 5, and the trend is much the same as before. As the thiosulfate level increases, the vanadium recovery decreases. At the start of the field trial, the thiosulfate level was 220 grams per liter, and the vanadium and ADA recoveries were 87% and 95% respectively. However, the initial processing rate was not high enough to maintain the thiosulfate concentration, and it rose to about 240 grams per liter. The solution coming from the balance tank pumps contained about 10% solid sulfur,whereas the solution processed in Freeport only contained about 4%. This high solids content lowered the filter capacity significantly.

After about 20 cycles, a preliminary settling tank was installed to lighten the load on the filters. A 20,000 gallon "frac tank" was used as a temporary settler. It is very important to note that this was temporary because a properly designed settler would be very small in comparison. This tank was filled with solution, and a new pump was installed with a suction about four feet above the bottom of the tank.

The settled solution was pumped through the filters at 100 gpm and back into the frac tank so the level only dropped by what was being processed in the recovery unit, about 700 gallons per day. When this level got low enough, the frac tank was refilled. When the tank was refilled around cycle 70, the thiosulfate concentration increased since it had continued to rise in the Stretford unit.

Once the thiosulfate level was in the range of 240-250 grams per liter, the vanadium recovery was only about 65%. Several attempts were made to improve the vanadium recovery by changing process conditions but to no

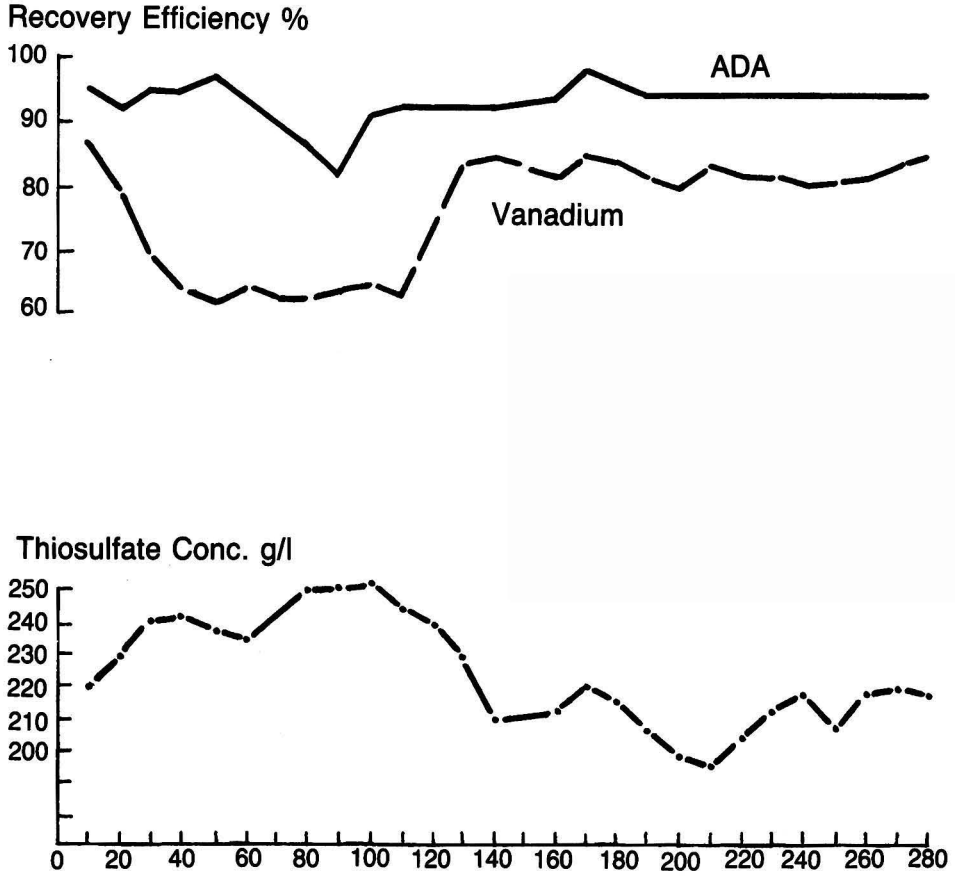

Figure 5. Field trial data.

BASIS
100,000 Gallon System Volume
95% ADA Recovery
80% Vanadium Recovery

	CASE 1	CASE 2
gram/liter ADA	2	3
gram/liter Vanadium	2.5	4
gram/liter Thiosulfate	160	200
Thiosulfate production rate, g/l day	2	3
gallons processed/day	1400	1670
gallon H_2O/gallon feed	2.6	4.0
gallon 25% NaOH/gallon feed	0.11	0.19
lbs. 150 psig steam/gallon feed	1.37	2.15
gallons product/gallon feed	1.77	2.76
gallons waste/gallon feed	1.94	2.43

(For both cases: 5000 watts electrical power, air and cooling water)

(1 Gallon = 3.785 Cubic Meters)

Figure 6. Operating data.

avail. After about 120 cycles, part of the solution was hauled out so the thiosulfate level was back below 220 grams per liter, and the vanadium recovery improved to over 80%.

It should be pointed out that the recovery unit used in the field trial was underdesigned for this Stretford unit. A larger recovery plant would be able to process enough solution to lower the thiosulfate concentration, thus avoiding the solution haul out. As it was, the recovery unit was, at best, just able to maintain a steady concentration. The fluctuations in the thiosulfate curve are explained by the batch type operation of the temporary settling tank.

The recovery unit did not seem to have any adverse effect on the Stretford plant and it was able to effectively purge the thiosulfate. The field trial did point out that there may be a need for a sulfur settling system in certain cases. Another alternative would be to add more filter modules to increase the capacity. An economic comparison must be made which involves the differences in equipment cost and pumping power required.

OPERATING DATA

Figure 6 shows operating data for two cases with varying plant conditions. The second case operates at a higher thiosulfate production rate and higher concentrations of ADA, vanadium, and thiosulfate. A comparison of some of these numbers helps explain how the plant operates.

Although Case 2 operates at a thiosulfate production rate of 1.5 times Case 1, the processing rate is only slightly higher. This is because Case 2 operates at a higher thiosulfate concentration so a smaller quantity of solution can be processed to remove the same amount of thiosulfate.

Another important number is the gallons of water used per gallon of feed which, of course, impacts the gallons of product and waste. The higher numbers for Case 2 are due to the high vanadium and ADA concentrations which cause the charcoal and resin columns to be much larger. Although the quantities of feed solution for the two cases don't differ much, this increase in column size increases the flow requirements of all phases of the regenerative process.

The quantity of product returned to the Stretford plant is important because the excess water needs to be removed in the cooling tower to maintain a constant level. The quantity of waste is especially important if it presents disposal problems. Other important aspects of the operating data are the low utility requirements and the fact that no chemicals or additives are used that are not compatible with the Stretford unit.

MODIFIED CYCLE

As mentioned above, the quantity of waste may need to be minimized if it presents disposal problems. Many plants have water treating facilities in which this waste stream would only be a small portion, but others may have to have the waste hauled off in trucks at quite an expense.

A modified cycle has been proposed that would help alleviate this problem. The key to this cycle is that all of the waste is not contaminated with Stretford chemicals. The effluent from the columns during the loading step is just flush water that was used in the previous cycle to lower the charcoal temperature and the resin pH. This slightly alkaline water could either be returned to the Stretford plant or used elsewhere. After all the flush water has been pushed through the columns, the waste stream will contain thiosulfate and should be handled accordingly. Similarly, at the end of the regeneration step, the water being flushed from the system is hot and has a high pH, but it is not contaminated with Stretford chemicals. As the flush step continues, the water temperatures and pH continue to drop until the end of the cycle. Again this water could be returned to the Stretford plant or used elsewhere. Obviously, the Stretford cooling tower would have to be capable of evaporating this additional water.

It should be pointed out that this is not the mode of operation used for the data in Figure 6. The data from Figure 6 corresponds to mode of operation used in the field trial which classifies all flows not containing vanadium and ADA as waste.

CONCLUSIONS

The Stretford Chemical Recovery Process represents a viable method of controlling the sodium thiosulfate level in Stretford plants while recovering the ADA and vanadium for return to the process. There is a correlation between the thiosulfate concentration and the vanadium recovery such that the vanadium recovery will not be as good at start-up if the initial thiosulfate level is high. In any case, once the thiosulfate level is under control, the vanadium and ADA recoveries will be about 85% and 95% respectively. In addition to the chemical savings, the process also has the potential for alleviating waste disposal problems due to vanadium and/or ADA.

C. Alan Hammond is an employee of Dow Chemical's GAS/SPEC Technology group in Freeport, Texas and is currently the project leader for the Stretford Chemical recovery process and Dow's hydrogen sulfide abatement process in geothermal power plants. Prior to joining GAS/SPEC, he received his BS in Chemical Engineering from Clemson University and worked six years as a design engineer for Dow's Research Engineering group.

Calcium Sulfite Hemihydrate: Crystal Growth Rate and Crystal Habit

The crystal growth rate of $CaSO_3 \cdot 1/2H_2O$ was measured by a pH-stat method in aqueous solution with pH 3.5 to 6.5, 1 to 25 mM dissolved sulfite, 0.01 to 0.3 M Ca^{++}, and 0 to 25 mM sulfate. The growth rate was a strong function of relative supersaturation and was strongly inhibited by dissolved sulfate. The growth rate per unit BET surface area, R' (mole/cm²-min), is given by: $9.7 \times 10^{-4} \exp(-10250/RT) \times (RS_{CaSO_3}\text{-}1)^2 \times RS_{CaSO_4}{}^{-1}$, where RS_{CaSO_3} and RS_{CaSO_4} are the relative saturations with respect to calcium sulfite and gypsum, respectively. Scanning electron microscopy and IR spectroscopy demonstrated that solids generated in the presence of dissolved sulfate contained solid solution sulfate and crystallized as agglomerates of very thin platelets. In the absence of solid or dissolved sulfate the solids were agglomerates of well-informed columnar, hexagonal crystals.

Philip C. Tseng and Gary T. Rochelle, Department of Chemical Engineering, The University of Texas at Austin, Austin, Texas 78712

INTRODUCTION

The crystallization of calcium sulfite hemihydrate is of importance in flue gas desulfurization processes which absorb SO_2 by a slurry of lime or limestone with simultaneous calcium sulfite/sulfate precipitation. Calcium sulfite crystallization affects the composition and chemical equilibria in the scrubbing solution, and therefore affects SO_2 absorption and limestone dissolution which are mass transfer controlled phenomena enhanced by equilibrium reactions [*1-5*]. The habit of the grown calcium sulfite crystals is of particular interest because it affects the ease of dewatering, and thus, the operation of solid-liquid separation processes [*6*]. Recently, limestone has been substituted for lime in dual-alkali processes [*7-8*]; the crystallization rate and crystal habit of calcium sulfite are critical to the development of this next generation of technologies.

The earliest study of $CaSO_3 \cdot 1/2H_2O$ crystallization rate was conducted by Ottmers, et al., [*9*]. A continuous-liquid/batch-solid method was used and the crystallization rate was found to be 1st order relative to the supersaturation of calcium sulfite. Nucleation was not significant when the relative supersaturation was below 3 or 4, and dominated above this level of supersaturation.

The ease of solids dewatering is strongly related to crystal size. Phillips et al., [*10*] developed a mathematical model to relate calcium sulfite crystal size distribution to FGD operating conditions. Discrepancies in crystal size measurement in the micrometer range by using different methods were investigated by Edwards, et al., [*11*]. The results confirmed the reliability of measurement by a Coulter Counter, which has been extensively used in recent crystal size studies [*4, 12-15*].

Since the flue gas is usually accompanied by air, some sulfite is oxidized to sulfate and a mixture of calcium sulfite/sulfate crystallization product is usually obtained. Jones, et al., [*16*] used X-ray, Differential Scanning Calorimetry and Infrared Spectroscopy to confirm the formation of a solid solution of calcium sulfate in calcium sulfite hemihydrate. It was indicated that the coprecipitation of sulfate with calcium sulfite hemihydrate is basically an equilibrium controlled process. Setoyama et al., [*17*] found that the solubility of calcium sulfate in calcium sulfite hemihydrate is a function of reaction temperature. The calcium sulfate substituted up to about 9 mol% to form solid solution with little changes in lattice parameters from X-ray diffraction, but calcium sulfate content greater than 9 mol% caused disorder of the calcium sulfite crystal.

Crystal habit is another important factor which determines the quality of the crystallization product. Kelly and Randolph [*15*] studied the effects of several crystal habit modifiers, mostly organic acids, on the size and morphology of calcium sulfite hemihydrate crystals. It was found that the presence of citric acid significantly reduces crystal growth rate and particle size, and produces spiny crystals; nitrilotris methylene triphosphoric acid (NMTP) on the other hand produces disc crystals. Meserole et al., [*18*] found that solution composition influenced the calcium sulfite crystal size and habit. Calcium sulfite precipitated in the presence of high sulfate concentration was rod shaped or globular with some foliated growth patterns, whereas that precipitated in the presence of high chloride concentration or in dilute solutions was lamellar or acicular in habit.

A number of results from industrial development strongly suggest that gypsum saturation affects the dewatering properties and crystal habit of calcium sulfite. In experiments simulating the hold tank of a $CaCO_3$ slurry scrubber, M. W. Kellogg found that large, easily dewatered $CaSO_3$ crystals were formed in the absence of sulfate [*19*]. Development of the limestone dual alkali process has shown that dewatering of the calcium sulfite solids is difficult at low ratios of dissolved sulfite to sulfate, but easy at high ratios [*8*]. Previous work has shown that low dissolved sulfite/sulfate ratios give solutions with higher gypsum saturation and higher sulfate content in the solids [*20*]. Recent work using sodium thiosulfate as an oxidation

inhibitor has shown that adequate levels of thiosulfate enhance dewatering of the calcium sulfite solids, probably because of the significantly reduced gypsum saturation [21-23].

In this paper, a correlation of $CaSO_3 \cdot 1/2H_2O$ crystal growth kinetics was obtained and the crystal habit was studied at conditions typical of flue gas desulfurization processes. The crystallization experiments were conducted at pH 3.5-6.5, with most runs at room temperature and some at 55°C. Relative supersaturations of calcium sulfite were 1.5 to 7. Typical scrubbing solution composition was varied from 0.01 to 0.3 M Ca^{++}, 0.2 to 0.9 M Cl^-, 1 to 25 mM total sulfite (S^{+4}), 0.3 to 0.9 eq/l ionic strength, and 0 to 250% gypsum saturation. The calcium sulfite seed crystals used in the experiments had different crystal morphology and sizes, and were agglomerates rather than single crystals.

EXPERIMENTAL

Seed Crystal Synthesis and Characterization

Three batches of calcium sulfite seed crystals were synthesized in the laboratory by reacting solutions of calcium chloride and sodium sulfite/sodium sulfate. The solids were rinsed with distilled water, filtered, and dried. These initial seed crystals were characterized (Table 1) by iodometric titration, differential scanning calorimetry (Perkin-Elmer DSC-2), X-ray powder diffraction, infrared spectroscopy (Nicolet, Model 7002), scanning electron microscopy (SEM, JEOL Model JSM-3C), BET surface area measurement (with Nitrogen adsorption), and particle size analysis by Coulter Counter (Model TAII) [24]. SEM photographs of the three samples are given in Figures 1, 2, and 3. Tseng and Rochelle [28] gives the detailed particle size distributions.

Crystal Growth Rate Measurement

Measurement of calcium sulfite crystal growth rates was performed in a batch stirred-tank reactor using the pH-stat method. The pH-stat apparatus was the same as that used previously for measurement of $CaCO_3$ dissolution [4] and sulfite oxidation [25]. The agitator speed was set at 480 rpm. The reactor was sparged with N_2 before the addition of the seed crystals and was blanketed with N_2 during the rate experiment. The pH was automatically controlled to ± 0.02 units by titrating with freshly-prepared 0.2 M Na_2SO_3. Calcium sulfite crystal growth rate was related to the titration rate by the stoichiometry:

$$Ca^{++} + SO_3^{=} + 1/2H_2O \rightarrow CaSO_3 \cdot 1/2H_2O\ (s)$$

The activities of Ca^{++} and $SO_3^{=}$ are strong functions of ionic equilibria in the scrubbing solutions. Supersaturations of calcium sulfite and gypsum were calculated by the Bechtel-modified Radian solution equilibrium program [26, 27]. The relative saturation of calcium sulfite, RS_{CaSO_3}, is defined as:

$$RS_{CaSO_3} = (a_{Ca^{++}}\ a_{SO_3^{=}})/K_{sp} \text{ of } CaSO_3 \cdot 1/2H_2O$$

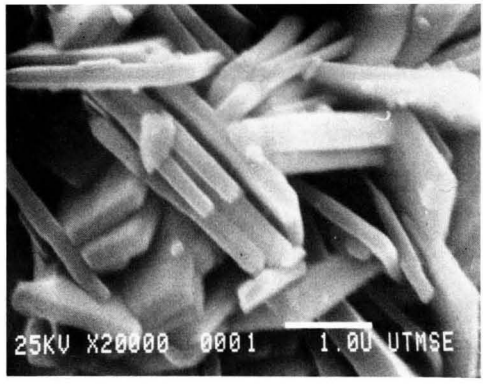

Figure 1. SEM photograph of seed 1.

Figure 2. SEM photograph of seed 3.

Corrected values of the $CaSO_3 \cdot 1/2H_2O$ solubility product (Table 2) were used based on previous work on calcium sulfite dissolution [28].

One mmole/liter seed crystal was put in the reactor at the beginning of each crystallization experiment, and was allowed to grow to 4-8 mmole/liter. Seed 1 (Figure 1) was used in most of the crystallization experiments, seeds 3 and 5 (Figures 2 and 3) were also used in some experimental runs to study the effect of seed crystal variation. During a batch experiment the pH and total dissolved sulfite were constant, and Ca^{++} concentration decreased by a negligible amount so that the solution composition could be assumed to be constant. The gas dispersion tube was lifted to allow sparging N_2 above the liquid level after the addition of Na_2SO_3 or Na_2SO_4 in the bulk solution to avoid stripping SO_2. Most of the experiments were performed at room temperature, but some runs were made at 55°C to study the effect of temperature.

TABLE 1. CALCIUM SULFITE SEED CRYSTALS

Sample No.	1	3	5
Synthesis Method	1 M Na_2SO_3 into 1 M $CaCl_2$	1.35 M Na_2SO_3, 0.15 M Na_2SO_4 into 1 M $CaCl_2$	2 M $CaCl_2$ into 2 M Na_2SO_3
$CaSO_4$ Concentration in Solids (Mole %)			
Iodometric titration	5.1	10.6	3.0
Infrared spectroscopy	3.4	10.7	1.0
Particle size (μm)	22 + 10	12 + 10	25 + 10
Platelet thickness (μm)	0.1	0.01	2
BET surface area (m^2/gram)	1.92	9.54	1.23

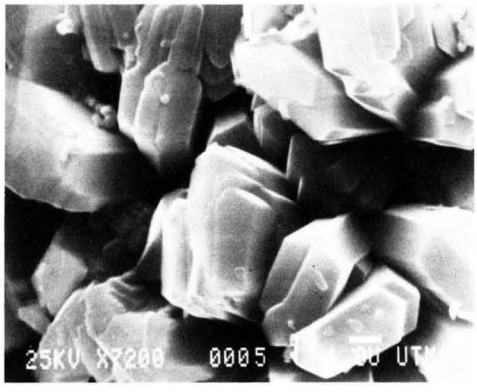

Figure 3. SEM photograph of seed 5.

A typical crystallization experiment is shown in Figure 4. The slurry density (mmole/liter) determined from the titration rate of Na_2SO_3 is plotted versus reaction time. The crystal growth rate is then calculated from the slope of the curve. Due to overshooting and fluctuation problems at the very beginning of some experiments, the crystal growth rates of all experiments were determined from the slope of the titration curves at the time when the slurry density has increased 50% relative to its initial value. the absolute growth rate was normalized by the BET surface area (N_2) of the initial seed.

The curve shown in Figure 4 is slightly concave upward. However, the slope change is small and the crystal growth rate is nearly independent of reaction time and crystal size/mass. The measured rates are two to three orders-of-magnitude slower than the rates predicted by the mass transfer model developed by Tseng and Rochelle [28] in their work on calcium sulfite dissolution. For Exp. No. 13, with an approximate driving force of 1 mM sulfite and a measured crystal growth rate of 1.6E-10 gmol/cm²-min, the calculated mass transfer coefficient is 2.6E-5 cm/s, three orders of magnitude less than would be reasonable. Therefore, calcium sulfite crystallization is not controlled by diffusion in the solution boundary layer.

SEM was used to characterize the shape and size of the crystal. Since calcium sulfite solids are not electrically conductive, the solids were sputtered or vacuum-evaporated with an alloy of Au and Pd to provide the necessary conducting medium for the SEM. IR was used to detect the presence of sulfate in the $CaSO_3 \cdot 1/2H_2O$ solids. The absorption structures of interest are the major sulfite band at approximately 990 cm^{-1} and the sulfate band near 1130 cm^{-1}. Peak heights of sulfite and sulfate absorption bands in the IR spectra were used to estimate the content of sulfate in the solids [29].

RESULTS AND DISCUSSION: GROWTH RATE

The experimental results are given in Table 3. Most of the data were obtained at 23°C with seed 1 at ionic strengths of 0.3 and 0.9 eq/l. Additional data were obtained at 55°C and with seeds 3 and 5.

Growth Rate Correlation

The growth rate, R′ (mole/cm²-minute), was empirically correlated as a function of calcium sulfite relative supersaturation, temperature, and gypsum saturation as follows:

$$R' = 9.7 \times 10^{-4}\, e^{-10250/RT} (RS_{CaSO_3} - 1)^2\, RS_{CaSO_4} - 1$$

The $CaSO_3 \cdot 1/2H_2O$ crystal growth rate is second order relative to the supersaturation of calcium sulfite, and is strongly inhibited by the presence of sulfate. The growth rate is inversely proportional to gypsum saturation.

Table 2. Corrected Values of K_{sp} of $CaSO_3 \cdot 1/2H_2O$ as a Function of Temperature and Solid Sulfate Content

Seed Crystal	1	3	5
Mole % $CaSO_4$	5.1	10.6	3.0
K_{sp} at 23°C (M^2)	2.67×10^{-7}	3.40×10^{-7}	2.40×10^{-7}
K_{sp} at 55°C (M^2)	1.12×10^{-7}	1.44×10^{-7}	1.01×10^{-7}

*K_{sp} is defined as the product of Ca^{++} and $SO_3^{=}$ activities.

Calculated values of the crystal growth rate are given in Table 3 for each experiment. When no sulfate was added to the solution, the gypsum saturation was assumed to be 0.025. The correlation is most effective at predicting rate with no added sulfate. The correlation was fitted to the first series of data on the effect of sulfate (Seed 1, 23°C, 0.9 eq/l ionic strength). It does not work well for other series where the gypsum saturation was on the order of 1.9.

Effect of Gypsum Saturation

The presence of dissolved sulfate reduces $CaSO_3 \cdot 1/2H_2O$ crystal growth rate significantly. In Figure 5, the growth rates with sulfate added at a $CaSO_3$ saturation of 4.3 to 4.6 are normalized to the growth rate at the "zero sulfate" condition. The rate of $CaSO_3 \cdot 1/2H_2O$ crystal growth is inversely proportional to the gypsum saturation. $CaSO_4$ is known to form a solid solution with $CaSO_3 \cdot 1/2H_2O$, and it comes as no surprise that gypsum saturation influences $CaSO_3 \cdot 1/2H_2O$ crystallization. Gypsum saturation also inhibits calcium sulfite dissolution.

Effect of Temperature, Sulfate and Seed Crystal Variation

The rate of crystal growth was measured with the three different seed crystals characterized in Table 1. The crystal growth rates per unit initial BET surface area are plotted versus relative supersaturation in Figure 6. It can be seen that $CaSO_3 \cdot 1/2H_2O$ crystal growth rate is proportional to the second order of calcium sulfite relative supersaturation, and the effects of temperature and gypsum sat-

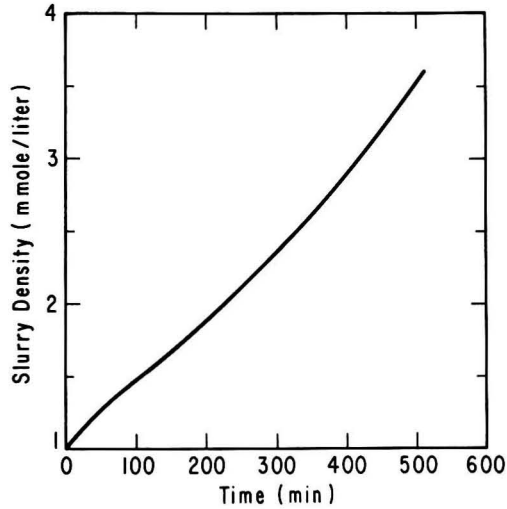

Figure 4. A typical crystallization experiment, seed 1, $RS_{CaSO_3} = 2.54$, Exp. No. 34.

TABLE 3. $CaSO_3$ CRYSTAL GROWTH RATE

Exp. No.	pH	Solution Composition (mM) Ca^{++}	S^{+4}	S^{+6}	Solid Saturation $CaSO_3$	$CaSO_4$	Solid $CaSO_4$ (mol %)	Growth Rate × 10^{10} (mole/cm²-min) meas	calc
Seed 1, 23°C, 0.9 eq/l ionic strength									
34	4.0	300	25	0	2.54	0	6	15.9	25.1
36	4.25	300	25	0	4.31	0	5.4	189.0	116.0
115	4.25	300	25	0	4.31	0	3.3	164.0	116.0
118	4.25	300	25	1	4.30	0.13	5.4	52.5	21.8
119	4.25	300	25	2	4.29	0.26	5.6	24.3	10.9
117	4.25	300	25	5	4.27	0.66	7.0	8.55	4.31
120	4.25	300	25	8	4.25	1.05	7.4	4.61	2.67
116	4.25	300	25	10	4.24	1.30	8.1	4.12	2.13
121	4.25	300	25	15	4.21	1.94	3.5	2.12	1.40
38	5.5	10	25	0	2.21	0	1.7	10.3	15.5
37	5.75	10	25	0	3.35	0	<1	5.29	58.4
33	6.0	10	25	0	4.75	0	4.4	136.0	149.0
43	6.0	10	25	10	4.66	0.05	4.2	57.5	73.7
44	6.0	10	25	20	4.58	0.09	6.6	42.0	36.4
108	6.0	10	25	20	4.58	0.10	<1	32.9	35.3
45	6.0	10	25	30	4.51	0.14	6.3	19.9	23.9
107	6.0	10	25	30	4.51	0.14	5.8	16.8	22.8
106	6.0	10	25	50	4.34	0.23	5.4	78.3	12.8
105	6.0	10	25	100	3.97	0.43	3.6	6.99	5.41
24	4.5	300	10	0	2.86	0	—	41.9	36.6
26	4.75	300	10	0	4.49	0	—	472.0	129.0
25	5.0	300	10	0	6.63	0	—	942.0	335.0
27	6.0	10	10	0	2.22	0	—	43.4	15.7
28	6.5	10	10	0	3.88	0	—	72.5	87.7
Seed 1, 23°C, 0.3 eq/l ionic strength									
84	4.7	100	10	0	1.99	0		7.33	10.4
81	4.8	100	10	0	2.42	0	<1	17.5	21.3
69	5.0	100	10	0	3.49	0	2.6	63.9	65.5
77	5.25	100	10	0	5.24	0	<1	204.0	190.0
35	5.25	100	10	20	4.83	1.91	9.8	9.82	2.03
88	5.25	100	10	20	4.83	1.91	14.6	6.08	2.03
89	5.5	100	10	20	6.85	1.90	11.3	37.6	4.76
39	5.5	100	10	20	6.85	1.90	18.0	41.9	4.76
90	5.75	100	10	20	8.96	1.89	9.4	157.0	8.86
40	5.75	100	10	20	8.96	1.89	—	189.0	8.86
20	5.7	20	10	0	3.10	0	—	41.6	46.6
19	6.0	20	10	0	4.73	0	—	223.0	147.0
21	6.5	20	10	0	7.57	0	—	812.0	456.0
11	5.2	100	5	0	2.47	0	—	23.8	22.8
9	5.5	100	5	0	3.71	0	—	54.4	77.6
10	6.0	100	5	0	5.70	0	—	217.0	234.0
13	6.5	100	5	0	6.87	0	—	669.0	364.0
18	5.55	100	2	0	1.50	0	—	7.69	2.64
16	6.0	100	2	0	2.29	0	—	39.5	17.6
14	6.5	100	2	0	2.76	0	—	109.0	32.7
15	7.0	100	2	0	2.95	0	—	196.0	40.2
17	7.5	100	2	0	3.02	0	—	374.0	43.1
Seed 1, 55°C, 0.3 eq/l ionic strength									
52	4.5	100	10	0	1.80	0	3.3	23.3	37.0
50	4.7	100	10	0	2.73	0	3.7	222.0	173.0
51	4.8	100	10	0	3.34	0	4.4	359.0	316.0
53	5.0	100	10	0	4.89	0	3.1	870.0	874.0
Seed 1, 55°C, 0.9 eq/l ionic strength									
49	3.75	300	25	0	1.88	0	4.4	104.0	44.7
48	4.0	300	25	0	3.28	0	5.4	732.0	300.0
55	5.25	10	25	0	1.49	0	1.6	29.5	13.9
54	5.5	10	25	0	2.39	0	1.8	236.0	112.0
Seed 3, 23°C, 0.3 eq/l ionic strength									
83	4.7	100	10	0	1.56	0	4.1	1.99	3.31
82	4.8	100	10	0	1.89	0	4.0	7.50	8.37
70	5.0	100	10	0	2.74	0	3.2	28.0	32.0
78	5.25	100	10	0	4.11	0	3.7	85.9	102.0
73	5.25	100	10	20	3.79	1.91	9.6	1.77	1.08
71	5.5	100	10	20	5.36	1.90	14.1	16.2	2.64
72	5.75	100	10	20	7.01	1.89	14.8	66.2	5.05
Seed 3, 55°C 0.3 eq/l ionic strength									
98	4.5	100	10	0	1.41	0	2.6	10.1	9.71
74	4.7	100	10	0	2.14	0	4.1	52.0	75.1
97	4.8	100	10	0	2.61	0	3.0	108.0	150.0
99	5.0	100	10	0	3.83	0	2.2	347.0	463.0

(Continued)

Seed 5, 23°C, 0.3 eq/l ionic strength									
68	4.7	100	10	0	2.21	0	<1	14.3	15.5
67	4.8	100	10	0	2.69	0	<1	37.5	30.2
66	5.0	100	10	0	3.88	0	2.1	135.0	87.7
62	5.25	100	10	0	5.83	0	1.3	487.0	247.0
63	5.25	100	10	20	5.38	1.91	9.3	17.9	2.65
87	5.25	100	10	20	5.38	1.91	8.4	16.9	2.65
64	5.5	100	10	20	7.61	1.90	11.9	66.3	6.08
92	5.5	100	10	20	7.61	1.90	11.7	74.8	6.08
65	5.75	100	10	20	9.96	1.89	12.3	283.0	11.2
93	5.75	100	10	20	9.96	1.89	12.9	283.0	11.2
Seed 5, 55°C, 0.3 eq/l ionic strength									
58	4.5	100	10	0	2.00	0	<1	63.9	57.8
75	4.7	100	10	0	3.04	0	2.3	210.0	240.0
60	4.8	100	10	0	3.71	0	2.7	675.0	424.0
61	5.0	100	10	0	5.44	0	<1	1740.0	1140.0

uration on crystal growth of the three seed crystals are the same. It also appears that initial BET surface area is better than initial particle size as a characteristic to distinguish seed crystals.

In Figure 6, temperature shows a strong effect on the growth rate. This also suggests that $CaSO_3 \cdot 1/2H_2O$ crystal growth is controlled by surface kinetics, not by mass transfer which normally shows a less significant effect of temperature. The growth rate at 55°C, as at 23°C, is second order relative to calcium sulfite supersaturation. The activation energy for $CaSO_3 \cdot 1/2H_2O$ crystal growth is estimated to be 10.3 kcal/gmole.

Another set of experimental data in Figure 6 were obtained with a gypsum saturation of 1.9. The crystal growth rate of $CaSO_3 \cdot 1/2H_2O$ at this high gypsum saturation has a stronger dependence on the relative supersaturation of calcium sulfite. There is apparently an interaction between the effects of gypsum saturation and calcium sulfite saturation on the crystal growth rete of calcium sulfite.

Effects of pH, Solution Composition, Temperature, and Ionic Strength

At typical operating pH ranges of FGD processes, total dissolved sulfite is mostly bisulfite, and calcium sulfite equilibrium is a strong function of pH as given by

$$Ca^{++} + HSO_3^- \leftrightarrow H^+ + CaSO_3\,(s)$$

Relative supersaturation of $CaSO_3 \cdot 1/2H_2O$ is also a function of the dissolved Ca^{++} and total sulfite. Higher pH, higher Ca^{++}, and higher total sulfite all increase the rate of $CaSO_3 \cdot 1/2H_2O$ crystallization.

In Table 3, two sets of experimental data were obtained at bulk solutions of high ionic strength (0.9 eq/l) and low ionic strength (0.3 eq/l). In each set of experimental data, the solution composition varied while the ionic strength was kept the same. When $CaCl_2$ was substituted by an equivalent ionic strength of NaCl, the crystal growth rate dropped significantly due to the decrease of Ca^{++} activity which directly determined the solubility product of calcium sulfite in the solutions. Therefore, a higher pH was needed to shift more HSO_3^- to $SO_3^=$ and thus increase the supersaturation of calcium sulfite to provide the driving force for crystal growth.

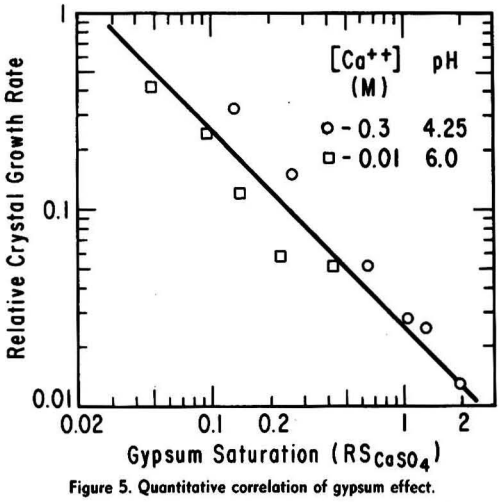

Figure 5. Quantitative correlation of gypsum effect.

RESULTS AND DISCUSSION: CRYSTAL HABIT

The grown crystals in the crystallization experiments were filtered, dried, and recovered for study of the crystal habit. Scanning electron microscopy and infrared spec-

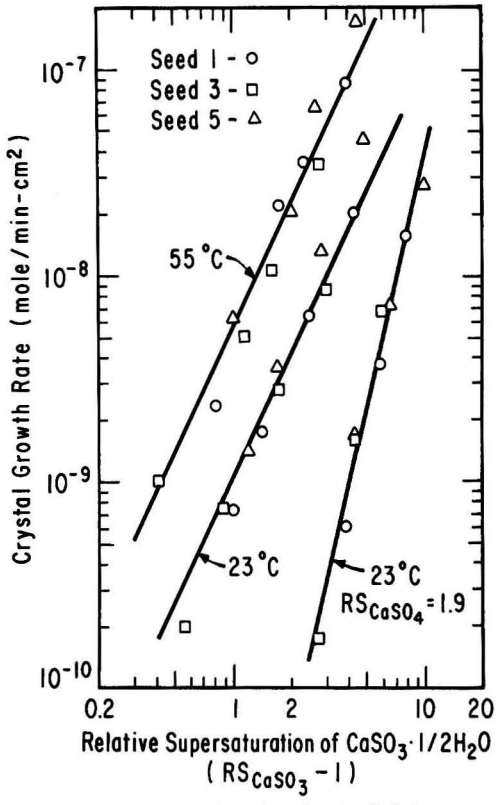

Figure 6. Calcium sulfite crystal growth as a function of relative supersaturation, temperature, and gypsum saturation for the three seed crystals.

troscopy have been applied to examine the changes in crystal morphology and solid composition. Seed 1 was used in most of the experimental runs; seeds 3 and 5 were used to study the effect of seed crystal variation.

The effects of solution composition, ionic strength, temperature, gypsum saturation and seed crystal variation on $CaSO_3 \cdot 1/2H_2O$ crystal habit were studied. Substances whose chemical properties are similar to those of the crystallizing component often become habit modifiers [30], and this is the case for $CaSO_4$, which has been found to be a strong habit modifier for $CaSO_3 \cdot 1/2H_2O$ crystallization.

Effect of Gypsum Saturation

Calcium sulfate has a very strong effect on $CaSO_3 \cdot 1/2H_2O$ crystal habit. Because of solution sulfate impurities, none of the rate studies give the extreme of low $CaSO_4$ (less than 1%) that gives large crystals in seed 5 (Figure 3). A dramatic change in crystal morphology was observed when the seeds were grown in a solution with 190 percent gypsum saturation (Figure 7) compared with that grown with very low sulfate in the solution (Figure 8). Agglomerates of very thin crystals were generated and IR spectroscopy indicated the increase of solid sulfate content. A probable explanation of this effect is that $CaSO_4$ selectively inhibits the growth of one crystal face as the other faces grow relatively more rapidly. The resulting crystal is a very thin platelet. This explanation is consistent with the earlier observation that $CaSO_4$ dramatically reduces the net growth rate of calcium sulfite crystals.

Seed Crystal Variation

A comparison of the SEM photographs of the grown crystals from all three seeds suggests that the calcium sulfite crystal habit is mainly determined by the gypsum saturation, solution composition, and temperature; seed crystal variation has only a minor effect.

The SEM photograph in Figure 9 exhibits a dramatic change in the crystal habit of seed 5 as it was grown in a solution of high gypsum saturation. Thin crystals were obtained even though the original seeds were thick. The SEM photographs of the partially grown crystals at 60 percent growth (Figure 10) shows clearly how the thick columner hexagonal seed crystals were grown into thin crystals during the transition period of the dramatic change in crystal habit.

Effects of Solution Composition, Temperature, and Ionic Strength

In the absence of $CaSO_4$, the crystal habit does not change significantly as a function of solution composition when the seed is grown in a high Ca^{++} environment, as shown in Figure 8. However, individual crystallites grow bulkier and thicker in Na^+ environment (Figure 11). Crystals grown at ionic strengths of 0.3 and 0.9 eq/l exhibit no significant change in crystal morphology. Variation of temperature in the range of 23 to 55°C shows no significant effect on $CaSO_3 \cdot 1/2H_2O$ crystal habit for most of the crystallization experiments.

Since seeds grow bulkier in Na^+ environment and thinner in $SO_4^=$ environment, the combination of these two effects was studied. The morphology of the grown crystals

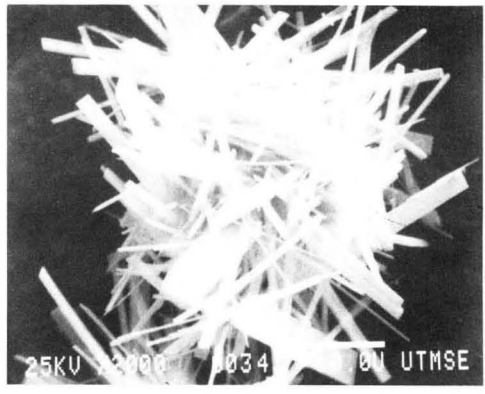

Figure 8. SEM photograph of the grown crystal in the absence of sulfate, 320% growth, Exp. No. 34.

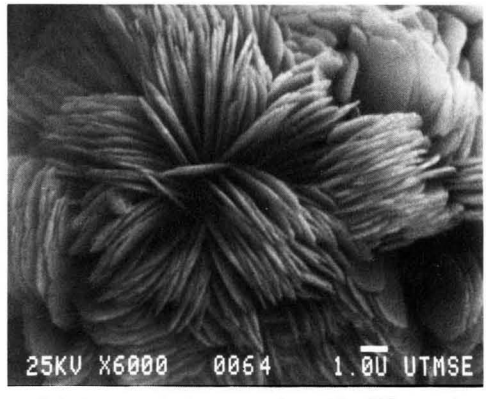

Figure 9. SEM photograph of grown crystals, seed 5 at 300% growth, with 1.9 gypsum saturation, Exp. No. 64.

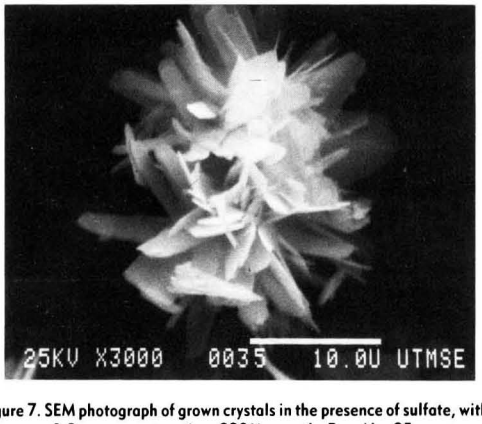

Figure 7. SEM photograph of grown crystals in the presence of sulfate, with 1.9 gypsum saturation, 320% growth, Exp. No. 35.

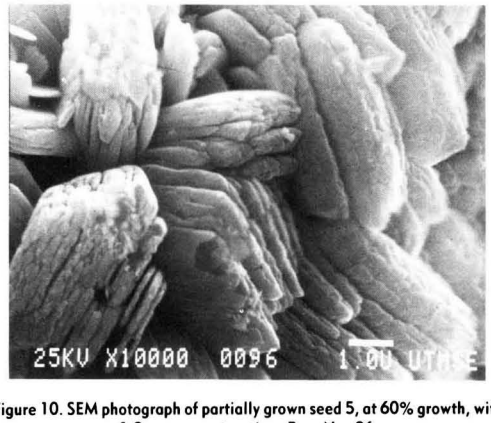

Figure 10. SEM photograph of partially grown seed 5, at 60% growth, with 1.9 gypsum saturation, Exp. No. 96.

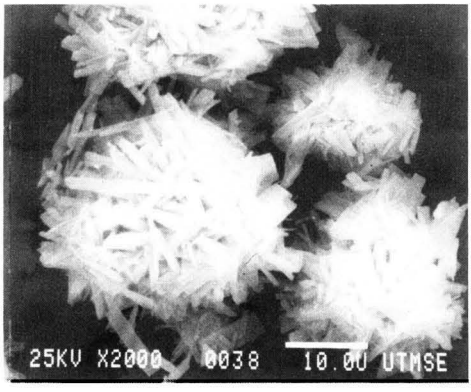

Figure 11. Crystal habit of grown crystal in Na^+ environment, seed 1, 1.7% sulfate in final solids, 210% growth, Exp. No. 38.

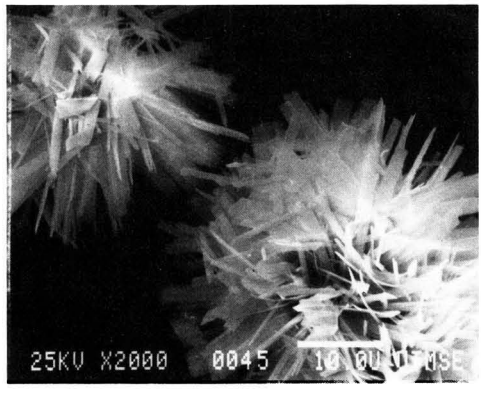

Figure 12. Crystal habit of grown crystals in Na^+ environment, 0.14 gypsum saturation, 6.2% sulfate in solids, 380% growth, Exp. No. 45.

demonstrated that gypsum saturation is a more important variable than Na^+ concentration (Figure 12).

NOMENCLATURE

a	activity (mole/liter)
K_{sp}	solubility product (M^2)
M	molarity (mole/liter)
R	gas constant = 1.987 (cal/mole-°K)
R′	crystal growth rate (mole/cm²-minute)
RS_{CaSO_3}	relative saturation of $CaSO_3 \cdot 1/2H_2O$
RS_{CaSO_4}	relative saturation of $CaSO_4 \cdot 2H_2O$
S^{+4}	total dissolved sulfite (as sulfite and bisulfite compounds)
T	temperature (°K)

LITERATURE CITED

1. Rochelle, G. T. and C. J. King, "The Effects of Additives on Mass Transfer in $CaO/CaCO_3$ Slurry Scrubbing of SO_2 From Waste Gases," *Ind. Eng. Chem. Fundam.*, **16**, 67-75 (1977).
2. Chang, C. S. and G. T. Rochelle, "SO_2 Absorption Into Aqueous Solutions," *AIChE J.*, **27**, 292-298 (1981).
3. Chang, C. S. and G. T. Rochelle, "Mass Transfer Enhanced by Equilibrium Reactions," *Ind. Eng. Chem. Fundam.*, **21**, 379-385 (1982).
4. Chan, P. K. and G. T. Rochelle, "Limestone Dissolution: Effects of pH, CO_2, and Buffers Modelled by Mass Transfer," *ACS Symp. Ser. 188*, 75-97 (1982).
5. Sada, E., H. Kumazawa, and H. Nishimura, "Absorption of Sulfur Dioxide into Aqueous Double Slurries Containing Limestone and Magnesium Hydroxide," *AIChE J.*, **29**, 60-65 (1983).
6. Borgwardt, R. H., "Proceedings: Symposium on Flue Gas Desulfurization," EPA Report 600/2-76-136a, 117-144 (1976).
7. Glancy, D. L., et al., "Proceedings: Eight Symposium on Flue Gas Desulfurization," EPA Report 600/9-84-017a, 280-299 (1984).
8. Chang, C. S. and N. Kaplan, "Proceedings: Eight Symposium on Flue Gas Desulfurization," EPA Report 600/9-84-017a, 300-328 (1984).
9. Ottmers, D. et al., "A Theoretical and Experimental Study of The Lime/Limestone Wet Scrubbing Process," EPA Report 650/2-75-006 (1974).
10. Phillips, J. L. et al., "Development of a Mathematical Basis for Relating Sludge Properties to FGD-Scrubber Operating Variables," EPA Report 600/7-78-072 (1978).
11. Edwards, L. O. et al., "Calcium Sulfite Crystal Sizing Studies," EPA Report 600/7-79-192 (1979).
12. Toprac, A. J. and G. T. Rochelle, "Limestone Dissolution in Stack Gas Desulfurization," *Env. Prog.*, **1**, 52-58 (1982).
13. Etherton, D. and A. D. Randolph, "Study of Gypsum Crystal Nucleation and Growth Rates in Simulated Flue Gas Desulfurization Liquors," EPRI Report CS-1885 (1981).
14. Erwin, J., C. C. Wang, and J. L. Hudson, "A Model of Oxidation in Calcium Sulfite Slurries," *ACS Symp. Ser. 188*, 191-220 (1982).
15. Kelly, B., B. Keough, and A. D. Randolph, "Some Effects of Crystal Modifiers on $CaSO_3 \cdot 1/2H_2O$ Crystal Habit, Growth and Nucleation," Presented at AIChE National Meeting, Houston, March 27-31, 1983.
16. Jones, B. F., P. S. Lowell, and F. B. Meserole, "Experimental and Theoretical Studies of Solid Solution Formation in Lime and Limestone SO_2 Scrubbers," EPA Report 600/2-76-273a (1976).
17. Setoyama, K. and S. Takahashi, "Solid Solution of Calcium Sulfite Hemihydrate and Calcium Sulfate," *Yogyo-Kyokai-shi*, **86**, 56-62 (1978).
18. Meserole, F. B., T. W. Trofe, and D. A. Stewart, "Proceedings: Eight Symposium on Flue Gas Desulfurization," EPA Report 600/9-84-017a, 466-491 (1984).
19. Cares, R., Personal communication, M. W. Kellogg, Houston (1982).
20. LaMantia, C. R. et al., "Proceedings: Symposium on Flue Gas Desulfurization-Atlanta," EPA-650/2-74-126a, 549 (1974).
21. Wang, S. C., Personal communication, Bechtel Corp., San Francisco (1982).
22. Acurex Corp., "Operation of EPA-Owned Pilot SO_2 Scrubber," Progress Report for January, 1984, EPA Contract 68-02-3648.
23. Barkley, et al., "Evaluation of Sodium Thiosulfate Additive on the Performance of a Spray Tower Scrubber System Using Limestone Slurry," TVA/OP/EDT-84/7 (1983).
24. Tseng, P. C., "Calcium Sulfite Hemihydrate Dissolution and Crystallization," Ph.D. Dissertation, University of Texas, Austin, Texas (1984).
25. Ulrich, R. K., R. E. Prada, and G. T. Rochelle, "Enhanced Oxygen Absorption into Bisulfite Solutions Containing Transition Metal Ion Catalysts," Submitted to *Chem. Eng. Sci.*, (1984).
26. Lowell, P. S. et al., "A Theoretical Description of The Limestone Injection-Wet Scrubbing Process," Radian Corporation, Contract No. CPA-22-69-138 (1970).
27. Epstein, M. and J. E. Williams, "EPA Alkali Scrubbing Test Facility: Summary of Testing Through October 1974," EPA-650/2-75-047 (1975).
28. Tseng, P. C. and G. T. Rochelle, "$CaSO_3 \cdot 1/2H_2O$ Dissolution in Flue Gas Desulfurization Processes," *Environ. Progr.*, **5**, 34-40 (1986).
29. Meserole, F. B., Personal communication, Radian Corporation, Austin, 1983.
30. Toyokura, K., "Encyclopedia of Chemical Processing and Design," edited by J. J. McKetta and W. A. Cunningham, **7**, 407-420, M. Dekker, Publisher, New York (1980).

Hazardous Waste Characterization Extraction Procedures for the Analysis of Blast-Furnace Slag From Secondary Lead Smelters

Quantitative data from actual field tests show that the carbonic-acid content of the landfill area is critical.

Nancy Karen Fish Woodley, Tuscaloosa Testing Laboratory, Inc., Tuscaloosa, Ala. 35403
James V. Walters, University of Alabama, University, Ala. 35486

Slag from the secondary-lead-smelter industry is the solid waste that caused the industry to be selected as one of fifteen priority industries to be surveyed under the Resource Conservation and Recovery Act, RCRA. Before RCRA the slag was a problem because it is a voluminous solid waste that was disposed in landfills. The RCRA criteria under which the slag might be determined to be a hazardous waste were the toxic-metal-concentration limits allowable in the leachate from the Extraction Procedure, EP, Toxicity Test adopted by the USEPA.

The EP Toxicity Test is specified in EPA publication SW-846 *Test Methods for Evaluating Solid Waste*, a manual for determining the hazardousness of solid wastes that was published in 1980. The EP Toxicity Test provides for the subjection of samples to a Structural Integrity Test, SIT, prolonged leaching of the sample in an agitated acetic acid solution, and the analyzing of the leachate for the concentration of eight metals.

The Secondary Lead Smelters Association, the technical association of the industry, was concerned that the EP Toxicity Test might over conservatively determine that the smelter slag is hazardous because the slag contains significant amounts of lead, because lead acetate is one of the most soluble of lead compounds, and because it is extremely unlikely that a lead-smelter-slag monolandfill in the real world will ever be leached by a relatively highly concentrated solution of acetic acid.

The Association sponsored this research so that the nature of the slag from most of the procedures in the industry could be evaluated. The alternative test was believed to be more representative of possible landfill field conditions.

MATERIALS AND METHODS

Materials

The objective of the laboratory portion of this research was to contrast EPA EP Toxicity Test results obtained on 27 blast furnace slag samples with the results obtained when the EPA EP Toxicity Test was modified to use carbonic acid instead of acetic acid in the leaching solution. Each of nine secondary lead smelters sent three split samples of slag from one week's operation—generally, one from Monday, one from Wednesday, and one from Friday.

From each plant, the three split samples were collected by placing two 60.73-ml refractory clay molds on a flat sheet of iron and ladling molten slag simultaneously into the molds from slag pots that had been cooled for four-to-five minutes. An angle iron was used to split the sample as it flowed into the two molds.

A sample collection procedure was developed and conducted to provide a statistically representative sample of each plant's slag, to minimize the anticipated nonuniformity in the process that generated the slag, and to determine the value for specific properties of the slag. All of the plants sent in their samples between December 9, 1982, and January 5, 1983.

The slag samples were in the form of a cylindrical core of 3.3-cm diameter and 7.1-cm length when removed from their molds. All were monolithic cores of black slag. Seventy five percent of the samples were in one to four large pieces when removed from the molds. The remaining 25 percent broke into small pieces during removal from the molds. The mass of the blast furnace slag samples varied, ranging from 158 grams to 282 grams.

Sample Preparation

This slag extraction project used the methods approved by EPA as a basis for designing the sampling program to insure acceptability of the sample collection procedure by EPA and to provide uniformity in how the slag was collected by the participating plants.

Sample preparation for the EPA and modified EPA Extraction Procedures involved a "Structural Integrity Procedure" in which each sample was placed in a compaction tester and subjected to EPA-prescribed compaction. The investigator then placed the sample in a 4000-ml polyethylene bottle with a volume in milliliters of deionized water equivalent to 16 times the sample's weight in grams. The pH of the extraction liquid with the sample in the bottle was recorded prior to commencement of the EPA EP and the modified EPA EP Toxicity Tests.

Extraction Procedures

The two extraction procedures used in this project were the EPA Extraction Procedure (EP) Toxicity Test and a modified EPA EP Toxicity Test. The EPA EP Toxicity Test is described in detail in the May 19, 1980, *Federal Register* on pages 33127 and 33128.

The modified EPA EP test was similar to the EPA protocol except that carbonic acid was used to leach the toxic contaminants instead of 0.5 *N* acetic acid. The extraction period started with the same 16:1 liquid to solid ratio, and CO_2 was bubbled into the mixture during pH-reading and pH-adjustment periods. Since no acetic acid was being added during the extraction period, the CO_2 was measured by time and flow rate for an approximation of the amount of CO_2 being bubbled through the extraction liquid. The similarities and differences between the two selected extraction procedures are summarized by Table 1.

One of the critical factors in conducting the EPA EP Toxicity Test involves selecting a suitable extractor. Since blast furnace slag is a heavy monolithic waste that can be fixed as a core when tapped from the furnace, the type of extractor that would ensure continuous surface contact with a well mixed extraction fluid and prevent stratification of the sample and extraction liquid would be a "rotary" extractor.

The "stirrer" extractor as shown in Figure 1 would not be able to mix a 150-plus-gram sample with the extraction liquid without abrading the metal walls, or jamming the blades. A "stirrer" would also be unable to prevent stratification of the solid and liquid, given the physical nature of slag. A "rotary" extractor avoids these problems by its end-over-end agitation. Figure 2 illustrates the prototype extractor used in this research project. Although the polyethylene bottles were abraded by the tumbling slag, the plastic particles were filtered out after the extraction period and didn't interfere with the metal analyses.

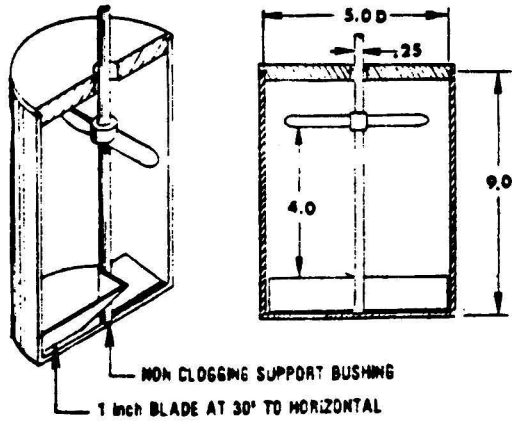

Figure 1. ERA-approved stirrer-extractor. (Source: US EPA, 1980, "Test Methods for Evaluating Solid Waste—Physical/Chemical Methods," SW-846).

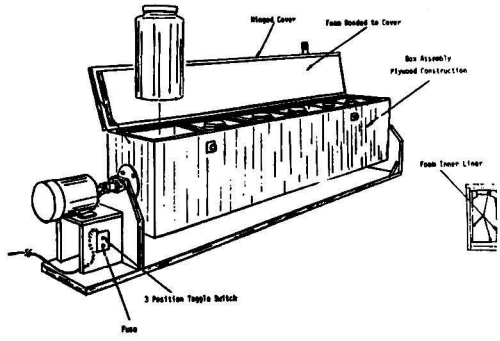

Figure 2. EPRI/ACUREX rotary extractor. (Source: US EPA, "Test Methods for Evaluating Solid Waste—Physical/Chemical Methods," SW-846).

Analytical Procedures

Because dross and other lead-bearing materials are the major feed stock to the blast furnace, lead is generally the primary contaminant of concern to the industry today. Thus in this project all slag samples were analyzed for lead, and randomly selected slag samples were analyzed for the other seven metals that have EP Toxicity characteristics.

Since slag is exposed to such high temperatures in the blast furnace (at least 1,200°C), the eight EP toxic metals should be the only contaminants possibly present. Organic EP Toxic Contaminants would be destroyed by the high operating temperature in the blast furnace.

The number of samples randomly selected for analysis of all eight toxic metals were 17 split samples. According to the 1977 NIOSH *Occupational Exposure Sampling Strategy Manual,* analyzing 17 out of an original group of 27 split samples for all eight metals would give a 95% confidence level that at least one of the three (i.e., 10% of 27) split samples with the highest metal concentrations would be included in the partial sample. Each split sample was assigned a number from 1 to 27 in the blast furnace slag group—for example, 1A and 1B. Then the first 17 numbers that fell within the 1 to 27 group were selected on a table of random numbers. The split samples that had one of the randomly selected numbers were analyzed for all eight toxic metals. The remaining ten split samples were analyzed only for lead concentrations.

Methods for analyzing metals in the EP extract were identified by EPA and published in *Methods for Analysis of Water and Wastes* in March, 1979. In this project, cadmium, chromium, lead, and silver were digested and analyzed by atomic absorption spectrophotometry.

A Varian Model 1100 Atomic Absorption Spectrophotometer and the method of standard additions (USEPA 1980) were used for all analyses.

An inductively coupled argon plasma (ICAP) spectrometer, Jarrell-Ash ICAP 9000, was used as an estimator for sample preparation for AA analysis and as a quality control for the precision of the Varian AA Spectrophotometer.

TABLE 1. COMPARISON OF EPA'S EP TO ALTERNATIVE EP FOR BLAST FURNACE SLAG

Factor	EPA Method	Alternative Method
Sample Size	100-g minimum	100-g minimum
Sample Preparation	Structural Integrity Test (SIT)	Structural Integrity Test (SIT)
Liquid: Solid Ratio	20 ml:1 g	20 mL:1 g
Composition of Leaching Solution	0.5 *N* acetic acid 4, ml/g maximum	CO_2 gas (to pH of not less than 4.8)
pH Control	4.8 to 5.2	4.8 or lowest attainable if > 5.2
Type and Degree of Mixing	Stirring device, tumbling device or equivalent 24 hour plus 4 hour if pH > 5.2	Same
Method of Liquid/ Solid Separation	4.5×10^{-7} meters filtration	4.5×10^{-7} meters filtration

EXTRACTION PROCEDURE TOXICITY TESTS

EPA EP Toxicity Test

Aside from the highly variable results obtained with EPA's EP Toxicity Test for identifying the hazardousness of a waste, the application of the test to determine adequate disposal methods is also questionable. One problem is the lack of information that correlates test results with actual field conditions. There are numerous chemical, physical, and biological variables that could affect the metals released in the tests, as well as those released under field conditions. Particularly, there is an absence of experimental data from field correlated leaching tests of blast furnace slag. This limits any effective use of the EP Toxicity Test as a design tool for landfill disposal of the slag.

Another major problem involves the representative nature of the EP. While use of a standard procedure allows interlaboratory data comparisons, the procedures may not represent normal management practice for various wastes. For example, the EPA EP simulates codisposal with a pH of 5.0 ± 0.2. The procedure's pH conditions however can't be met if a highly alkaline waste uses the maximum allowable (4 ml per gram of sample) acetic acid and still cannot meet the 5.0 ± 0.2 pH condition. Under these circumstances, the procedure would not be appropriate for evaluating the leaching properties of this waste. Also, the monolandfilling of such wastes with other alkaline wastes would not be reflected by a leach test that has acetic acid as a pH modifier.

The problems of reproductibility, procedure appropriateness, and field condition simulation should be kept in mind when interpreting the results from EPA's EP Toxicity Test. If the EP test were to be used to estimate leaching properties of a waste under site-specific conditions, important variables should be incorporated to reflect field conditions. Sample preparation, dilution ratio, type and extent of agitation, elution medium, and time are all important factors that could affect the behavior of landfilled waste. If the standard laboratory EP is followed, interpretation of the results would have limited values in determining landfill design.

Limitations to the precision of analyzing the slag samples were the detection limit and interferences associated with the atomic absorption spectrophotometer approved for use in sample analysis under the RCRA. A Varian Model 1100 was used in this project. This spectrophotometer is most precise when measuring concentrations which lie within an "optimum range" and losses that degree of precision as the concentrations approach the lower detection limit or greatly exceed the "optimum range" values. In order to prepare the slag sample extracts to fall within the "optimum range" for each of the surveyed metals, a Jarrell-Ash ICAP 9000 was used to obtain a preliminary estimate of the concentration values.

EPA EP Toxicity Test Results

Data results from extracting the 27 samples of blast furnace slag according to EPA protocol are presented in Table 2. Note that the first value is the Varian AA estimate and the second value is the ICAP 9000 estimate. The "A" denotes that the EPA EP protocol was used.

The results show for AA values that lead and cadmium may leach from the slag in amounts that exceed toxicity levels. Lead leachate concentrations vary widely—even those from slag samples taken at the same plant. However, one pattern was observed—seven of the ten highest lead concentrations in leachates were also among the ten

TABLE 2. SECONDARY LEAD SMELTER BLAST FURNACE SLAG EPA EXTRACTIVE PROCEDURE TOXIC METAL CONCENTRATIONS AA-ICAP (mg/L)

Sample	As	Ba	Cd	Cr	Pb	Hg	Se	AG
1A	0.11	0.83	<0.02	0.07	2.83-7.02	<0.02	0.06	<0.03
2A	2.35-0.52	<1.00-0.36	0.26-<0.02	0.03-<0.05	209-619	0.02-0.04	0.45-0.15	<0.10-<0.03
3A	0.17-0.05	<1.00-1.08	0.64-<0.02	0.05-0.07	0.53-0.39	0.01-0.04	0.04-0.09	<0.10-<0.03
4A	0.76	1.14	<0.02	<0.05	1,300-934	0.10	0.26	<0.03
5A	0.26-0.05	1.76-0.06	0.92-<0.02	0.16-0.07	3.86-3.67	<0.002-<0.03	0.32-0.15	<0.10-<0.03
6A	1.54-0.21	7.17-6.74	1.22-0.01	0.17-0.07	141-91.6	0.004-0.04	0.13-0.21	0.11-<0.03
7A	2.03-0.39	12.4-0.75	0.49-0.05	0.11-0.17	543-438	<0.002-0.07	0.04-0.15	<0.10-<0.03
8A	0.21	0.40	0.01	0.03	21.9-22.4	0.03	0.15	<0.03
9A	0.17	0.52	0.01	0.07	125-147	0.03	0.18	<0.03
10A	1.25-0.14	23.1-12.0	0.25-<0.02	0.37-0.07	17.9-9.50	<0.002-0.06	0.06-0.15	<0.10-<0.03
11A	0.05	6.50	<0.02	0.17	4.88-1.44	0.04	0.06	<0.03
12A	0.23	8.54	<0.02	0.14	31.8-22.1	0.03	0.18	<0.03
13A	* -0.79	2.90-0.25	0.73-0.03	0.67-0.10	774-797	0.04-0.09	0.40-0.24	<0.10-<0.03
14A	1.59-0.50	32.1-32.9	1.78-0.81	0.70-0.17	493-492	0.18-0.10	0.48-0.26	0.21-<0.03
15A	1.86-0.33	11.3-1.03	1.04-<0.02	0.41-0.07	409-408	0.10-0.06	0.56-0.15	0.15-<0.03
16A	0.18-0.11	1.84-1.01	0.15-0.01	0.30-0.07	1.58-0.91	0.01-0.06	0.65-0.24	0.45-<0.03
17A	0.08	1.12	<0.02	<0.05	21.2-7.85	<0.03	0.09	<0.03
18A	0.64	15.9	0.03	0.21	16.6-8.69	0.16	0.38	<0.03
19A	0.04-0.22	0.82-0.67	<0.02-0.02	<0.05-<0.05	35.3-39.1	0.03-<0.02	<0.02-0.14	<0.10-<0.03
20A	0.72-0.18	7.38-0.51	1.22-0.01	0.37-0.03	15.7-20.3	0.02-<0.02	0.04-0.09	0.35-<0.03
21A	0.13	0.75	0.02	<0.05	59.1-60.0	<0.02	0.09	<0.03
22A	0.09	2.15	<0.02	0.03	2.26-1.00	0.03	0.14	<0.03
23A	1.39-1.61	11.0-11.0	1.38-0.09	0.80-0.21	291-283	0.02-0.33	0.39-2.43	0.50-<0.03
24A	2.90-0.19	8.18-4.89	1.31-0.02	0.40-0.07	4.18-2.86	0.01-0.05	0.26-0.37	0.15-<0.03
25A	1.27-0.63	14.6-8.25	1.45-0.04	0.74-0.10	380-274	<0.002-0.11	0.13-0.71	0.19-<0.03
26A	1.36-0.70	25.7-9.43	3.65-0.03	0.73-0.07	39.4-31.5	0.02-0.11	0.12-0.71	<0.10-<0.03
27A	4.87-1.30	21.9-31.7	0.10-0.08	<0.05-0.21	340-208	0.13-0.24	0.52-1.46	<0.10-<0.03
Toxic Concentration	5	100	1	5	5	0.2	1.0	5.0
Optimum Range (AA)	0.002-0.02	1-20	0.05-2	0.5-10	1-20	0.0002-0.01	0.002-0.02	0.1-4

* Laboratory Accident

samples with the largest amounts of 0.5 *N* acetic acid added.

Another observation was that there did not appear to be any direct relationship between easily broken slag samples and high lead concentrations. Table 3 is a tabulation of lead concentrations, slag surface descriptions, and acetic acid additions for blast furnace slag samples which underwent the EPA EP toxicity test.

Alternative EP Toxicity Test

The remaining 27 split samples from blast furnace smelters were subjected to the same EPA EP protocol except that CO_2 was bubbled into the extraction liquid at appropriate intervals instead of adding 0.5 *N* acetic acid. Table 4 summarizes the AA and ICAP metal concentrations for the "B" or split samples of 1 through 27.

The "B" samples were exposed to identical conditions as the "A" samples except that CO_2 was used to adjust the pH. Since the CO_2 was added as a gas, the balance of the total amount of deionized water (20 times the weight of the sample) was added during the test when the pH could not be adjusted lower than 5.2. There were two reasons for adding the deionized water supplement when the pH of 5.2 could not be reached. The additional water would provide more holding capacity for the CO_2 and the pH of the deionized water itself ranged from 5.4 to 5.9 as the result of the sorption of CO_2 from the air.

Alternative EP Toxicity Test Results

The salient findings of extracting the eight metals with CO_2 instead of 0.5 *N* acetic acid for slag samples 1 through 27 are as follows:

1. All 27 "B" samples, except for sample No. 21B, had lead concentrations smaller than 5 mg/L in their leachate;
2. Sample 21B had an AA value of 5.65 mg/L lead and an ICAP value of 2.30 mg/L lead, which suggests that 21B may possibly have a lead concentration less than 5 mg/L;
3. While cadmium and lead were the only metals that exceeded toxicity levels in the "A" samples, they did not exceed "toxic" levels in the "B" or split samples. The only exceptions being 21B for lead as noted above and 5B for cadmium. In both these cases, there is a difference between the AA and ICAP estimate which indicates that there possibly is not a toxic amount present in these two samples;
4. The metals that appeared to be more affected by CO_2 leaching were arsenic and mercury. Some "B" samples leached concentrations of these two metals that exceeded "toxic" levels;
5. In comparing the "A" samples to the "B" samples, particularly for lead concentrations, the means and standard deviations from 9 plants were much larger and coefficients of variations were generally larger for "A" samples than for "B" samples. The results indicate that "A" and "B" samples must be from different distributions.

TABLE 3. A TABULATION OF LEAD CONCENTRATIONS, SLAG SURFACE DESCRIPTIONS, AND REQUIRED ACETIC ACID ADDITIONS

Sample Number "A"	Lead Concentration (mg/L)	Surface Area Condition*	Acetic Acid Addition (mL)	Acetic Acid As a percent of the elutriate
1	2.83	L	11.8	0.3
2	209.0	1	65.23	2.2
3	0.53	1	20.68	0.6
4	1,300.0	1	68.0	2.1
5	3.86	1	10.62	0.2
6	141.0	1	47.9	1.3
7	543	S	42.0	1.3
8	21.9	S	12.0	0.3
9	125.0	S	19.4	0.6
10	17.9	1	23.66	0.7
11	4.88	1	7.5	0.2
12	31.8	1	35.1	1.1
13	774	3	72.9	1.7
14	493	1	36.6	1.0
15	409	3	52.0	1.3
16	1.58	1	21.0	0.7
17	21.2	3	8.91	0.3
18	16.6	S	109.0	3.6
19	35.3	S	16.36	0.5
20	15.7	S	13.88	0.4
21	59.1	L	17.0	0.4
22	2.26	1	33.5	1.0
23	291	S	622	15.9
24	4.18	L	61.0	2.0
25	380	1	158.0	5.0
26	39.4	3	148.8	4.8
27	340.0	1	364.0	11.1

* 1, 2, 3 = 1, 2 or 3 large pieces
L = large chunks, >3 pieces
S = small pieces

CONCLUSIONS AND RECOMMENDATIONS

Although the EPA EP Toxicity Test protocol which used 0.5 *N* acetic acid yielded lead concentrations in excess of 5 mg/L in the leachates, the alternate protocol, using gaseous CO_2 on split samples, yielded lead concentrations in the leachates of less than 5 mg/L (the EPA assigned toxic concentration limit for lead) in all but one sample.

Since EPA's interpretation of the EP Toxicity Test is now primarily used for identifying hazardous wastes and not for determining leachate concentrations in actual field conditions, it would seem reasonable to use the CO_2 induced leachate lead concentrations as more realistic values for depicting field values. The presence of CO_2 in the atmosphere, its transmission into the soil via precipitation and its production by organisms in the soil support the position that a CO_2 induced acid condition is much more likely to occur at a monolandfill site than acetic-acid-induced acid conditions.

The leachate from a monolithic, alkaline, dry waste such as blast furnace slag should be fairly low in lead concentrations if the carbonic acid condition occurs during rainfall events because the laboratory data shows that, even at a pH of 5 ± 0.2, there were not toxic levels of lead in the CO_2-induced acidic leachate. The same samples (splits) yielded toxic levels of lead when leached with acetic acid at a pH of 5 ± 0.2.

CONCLUSIONS

1. Although EPA has included the Structural Integrity Test as part of the EP, it does not appear that the SIT has a significant impact on increasing the amount of lead leached by the acetic acid EP (see Table 3). It appears that the greater the porportionate amount of acetic acid added, the greater the lead concentration in the leachate.

2. Another major conclusion that can be stated is that the carbonic acid EP shows much less lead in the leachate than the acetic acid EP. (See Tables 2 and 4.) Since carbonic acid is the kind of acid most likely to be present in soils, especially in a slag monolandfill, the carbonic acid EP should be the most logical extracting medium used to simulate conditions in an actual monolandfill.

3. Comparisons between the values obtained in the carbonic acid EP and actual field data from two secondary lead smelter slag landfills show the carbonic acid EP is a better predictor of groundwater and leachate concentra-

TABLE 4. SECONDARY LEAD SMELTER BLAST FURNACE SLAG ALTERNATIVE EXTRACTIVE PROCEDURE TOXIC METAL CONCENTRATIONS
AA-ICAP (mg/L)

Sample	As	Ba	Cd	Cr	Pb	Hg	Se	AG
1B	3.85	1.67	0.01	<0.05	0.44-0.24	0.20	0.79	<0.03
2B	3.73-4.12	<1.00-3.07	0.41-0.01	<0.05-<0.05	0.22-3.59	0.07-0.18	0.52-0.74	<0.10-<0.03
3B	3.98-2.89	<1.00-0.80	0.66-<0.02	0.07-<0.05	0.10-0.19	0.10-0.13	0.31-0.56	<0.10-<0.03
4B	3.53	0.66	0.03	0.10	0.42-0.33	0.24	1.24	<0.03
5B	2.30-1.85	3.11-0.13	1.10-<0.02	0.15-<0.05	0.72-0.76	0.01-0.08	0.26-0.38	<0.10-<0.03
6B	1.88-1.55	6.45-1.28	0.89-<0.02	0.15-0.03	2.10-3.20	0.01-0.07	0.08-0.44	<0.10-<0.03
7B	15.2-7.58	23.2-1.65	0.52-0.16	0.43-<0.05	0.15-0.24	0.12-0.16	0.03-0.74	0.12-<0.03
8B	2.35	0.53	0.01	<0.05	4.47-1.80	0.11	0.41	<0.03
9B	6.76	0.78	0.06	<0.05	0.37-0.24	0.22	1.06	<0.03
10B	2.16-1.12	7.84-6.87	0.06-<0.02	0.25-<0.05	0.91-0.69	<0.002-0.07	0.06-0.29	<0.10-<0.03
11B	2.15	9.29	<0.02	<0.05	0.97-0.33	0.12	0.50	<0.03
12B	1.36	6.38	<0.02	<0.05	0.85-0.15	0.05	0.29	<0.03
13B	1.69-8.77	0.61-0.31	0.10-0.05	1.90-<0.05	0.47-0.44	0.81-0.50	0.61-2.27	<0.10-<0.03
14B	1.52-7.62	4.55-5.39	0.10-0.06	2.30-<0.05	0.52-0.35	1.01-0.35	0.40-1.77	<0.10-<0.03
15B	1.82-8.20	1.42-9.46	0.15-0.06	0.71-<0.05	0.42-0.41	0.11-0.40	0.43-2.03	0.28-<0.03
16B	1.73-5.11	1.98-0.84	0.14-<0.02	0.39-<0.05	0.50-0.11	0.07-0.22	0.30-0.91	0.33-<0.03
17B	1.70	0.67	0.03	0.21	1.64-0.70	0.07	0.35	0.05
18B	6.70	12.8	0.02	<0.05	0.72-0.30	0.34	1.50	<0.03
19B	5.18-4.09	0.88-0.70	<0.02-0.03	<0.05-<0.05	1.48-1.28	0.32-0.13	0.05-0.77	0.13-<0.03
20B	1.37-2.03	0.51-0.51	0.71-0.02	0.42-<0.05	1.84-1.85	0.02-0.04	0.36-0.43	0.14-<0.03
21B	2.70	1.04	0.02	<0.05	5.65-2.29	0.07	0.54	<0.03
22B	2.88	1.04	0.03	<0.05	0.60-0.21	0.07	0.63	<0.03
23B	1.56-3.55	4.16-5.26	0.16-0.07	1.35-<0.05	0.57-0.36	0.25-0.21	0.37-1.31	0.12-<0.03
24B	1.24-5.55	4.85-3.43	0.17-<0.02	0.46-<0.05	0.44-0.21	0.11-0.28	0.29-1.26	<0.10-<0.03
25B	1.96-7.91	5.05-4.37	0.19-0.09	4.97-<0.05	0.71-0.40	0.09-0.39	0.17-2.09	<0.10-<0.03
26B	1.81-8.85	4.6-5.46	0.18-0.05	0.48-<0.05	0.70-0.34	0.10-0.47	0.01-1.91	<0.10-<0.03
27B	12.1-10.2	32.1-25.2	0.09-0.07	<0.05-<0.05	0.78-0.48	0.13-0.56	<0.02-2.60	<0.10-<0.03
Toxic Concentration	5.0	100.0	1.0	5.0	5.0	0.2	1.0	5.0
Optimum Range (AA)	0.002-0.02	1-20	0.05-2	0.5-10	1-20	0.0002-0.01	0.002-0.02	0.1-4

tions of lead than the acetic acid EP. Therefore, it can be concluded that the carbonic acid EP would be a better test than the acetic acid EP for determining the hazardousness of secondary lead blast furnace slag.

4. Because the carbonic system is much more prevalent in soils and water than the acetic system, lead leaching in monolandfills can be limited significantly by the carbonate species already present in the soil and water in the landfill.

Recommendations

The need and justification for adding the Alternative EP Toxicity Test to Part 261's testing methods can be found in numerous research documents, particularly the 1979 *Background Study on the Development of a Standard Leaching Test* by Ham *et al.* This waste furnace slag investigation supports the contention made by Ham *et al.* that "... no one media [sic] can give results adequate to describe properly the leaching characteristics of a waste ..." The use of deionized water with gaseous CO_2 to model monolandfilling blast furnace slag is much more realistic for simulating field conditions than the use of deionized water with 0.5 *N* acetic acid. General scientific knowledge of soil chemistry, the thermodynamic properties of lead, and the atmospheric-hydrologic behavior of CO_2 in the environment indicates that an addition to EPA's EP Toxicity Test procedures for this particular type of waste is justifiable.

The Alternative EP Toxicity Test results were much closer in value than the EPA EP Toxicity Test results when compared with the limited lead leachate data collected at two secondary lead smelter slag disposal sites. The leach test data from this research for lead concentrations extracted by the Alternative EP and EPA EP were as follows:

Alt. EP:	1.065 mg/L	mean
	1.239 mg/L	standard deviation
	116%	relative standard deviation
	1.53	variance (S^2)
EPA EP:	195.7 mg/L	mean
	297.7 mg/L	standard deviation
	152%	relative standard deviation
	88635	variance (S^2)

Unpublished data from ground water, lysimeter, and leachate monitoring at the two secondary lead blast furnace disposal sites ranged from 0 mg/L to 0.16 mg/L in the ground water with a maximum lead concentration of 0.60 mg/L found in the leachate collection system above the liner of one of the sites. For both sites, EPA leach-test concentrations are 100 to 1,000 times greater than actual monolandfill leachate concentrations. The Alternative EP Toxicity Test conducted for this should be used on samples from these two sites to see if there is a closer estimation by the leach test of field conditions than has been demonstrated for the EPA leach test and field conditions. Further research in comparing the proposed Alternative EP data results with actual ground water data would help substantiate these preliminary findings and provide better documentation for a petition to add the Alternative EP to test procedure under 40 CFR 261.24.

LITERATURE CITED

Daniels, S. L., "Development of Realistic Tests for Effects and Exposure of Solid Wastes, Hazardous Solid Waste Testing," First Conference, ASTM STP 760: ASTM, 345-365 (1981).

Fuller, W. H., A. Amoozegar-Fard, and G. E. Carter, "Predicting Movement of Selected Metals in Soils: Application to Disposal Problems," Solid and Hazardous Waste Research Division, Fifth Annual Research Symposium, Municipal Solid Waste, Land Disposal, USEPA (1979).
Ham, R., M. A. Anderson, R. Stegmann, and R. Stanforth, "Background Study on the Development of a Standard Leaching Test," USEPA, EPA-600/2-79-109 (1979).
Hem, J. D., "Inorganic Chemistry of Lead in Water," Geological Survey Professional Paper, 957, USGS (1976).
Hem, J. D., and W. H. Durum, "Solubility and Occurrence of Lead in Surface Water," *Journal AWWA* **65**, 562-568 (August, 1973).
Larson, R. J., P. G. Malone, T. E. Myers, and R. A. Shafer, "Evaluation of the Extraction Procedure Testing of Hazardous Industrial Wastes, Hazardous Solid Waste Testing," First Conference, ASTM STP 760: ASTM, 139-150 (1981).
LeGrand, H. E., "A Standardized System for Evaluating Waste-Disposal Sites," National Water Well Association, Worthington, Ohio, 42 (1980).
Leidel, N. A., K. A. Busch, and J. R. Lynch, "Occupational Exposure Sampling Strategy Manual" U.S. Department of HEW, NIOSH, Cincinnati, Ohio, 132 (1977).
Lowenbach, W., "Compilation and Evaluation of Leaching Test Methods," USEPA, EPA-600/2-78-095 (1978).
Turjoman, A. M., "The Behavior of Lead as a Migrating Pollutant in six Saudi Arabian soils: Ph.D. Dissertation, University of Arizona, 148 (1978).
U.S. Environmental Protection Agency, "Test Methods for Evaluating Solid Waste-Physical/Chemical Methods," Office of Water and Waste Management, SW-846 (1980).
U.S. Environmental Protection Agency, "Toxicity of Leachates," Office of Water and Waste Management, EPA-600/2-80-057 (1980).

Nancy K. Woodley is an environmental consultant associated with the Tuscaloosa Testing Laboratory, Inc. She earned a B.S. in Mathematics at the University of Massachusetts, in Amherst, Massachusetts. Her M.S.C.E. and Ph.D. degrees were earned at the University of Alabama in 1982 and 1984 respectively. She is a member of APCA, ASPE, AWWA, NSPE, WPCF, Tau Beta Pi, and Sigma Xi. She is an EIT in Alabama.

James V. Walters is Professor of Civil Engineering at the University of Alabama. He is a member of the University of Alabama Institute for Waste Management Studies and is the Chairman of the Board of Directors of Tuscaloosa Testing Laboratory, Inc. He earned B.C.E. and M.S.C.E. degrees at the Georgia Institute of Technology and the Ph.D. degree at the University of Florida in 1963. He is a member of APCA, ACS, ASCE, AWWA, TAPPI, WPCF, and Sigma Xi. He is a registered professional engineer in Alabama and in eighteen other states.

Volatile Organic Compounds at Hazardous Waste Sites and a Sanitary Landfill in New Jersey

An up-to-date review of the present situation.

John LaRegina and Joseph W. Bozzelli, New Jersey Institute of Technology, Newark, N.J. 07102
Ron Harkov and Sam Gianti, New Jersey Department of Environmental Protection, Trenton, N.J. 08625

The sampling and analysis of volatile organic compounds (VOC) at ambient levels has been performed since the early to mid-1970's in a variety of urban environments [1-5]. In New Jersey, a wide variety of locations have been looked at, from very industrial areas in and around Newark to rural locations such as the Pinelands in the rural south of the state [5].

The abundance of petrochemical industry in New Jersey has resulted in a great deal of chemical dumping activity over the past decades. The number of dumpsites is quite large and, although much analysis of the soil and groundwater has been performed, the air quality in and around the sites has rarely been investigated [6].

This present study attempted to collect data on the ambient levels of primarily chlorinated and aromatic VOC in and around five hazardous waste sites and one landfill in New Jersey.

SAMPLING LOCATIONS

The five hazardous sites chosen are currently on the National Priorities List of hazardous sites [7] and are generally located in rural areas. These sites will be referred to individually as hazardous sites A through E. The landfill site is presently receiving non-hazardous industrial and municipal waste and is situated in a more urban location.

Within each site, five locations were chosen which best reflected the environmental area to be sampled. Table 1 summarizes these locations and lists the features, such as leachate pools, buried drums, etc., that affected each.

SAMPLING AND ANALYSIS

Samples were collected for three consecutive 24 hour periods at each of the five locations within each hazardous waste site and at the landfill (Site A was sampled for five days). The method [8] consists of using portable battery powered samplers that draw 10-15 ml/min of air through a collection trap containing Tenax-GC adsorbent, for a total sample volume of 10-15 liters. The traps are capped, sealed in glass tubes, and transported back to the laboratory for analysis after collection.

The sample traps are thermally desorbed at 250°C into a 10 ml polished 316 SS cylinder maintained at −80°C (vacuum distilled 30 min; then purged with He, 40 ml at ATP). The concentrated sample is then analyzed twice. First, a 2 ml aliquot of sample at 20 psia is injected into a Varian 3700 gas chromatograph equipped with an SP 2100 quartz capillary column and parallel FI/EC detectors. Cryofocusing (−195°C) is used to concentrate the organics injected at the head of the column. The second analysis is performed on a Varian Mat-44 GC/Mass Spectrometer equipped with a similar capillary column and injection technique. This analysis allows back-up qualitative identification of target compounds and additional identification of other collected species present at or above approximately 0.05 ppbv. A typical chromatogram with target and non-target compounds identified is shown in Figure 1.

RESULTS

Average concentration data for the 26 VOC's quantified in this study are presented in Tables 2A through 2F. In the geometric mean calculations, the GC detection limit of 0.01 ppbv was substituted for zero concentrations when the compound was not detected. Benzene, toluene, and the xylenes were consistently detected in every sample,

TABLE 1. FEATURES FOUND AT SIX SAMPLING SITES

Location Inside Site	Hazardous Sites A	B	C	D	E	Landfill LF
	Off	BS	On	On	On	On
1	R	R			SD	Vent
	LP					
2	Off	On	On	On	On	On
	R		LP		Drum	
3	BS	On	BS	BS	On	BS
	LP	LP		LP		LP
4	On	Off	BS	BS	On	BS
5	Off	Off	Off	Off	Off	Off
	LP					Ind.

Feature Codes
LP Leachate Pools
R Proximity to Residences
BS Boardering Site
On On Site
Off Offsite
Drum Drums Exposed
Vents Vents
SD Soil Discolorations
Ind. Potential Industrial Input

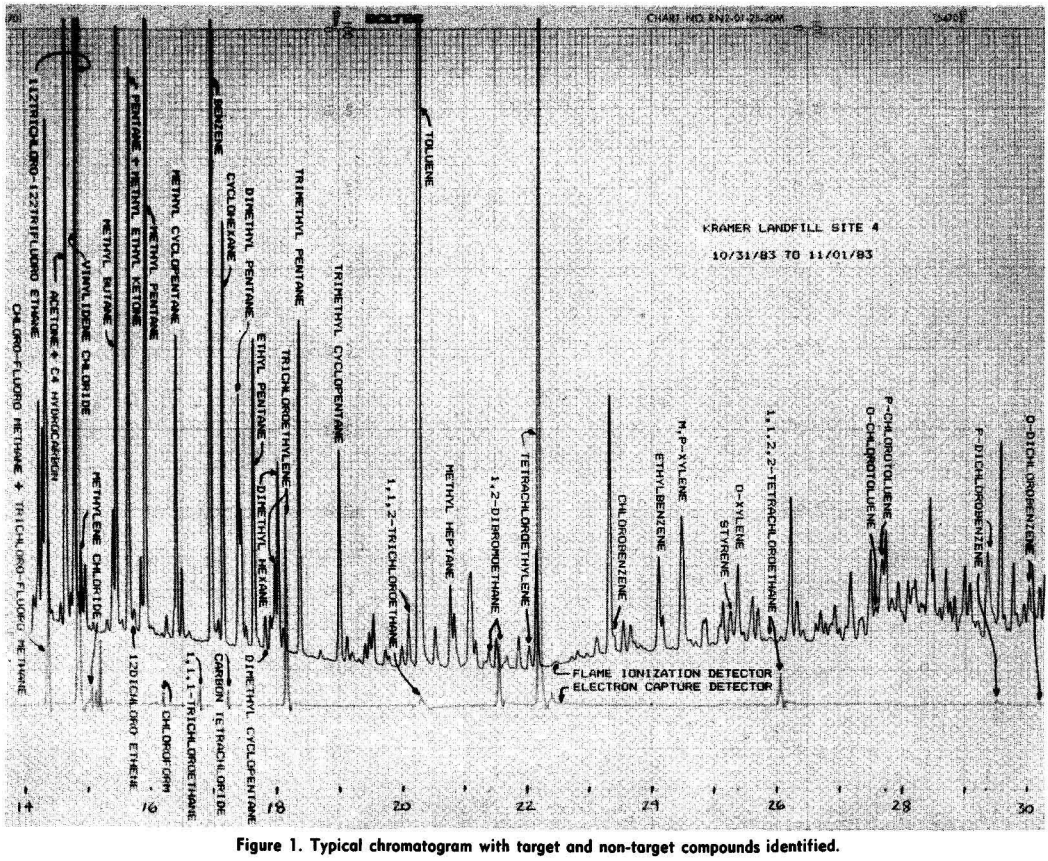

Figure 1. Typical chromatogram with target and non-target compounds identified.

TABLE 2A. SITE CONCENTRATION AVERAGES. HAZARDOUS WASTE SITE A. 24 SAMPLES

	Arth Mean PPBV	*Geom Mean PPBV	Non-Zero Values	Max Value PPBV
Vinylidene Chloride	0	0.01	0	0
Methylene Chloride	0.09	0.01	4	3
Chloroprene	0	0.01	0	0
Chloroform	0.33	0.03	12	5.23
1-2 Dichloroethane	0.01	0.01	1	0.35
1-1-1 Trichloroethane	0.38	0.1	30	4.49
Benzene	4.98	2.79	47	22.03
Carbon Tetrachloride	0.06	0.03	25	0.41
Trichloroethylene	0.39	0.19	38	1.66
Dioxane	0	0.01	0	0
1-1-2 Trichloroethane	0.02	0.01	6	0.27
Toluene	42.09	19.59	47	300.38
1-2 Dibromoethane	0.25	0.05	22	1.38
Tetrachloroethylene	0.92	0.53	45	7.84
Chlorobenzene	0.53	0.21	46	4.07
Ethylbenzene	3.56	1.71	47	28.91
M&P Xylene	9.95	4.35	47	84.91
Styrene	0.62	0.14	34	3.68
O Xylene	3.09	1.19	45	20.51
1-1-2-2 Tetrachloroethane	0.24	0.05	27	3.54
O-Chlorotoluene	0.4	0.18	44	2.02
P-Chlorotoluene	0.71	0.33	44	3.28
P-Dichlorobenzene	0.24	0.12	45	1.21
O-Dichlorobenzene	0.35	0.15	45	2.59
Nitrobenzene	1.38	0.29	38	14.48
Naphthalene	0.88	0.34	42	5.19

NJIT Air Pollution Research Laboratory

* Detection Limit of 0.01 Substituted for Zero Concentrations.

TABLE 2B. SITE CONCENTRATION AVERAGES. HAZARDOUS WASTE SITE B. 15 SAMPLES

	Arth Mean PPBV	*Geom Mean PPBV	Non-Zero Values	Max Value PPBV
Vinylidene Chloride	0.39	0.01	1	7.45
Methylene Chloride	0.49	0.01	1	9.4
Chloroprene	0	0.01	0	0
Chloroform	0.64	0.31	16	3.37
1-2 Dichloroethane	0	0.01	0	0
1-1-1 Trichloroethane	0.51	0.36	19	1.84
Benzene	2.55	1.83	19	7.7
Carbon Tetrachloride	0.12	0.06	17	0.6
Trichloroethylene	0.36	0.24	19	2.05
Dioxane	0	0.01	0	0
1-1-2 Trichloroethane	0.02	0.01	2	0.23
Toluene	11.52	7.44	19	37.99
1-2 Dibromoethane	0.25	0.03	7	3.08
Tetrachloroethylene	1.03	0.6	19	6.81
Chlorobenzene	0.09	0.05	18	0.45
Ethylbenzene	0.78	0.52	19	3.15
M&P Xylene	2.18	1.5	19	8.55
Styrene	0.27	0.08	13	1.88
O Xylene	0.93	0.59	19	2.65
1-1-2-2 Tetrachloroethane	0.05	0.02	5	0.44
O-Chlorotoluene	0.06	0.02	15	0.48
P-Chlorotoluene	0.06	0.02	15	0.72
P-Dichlorobenzene	0.1	0.03	18	0.77
O-Dichlorobenzene	0.11	0.04	18	0.87
Nitrobenzene	0.23	0.15	18	0.69
Naphthalene	0.2	0.12	19	0.56

NJIT Air Pollution Research Laboratory

* Detection Limit of 0.01 Substituted for Zero Concentrations.

TABLE 2C. SITE CONCENTRATION AVERAGES. HAZARDOUS WASTE SITE C. 14 SAMPLES

	Arth Mean PPBV	*Geom Mean PPBV	Non-Zero Values	Max Value PPBV
Vinylidene Chloride	36.44	19.08	19	96.69
Methylene Chloride	11.34	6.64	20	53.78
Chloroprene	0.01	0	1	0.22
Chloroform	0.91	0.17	14	6
1-2 Dichloroethane	0.28	0.02	2	5.15
1-1-1 Trichloroethane	3.04	1.66	20	18.97
Benzene	7.66	5.33	20	26.12
Carbon Tetrachloride	0.1	0.05	19	0.59
Trichloroethylene	2.86	0.95	20	19.95
Dioxane	0.01	0	1	0.17
1-1-2 Trichloroethane	1.26	0.27	16	6.91
Toluene	51.91	27.71	20	273.81
1-2 Dibromoethane	0.36	0.02	10	6.71
Tetrachloroethylene	2.03	1.08	20	8.51
Chlorobenzene	0.78	0.31	20	4.49
Ethylbenzene	3.91	1.87	20	17.37
M&P Xylene	7.72	3.26	20	32.95
Styrene	1.3	0.41	20	15.49
O Xylene	2.27	1.34	20	11.94
1-1-2-2 Tetrachloroethane	0.59	0.02	5	11.38
O-Chlorotoluene	0.43	0.06	10	5.34
P-Chlorotoluene	0.39	0.07	10	1.7
P-Dichlorobenzene	0.51	0.22	20	4.19
O-Dichlorobenzene	0.77	0.23	20	8.4
Nitrobenzene	0.48	0.09	14	4.7
Naphthalene	0.27	0.13	19	1.99

NJIT Air Pollution Research Laboratory

* Detection Limit of 0.01 Substituted for Zero Concentrations.

TABLE 2E. SITE CONCENTRATION AVERAGES. HAZARDOUS WASTE SITE E. 14 SAMPLES

	Arth Mean PPBV	*Geom Mean PPBV	Non-Zero Values	Max Value PPBV
Vinylidene Chloride	1.6	0.57	15	6.32
Methylene Chloride	1.14	0.39	14	4.51
Chloroprene	0	0.01	0	0
Chloroform	0.08	0.05	12	0.29
1-2 Dichloroethane	0	0.01	0	0
1-1-1 Trichloroethane	0.57	0.43	17	1.22
Benzene	0.6	0.51	18	2.01
Carbon Tetrachloride	0.03	0.02	13	0.1
Trichloroethylene	0.08	0.06	16	0.35
Dioxane	0	0.01	0	0
1-1-2 Trichloroethane	0.29	0.15	14	0.82
Toluene	3.28	1.84	18	9.67
1-2 Dibromoethane	0.05	0.03	11	0.28
Tetrachloroethylene	0.12	0.1	18	0.26
Chlorobenzene	0.09	0.05	15	0.53
Ethylbenzene	0.13	0.09	17	0.41
M&P Xylene	0.37	0.25	17	1.33
Styrene	0.13	0.08	14	0.33
O Xylene	0.15	0.1	17	0.43
1-1-2-2 Tetrachloroethane	0.01	0.01	1	0.26
O-Chlorotoluene	0.02	0.01	4	0.22
P-Chlorotoluene	0.04	0.02	4	0.55
P-Dichlorobenzene	0.04	0.02	7	0.38
O-Dichlorobenzene	0.06	0.02	7	0.69
Nitrobenzene	0.01	0.01	2	0.11
Naphthalene	0.1	0.06	18	0.63

NJIT Air Pollution Research Laboratory

* Detection Limit of 0.01 Substituted for Zero Concentrations.

with 111-trichloroethane, trichloroethylene, and tetrachloroethylene nearly always found.

The concentrations for the VOC varied considerably from site to site, as would be expected. For example, toluene ranged from an average 3.28 ppbv at hazardous site D to 51.91 ppbv at site C. At sites A and C individual sample concentrations of toluene exceeded 100 ppbv reaching as high as 300 ppbv at A. Within each site, there is significant

TABLE 2D. SITE CONCENTRATION AVERAGES. HAZARDOUS WASTE SITE D. 15 SAMPLES

	Arth Mean PPBV	*Geom Mean PPBV	Non-Zero Values	Max Value PPBV
Vinylidene Chloride	3.46	0.87	16	14.75
Methylene Chloride	0.9	0.11	10	4.85
Chloroprene	0	0	0	0
Chloroform	0.21	0.13	18	0.76
1-2 Dichloroethane	0.03	0	1	0.59
1-1-1 Trichloroethane	0.84	0.49	19	2.89
Benzene	1.33	1.16	21	5.55
Carbon Tetrachloride	0.04	0.03	17	0.19
Trichloroethylene	0.21	0.12	20	1.88
Dioxane	0	0	0	0
1-1-2 Trichloroethane	0.32	0.14	15	0.94
Toluene	15.16	10.79	21	40.81
1-2 Dibromoethane	0.06	0.03	13	0.28
Tetrachloroethylene	0.38	0.23	21	3.08
Chlorobenzene	0.32	0.11	16	1.5
Ethylbenzene	0.61	0.32	20	2.11
M&P Xylene	1.52	0.95	21	4.59
Styrene	0.11	0.04	9	0.81
O Xylene	0.42	0.26	20	1.15
1-1-2-2 Tetrachloroethane	0.02	0.02	5	0.17
O-Chlorotoluene	0.05	0.02	3	0.84
P-Chlorotoluene	0.07	0.02	3	0.83
P-Dichlorobenzene	0.08	0.03	8	0.45
O-Dichlorobenzene	0.11	0.03	8	0.7
Nitrobenzene	0.12	0.02	4	1.41
Naphthalene	0.11	0.04	10	0.73

NJIT Air Pollution Research Laboratory

* Detection Limit of 0.01 Substituted for Zero Concentrations.

TABLE 2F. SITE CONCENTRATION AVERAGES. LANDFILL LF. 15 SAMPLES

	Arth Mean PPBV	*Geom Mean PPBV	Non-Zero Values	Max Value PPBV
Vinylidene Chloride	2.61	0.96	14	6.56
Methylene Chloride	1.58	0.26	11	6.36
Chloroprene	0	0.01	0	0
Chloroform	0.12	0.11	17	0.4
1-2 Dichloroethane	0	0.01	0	0
1-1-1 Trichloroethane	1.29	0.47	15	7.15
Benzene	3.33	2.63	17	6.72
Carbon Tetrachloride	0.02	0.02	10	0.08
Trichloroethylene	0.34	0.18	17	1.24
Dioxane	0	0.01	0	0
1-1-2 Trichloroethane	0.11	0.04	8	0.3
Toluene	27.79	18.35	17	74.81
1-2 Dibromoethane	0.02	0.01	4	0.23
Tetrachloroethylene	1.53	0.59	17	6.53
Chlorobenzene	0.15	0.1	16	0.48
Ethylbenzene	1.53	0.89	17	5.02
M&P Xylene	3.35	2.21	17	10.41
Styrene	0.41	0.27	17	1.52
O Xylene	0.9	0.63	17	2.82
1-1-2-2 Tetrachloroethane	0.01	0.01	1	0.19
O-Chlorotoluene	0.01	0.01	4	0.12
P-Chlorotoluene	0.03	0.02	4	0.38
P-Dichlorobenzene	0.06	0.03	7	0.44
O-Dichlorobenzene	0.06	0.03	7	0.53
Nitrobenzene	0	0.01	0	0
Naphthalene	0.08	0.05	14	0.31

NJIT Air Pollution Research Laboratory

* Detection Limit of 0.01 Substituted for Zero Concentrations.

fluctuation from one location to another (as well as on different sampling days). Table 3 shows this for site C. This table also shows a pair of duplicate samples taken side by side at one location. The overall precision of this series of analysis is shown in Table 4. These data on precision are very similar to results from previous studies such as the ATEOS project in New Jersey [9, 10] and those of Fehsenfeld *et al.* [11].

It is interesting to compare average levels from the six sites investigated with urban and rural levels obtained from other work. Table 5 lists some ambient VOC concentration data from 3 urban sites and 3 rural areas in the United States. Notice that, for many of the target compounds, the levels found at the hazardous waste sites (except E) are generally much higher than the reported levels at rural locations. Sites A, B, C, and D all have toluene concentrations between 10 and 50 ppbv, as compared to less than 1 ppbv at rural locations. These levels are also higher than the three urban sites listed. The average levels at the urban landfill, LF, are nearly 30 ppbv, also higher in comparison with the data in Table 5. It would appear from this comparison that sites A, B, C, D, and the landfill are emitting toluene into the ambient atmosphere but that site E is not.

The levels of chlorinated target VOC's at site C are much higher than at the other sites. For example, vinylidene chloride had an average concentration of 36.44 ppbv. Methylene chloride was 11.34. These levels are extremely high when examined with the comparison data in Table 5. Other chlorinated solvents show similar increases at site C, but not nearly as large as vinylidene chloride and methylene chloride. Figures 2a and 1b show these facts, and it would appear from this comparison that site C has a much greater rate of emission for these chlorinated solvents than the other sites.

Variation in concentration of the VOC due to specific site characteristics and weather can be seen in a plot of concentration for a particular VOC with respect to day and location. Sampling location 1 at the landfill had a vent nearby and location 3 was near a leachate pool. A snow storm began at midday on day 2 and lasted until the next morning. The temperature was 25-30°F for days 1 and 2 and 30-40°F for the last day. Figures 3a, b, and c show the possible effect of the snow storm and temperature drop on trichloroethylene, tetrachloroethylene, and carbon tetrachloride levels. Figures 3d, e and f show larger concentrations on day 2 for site 1, near the vent; for aromatics. This indicates that these aromatic compounds could be emitted from this vent and that other compounds are not. For napthalene, the concentration is highest near the leachate pool on the first day and it drops off rapidly, thus indicating that the blanket of snow may have reduced the effluent from this pool. Levels of toluene at locations 1 and 2 are over ten times the average level found in the ATEOS [5] sampling at Newark, NJ. Since these two sampling locations are near homes, this may be of concern.

At hazardous site C, the first two days of sampling were sunny, followed on the third day by clouds and then rain. Sampling location 2 was near a leachate pool. Figures 4a, b, and c show higher levels for toluene, trichloroethylene,

TABLE 4. PRECISION ESTIMATES ON A SITE BASIS

Site	Number of Duplicates	Number of Compounds	% Error ±	X^a PPBV
A	23	17	42.0	4.00
B	4	13	43.0	1.42
C	6	10	25.0	12.7
D	6	10	40.0	2.90
E	4	10	39.0	0.78
LF	2	10	36.0	4.18

Note: While concentrations of some compounds may be high, bringing the X^a values up, many compounds are present in the 10 to 100 PPTv range and a precision of ± 50% at these levels is very difficult.

TABLE 3. SITE SUMMARY. HAZARDOUS WASTE SITE C. SAMPLING LOCATION 1

	Day 1 Right	Day 1 Left	Day 2 Right	Day 3 Right	Arth Mean	Geom Mean
Vinylidene Chloride	*2.01	*6.58	*94.61	12.4	28.9	11.16
Methylene Chloride	*3.13	*1.03	*14.79	2.16	5.28	3.19
Chloroprene	0	0	0	0	0	0.01
Chloroform	0	0	0	0	0	0.01
1-2 Dichloroethane	0	0	0	0	0	0.01
1-1-1 Trichloroethane	0.67	*1.63	2.11	0.65	1.27	1.11
Benzene	*1.95	*3.17	*6.21	*1.61	3.24	2.8
Carbon Tetrachloride	0.01	0.05	*0.29	0.01	0.09	0.03
Trichloroethylene	*0.25	*1.22	1.26	*0.44	0.79	0.64
Dioxane	0	0	0	0	0	0.01
1-1-2 Trichloroethane	0.1	0	0	0	0.02	0.02
Toluene	*6.07	*11.94	*49.31	*7.2	18.63	12.67
1-2 Dibromoethane	0.01	0	0	0	0	0.01
Tetrachloroethylene	*0.32	*0.59	*1.57	*0.29	0.69	0.54
Chlorobenzene	0.04	*0.26	*0.52	*0.03	0.21	0.11
Ethylbenzene	*0.39	*2.72	*7.19	*0.28	2.65	1.21
M&P Xylene	*0.78	*5.39	*10.03	*0.65	4.21	2.29
Styrene	*0.08	*0.95	*1.27	*0.06	0.59	0.28
O Xylene	*0.33	*1.97	*3.55	*0.31	1.54	0.92
1-1-2-2 Tetrachloroethane	0	0	0	0	0	0.01
O-Chlorotoluene	0	0	0	0	0	0.01
P-Chlorotoluene	0	0	0	0	0	0.01
P-Dichlorobenzene	*0.17	*0.67	*0.39	*0.03	0.31	0.19
O-Dichlorobenzene	*0.08	*0.62	*0.39	*0.04	0.28	0.17
Nitrobenzene	0.07	*0.27	0.14	0.03	0.13	0.09
Naphthalene	*0.3	*0.27	0.42	*0.04	0.26	0.19

Concentrations in Parts Per Billion

'*'-Compound Identified on GC/MS

NJIT Air Pollution Research Laboratory

TABLE 5. COMPARISON VOC CONCENTRATION DATA

	Urban Areas		
	*Newark, NJ 1982 (5)	Houston, Texas 1981 (2)	Staten Island NY 1981 (2)
Vinylidene Chloride	0.17	0.25	0
Methylene Chloride	0.54	0.57	1.61
Chloroform	0.17	0.42	0.15
12-Dichloroethane	0.01	1.52	0.26
111-Trichloroethane	N/A	0.35	0.47
Benzene	2.52	5.78	4.2
Carbon Tetrachloride	0.02	0.40	0.31
Trichloroethylene	0.59	0.14	0.17
112-Trichloroethane	0.05	0.03	0.01
Toluene	4.20	N/A	N/A
12-Dibromoethane	0.01	0.06	0.02
Tetrachloroethylene	0.42	0.40	0.29
Ethylbenzene	0.47	N/A	N/A
M/P-Xylene	1.72	N/A	N/A
O-Xylene	0.41	N/A	N/A
	Rural Areas		
	Batsto, NJ 1979 (10)	Smokey Mountains, NC 1981 (11)	Talledga Forest, AL 1981 (12)
Benzene	0.52	0.89	0.40
Carbon Tetrachloride	0	N/A	N/A
Trichloroethylene	0.08	N/A	N/A
Toluene	0.56	0.96	0.40
Tetrachloroethylene	0.04	N/A	0.20
M/P-Xylene	0.25	N/A	N/A
O-Xylene	0.41	N/A	N/A

Concentrations in PPBv
N/A — Not Analyzed
* Geometric Mean

and tetrachloroethylene at location 2 than at any other location, possibly indicating their presence and emission from the pool. The chlorinated solvents drop in concentration on day 3, probably because of the rain.

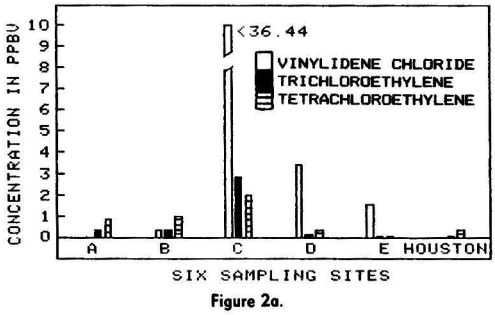

Figure 2a.

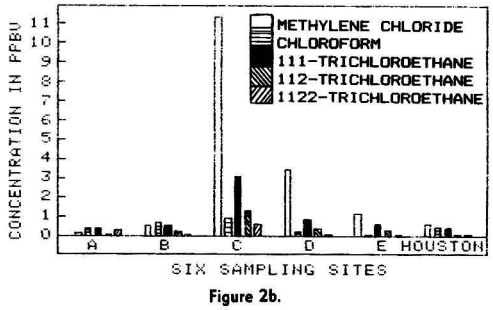

Figure 2b.

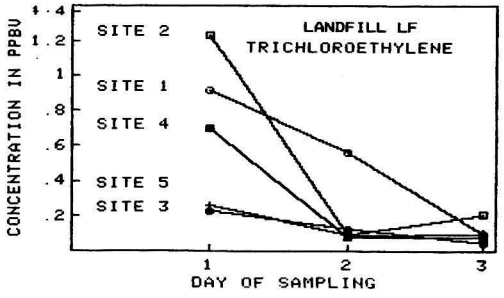

Figure 3a.

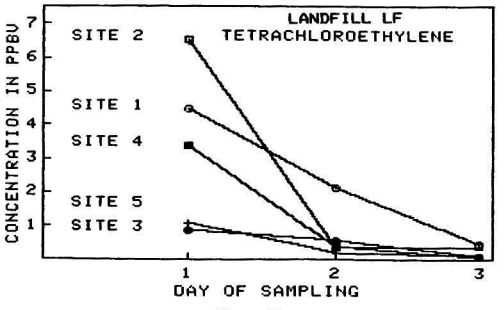

Figure 3b.

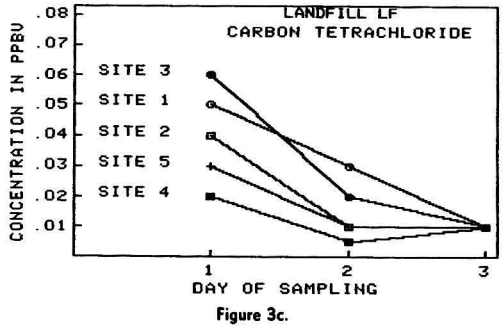

Figure 3c.

Hazardous site B had clear sunny weather for the first two days, followed by rain. Location 3 was near a leachate pool. Figure 5a shows that the levels for benzene are higher here than for the other locations, again indicating the possible presence of this aromatic in the pool. Figures 5b through 5e show higher concentrations on day 1, with a drop off on later days. This could be due to changing weather and the rainfall.

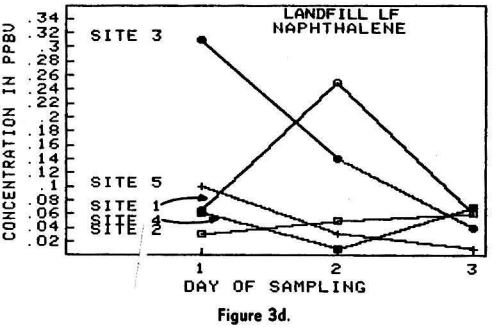

Figure 3d.

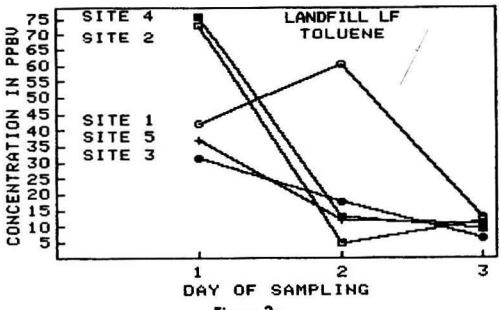

Figure 3e.

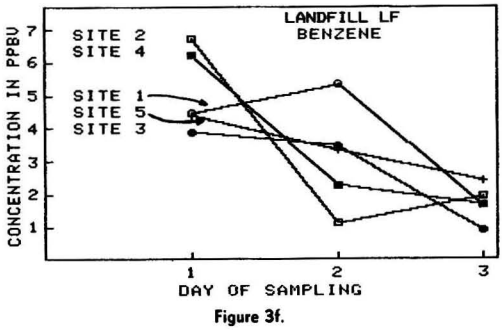

Figure 3f.

Hazardous site A had leachate pools near locations 1, 3, and 5, where one can observe that aromatic species such as benzene, toluene, and xylene have a very similar concentration pattern (Figures 6a, b, and c). This indicates they are, most likely, all from the same source, possibly the leachate pools. Their concentrations would vary directly with the amount of impact the pools have on the samplers,

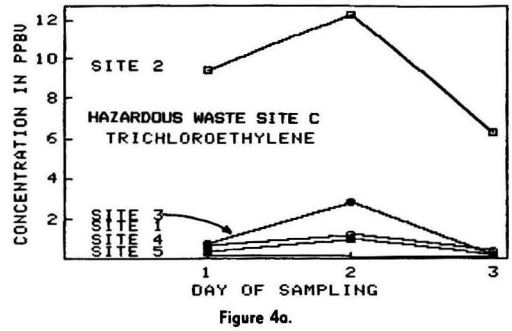

Figure 4a.

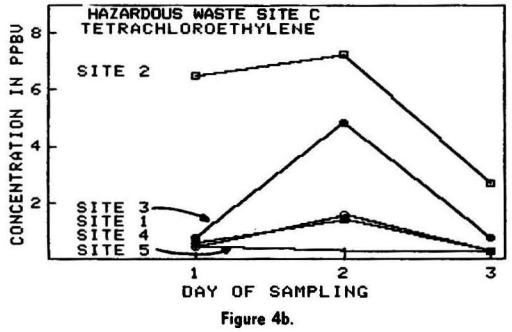

Figure 4b.

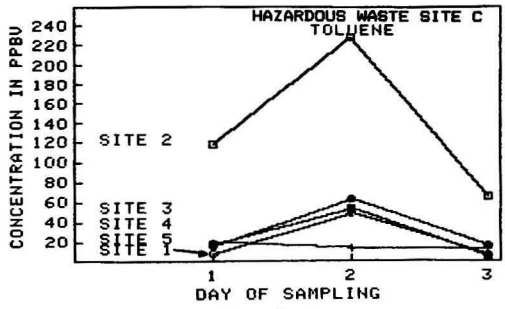

Figure 4c.

which, in turn, depends on such variables as wind directions, snow covering, etc. The temperature also seems to have an effect, as it varied from low on day 1 (low 50, high 70) to high on day 4 (low 64, high 90) and then dropped off to about 70°F (avg.) on day five. The concentrations for benzene, toluene, and xylene do reach a low point on day 2 and rise to their maximum on day 4, dropping off on day 5

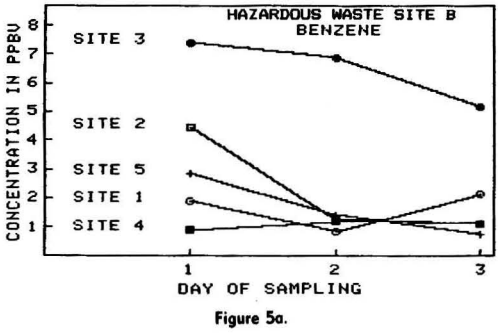

Figure 5a.

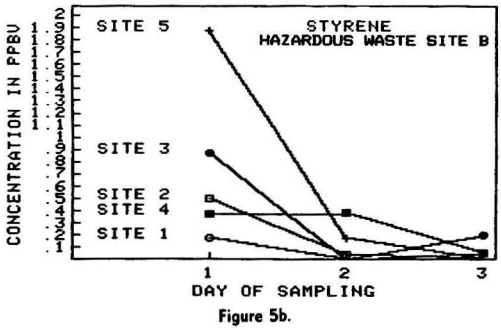

Figure 5b.

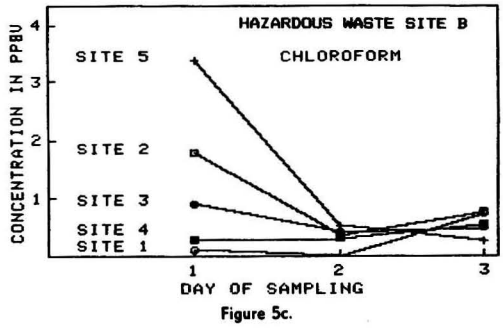

Figure 5c.

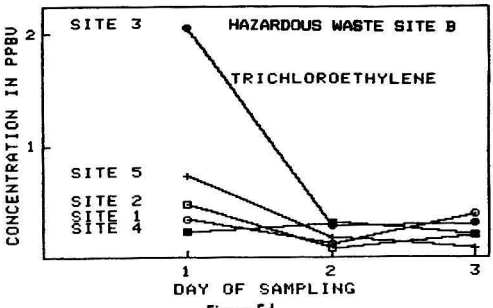

Figure 5d.

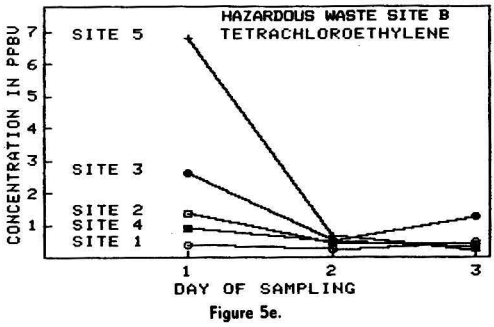

Figure 5e.

at leachate pool locations 1 and 3. One could speculate that the sampler at location 5 did not receive as much input from its surroundings due to possible local wind movements.

For some compounds, such as tetrachloroethylene at site D (Figure 7), the concentration varied very little from day to day, location to location. The relatively low values similar to those of ambient air indicate that this site is not a source of VOC.

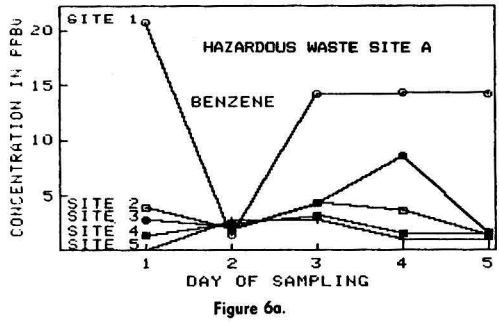

Figure 6a.

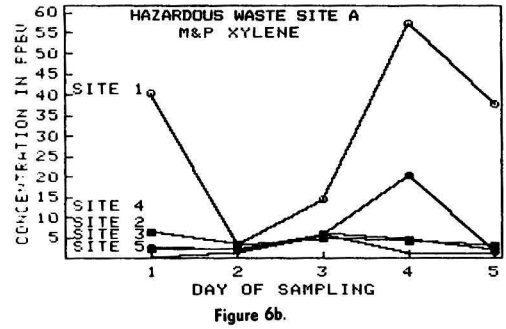

Figure 6b.

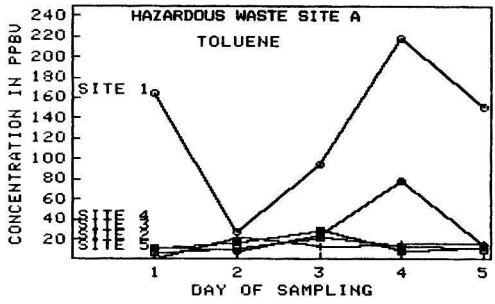

Figure 6c.

Figure 8 shows a plot of site averaged concentration for three aromatics at the landfill, LF. The fluctuation of concentrations is very similar, giving further evidence that these VOC are being evolved from the site. At hazardous site D, xylene and toluene fluctuate a great deal while the levels of benzene remain constant, indicating that, perhaps, benzene is not emitted from site D (Figure 9).

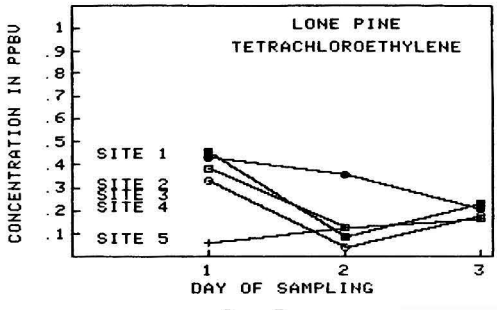

Figure 7.

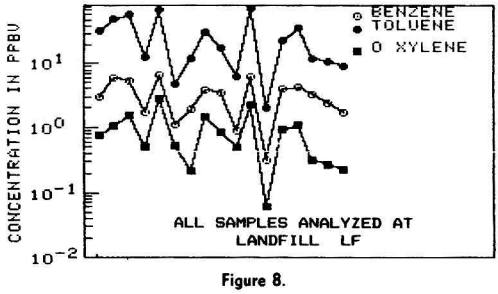

Figure 8.

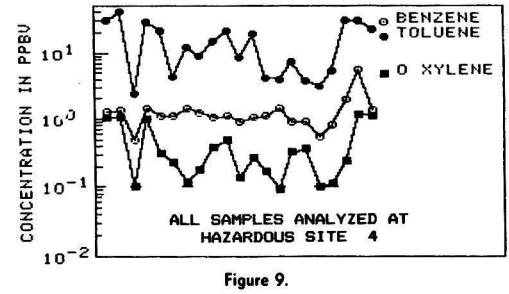

Figure 9.

QUALITY CONTROL AND ASSURANCE

A program of quality control and assurance is applied to all sampling and analysis of VOC in these laboratories. The Tenax traps are carefully assembled to insure that each has the same amount of material (0.5g) and that, once packed, the pressure drop for each is close to 2 in. H_2O for 20 ml/min flow. Traps are conditioned by passing 10 ml/min of clean N_2 gas through the traps while heating to 300°C for 48 hours. After conditioning, one trap from each batch is analyzed as a sample with typical sample volumes and instrument calibration factors used to quantify the impurities. A second measure is when a set of traps is sent to the field; several traps are not used for sample collection, but as controls. These control traps routinely show less than 0.1 ppbv for the pollutants, but occasionally show significant contamination for 1 or 2 specific chemicals as summarized in Table 6.

One control trap from site D, for example, had an estimated toluene concentration of 27 ppbv. This level is higher than many detected levels in the samples and caused significant concern. Trap history examination showed that a probable explanation for such high levels of contamination may involve traps that had been previously used to sample at sites where the levels were very high. In the example cited, the control trap found to contain 27 ppbv of toluene had been previously used to sample site A where the level was 60.4 ppbv. At such a high concentration, perhaps the Tenax pore structure is heavily loaded with the toluene, and normal desorption and conditioning does not fully remove all the compound from deep within the pore structure. It then slowly effuses out and builds up a static-sealed storage condition. The Toluene could then be detected after the trap is redesorbed as a control. It is felt that the other possibility of the traps becoming contaminated while sitting idle due to atmospheric exposure, through leaking seals, etc., is unlikely. Such a process should show impurities of all the atmospheric contaminants, while only one or two contaminants are actually observed.

Specific analysis of trap history, along with observation of unusually high levels for each trap used throughout this campaign (all traps were new at campaign start up), showed no likely errors in the campaign measurements due to this effect. A procedure involving analyzing the cleaned trap which in prior analysis showed the highest concentration, sealing it for seven days, and then reanalyzing it, was also initiated midway through the project. One other possible solution would be vacuum conditioning at the desorption temperature to increase the diffusion and volatilization rates of contaminant removal, where a small purge gas flow would effect transfer of the volatiles out of the traps. Further studies will have to be done to gain a better understanding of the efficiency of such vacuum conditioning.

Contamination could also be partly responsible for the level of precision exhibited in duplicate samples. Since sample pumps are carefully calibrated and yield errors in flow of only 2.3% to 6.4% with a mean of 3.6%, this contribution to the imprecision is considered small.

TABLE 6

Arithmetic means of laboratory and field blank data (ppbv)

Compound	Lab Blanks	Max.[a]	Field Blanks	Max.[b]
	(n = 12)		(n = 14)	
Vinylidene Chloride	0	0	1.0	7.78
Methylene Chloride	0	0	0.51	2.54
Chloroprene	0	0	0	0
Chloroform	0	0	0.16	0.95
1,2-Dichloroethane	0	0	0	0
1,1,1-Trichloroethane	0	0	0.27	1.48
Benzene	0.18	0.70	0.44	0.99
Carbon Tetrachloride	0	0	0	0
Trichloroethylene	0.01	0.06	0.03	0.13
Dioxane	0	0	0	0
1,1,2-Trichloroethane	0.05	0.34	0.05	0.36
Toluene	0.17	0.54	3.66	27.0
1,2-Dibromoethane	0	0	0.01	0.11
Tetrachloroethylene	0.02	0.07	0.06	0.20
Chlorobenzene	0	0	0	0
Ethylbenzene	0.02	0.07	0.04	0.16
M,P-Xylene	0.04	0.11	0.15	0.48
Styrene	0	0	0.01	0.04
O-Xylene	0.01	0.06	0.06	0.29
1,1,2,2-Tetrachloroethane	0	0	0.01	0.06
O-Chlorotoluene	0	0	0	0
P-Chlorotoluene	0	0	0	0
P-Dichlorobenzene	0	0	0	0
O-Dichlorobenzene	0	0	0	0
Nitrobenzene	0.04	0.53	0	0
Naphthalene	0.07	0.32	0.01	0.05

a — Maximum concentration found in laboratory blanks.
b — Maximum concentration found in field blanks.

ADDITIONAL MASS SPECTOMETER IDENTIFICATION

More than 95% of all samples were analyzed on a Varian Mat-44 GC/MS to validate identification of the 26 target VOC's as well as to supply additional identification of other VOC's collected. The identification of these non-target compounds is performed manually by comparing the spectra obtained with reference spectra [*14*]. Since the mass spectrometer is not as sensitive as that of an electron capture detector, electronegative species would frequently go undetected on the MS while being observed during the GC analysis. For non-target hydrocarbons, the MS detection limit is approximately 0.1 ppbv, and operated at somewhat less sensitivity, site A samples. The Tenax collection method and the mass spectrometer operation allows identification from light C_3 hydrocarbons and halocarbons up to compounds such as biphenyl. Generally, beyond substituted C_8 aliphatic hydrocarbons, it is very difficult to distinguish between isomers, so specific isomers were not always elucidated. It should also be pointed out that concentrations of the less volatile compounds such as nitrobenzene must be significant or they would not be detected.

Table 7 lists non-target compounds that were detected at each site and their relative occurrence. Sites B and C had a great variety of halocarbon compounds. Site C had the greatest variety of materials, although most were chained,

TABLE 7.
NON-TARGET VOC MASS SPECTROMETER IDENTIFICATIONS

	B	C	D	E	LF	
Chloro Methane	2	1		2	1	
Bromo Methane	1					
Iodo Methane	2					*
Chloro-fluoro Methane		1				*
Chloro-bromo Methane		1				*
Dichloro-bromo Methane	1	1				*
Dichloro-difluoro Methane	1					*
Dibromo-chloro Methane	2	1				*
Dibromo-difluoro Methane		4	3	3	3	*
Trichloro-fluoro Methane	2	4	4	4	3	+
Difluoro-chloro-bromo Methane		1				*
Fluoro-dichloro-bromo Methane		1				*
Chloro Ethane	2					
111-Trichloro-222-trifluoro-ethane	2					*

(Continued on Next Page)

TABLE 7. *(Continued)*

112-Trichloro-122-trifluoro-ethane		2	1	1	2	
12-Dichloro Ethylene	4	4		4		
Dichloro Propane	2					*
Acetone	4	4	4	4	4	+
Methyl Isobutyl Ketone				1		
Methyl Ethyl Ketone	1	3	1	1	1	
Tetrahydrofuran	1	1				*
Trimethyl Benzene	4	3	2	3	2	
Methyl Ethyl Benzene		2	1	2		
Dimethyl Ethyl Benzene			2		2	
Methyl N-Propyl Benzene					3	
Methyl Tertbutyl Benzene				1		*
Isopentyl Methyl Cyclohexane			1			*
Chloro Ethyl Benzene		1				*
Methyl Naphthalene		1				*
Biphenyl	1	2	1	3	1	*
Methyl biphenyl		2				*
Benzaldehyde	4	1	1	3	4	
Dibenzofuran	1	3	1	1	2	*+
Butene	2	3	3	4	4	
Butane			4		4	
Dimethyl Propene	2					*
Methyl Butene	1	2	1	1	3	
Methyl Butane		2	3	4	4	
Dimethyl Butane		2				
Pentene		2	1	3	1	
Pentane		2	2	3		
Hexane			2	4		
Methyl Pentane	4	4	3	4	4	
Dimethyl Pentene			3	3	2	
Methyl Cyclopentane	3	4	2	2	4	
Dimethyl Pentane		4	3	4	4	
Ethyl Pentane		4	3	4	4	
Dimethyl Cyclopentane	1	3	2	1		
Trimethyl Cyclopentane		4				
Trimethyl Pentene		3			1	
Trimethyl Pentane		2	1			
Methyl Hexane	2	1				
Dimethyl Hexane	2	3	4		4	
Cyclohexane	4	4	4	4	4	+
Methyl Cyclohexane	3	1	1			
Dimethyl Cyclohexane	1	4	2		1	
Methyl Heptane	1	3	3	3	2	
Trimethul Hexene	1	1				
Dimethyl Heptane	1	1	2	1	2	
Dimethyl Ethyl Pentane		1				
Octane		2				
Nonane		1				
Methyl Decane		1				
Methyl Ethyl Cyclohexane		1				
Diethyl Cyclohexane		1				
Isopropyl Cyclohexane		1				
SEC Butyl Cyclohexane			1			
Butadiol		1				*
Isopropyl Alcohol		2	2	1	3	*

Code	% Times Identified at Site
4	75%-100%
3	50%-75%
2	25%-50%
1	1%-25%
No Code	Not Identified

* Not identified in previous NJIT ambient sampling studies.
\+ Higher apparent concentration than ambient levels.

branched, or cyclic hydrocarbons. With the exception of site A, site C had the highest overall levels of target VOC. It is not surprising that more compounds would be detected, because their relative levels would be higher and more compounds would be present above the MS detection limit. Site A should have had the greatest number of non-target compounds identified, but the operating sensitivity of the MS instrument was low during this analysis. Most of the compounds in Table 7 have been identified during previous sampling of ambient air [*10*]. Some compounds, such as cyclohexane, appeared to have much higher concentrations than the levels observed before [*9, 10*]. It is also interesting to note that the apparent concentration of cyclohexane at all sites paralleled that of benzene, with the possibility that it is a decomposition product or a benzene precursor in highly contaminated ground and leachate pools.

CONCLUSIONS

First, it is clear that VOC levels at hazardous sites and landfills vary greatly from site to site and at locations within each site. Indeed, such variation is exhibited in any ambient sampling that takes place. However, the overall levels were higher than that found in urban environments for some specific VOC's, and it seems likely that the high levels are due to the sites themselves. At site A, for example, average levels of toluene are on the order of 10 times that normally found at urban locations.

Second, this study has shown that the effects of site characteristics and meteorological events on the levels of VOC in the ambient air are not very clear. Although samples did show higher levels of some VOC near leachate pools or vents, no real trends were evident. Understanding how such vents, leachate pools, and local weather effect the emission of VOC would require a more concentrated sampling schedule at one place with complete records of relevant meteorological data, in addition to modelling.

Finally, the problems associated with the proper quality assurance of Tenax must be controlled with rigorous cleaning and maintenance procedures and perhaps more studies into the pore effects involved.

LITERATURE CITED

1. Harkov, R., R. Katz, J. Bozzelli, B. Kebbekus, "Toxic and Carcinogenic Air Contaminants in New Jersey — Volatile Organic Substances," *Proceedings, Toxic Air Contaminants, VIP—I*, Air Pollution Control Association, Pittsburgh (1981).
2. Singh, H. B., L. J. Salas, A. J. Smith, and H. Shigeishi, "Measurements of Some Potentially Hazardous Organic Chemicals in Urban Atmospheres," *Atmos. Environ.* **15,** 601 (1981).
3. Lillian, D., H. B. Singh, A. Appleby, L. Lobban, R. Arnts, R. Gumpert, R. Hague, J. Tosney, Jr., M. Kazzazis, D. Antell, and B. Scott Hansen,, "Atmospheric Fates of Halogenated Compounds," *Environ. Sci. Technol.* **9,** 1042 (1979).
4. Pellizzari, E. D., M. D. Erickson, R. A. Zweidinger, "Formulation of a Preliminary Assessment of Halogenated Organic Compounds in Man and Environmental Media," EPA-560/13-79-010, U.S. Environmental Protection Agency, 1979.
5. Harkov, R., B. Kebbekus, J. Bozzelli, and P. Lioy, "Measurements of Selected Volatile Organic Compounds at Three Locations in New Jersey during the Summer Season," *JAPCA* **33,** 1177 (1983).
6. Pellizzari, E., "Analysis for Organic Vapor Emissions Near Industrial and Chemical Waste Disposal Sites" *Environ. Sci. and Technol.* **16,** 781 (1982).
7. Hazardous Waste Sites — National Priorities List, U.S. Environmental Protection Agency HW-7.1, 60 pp., August 1983.
8. Bozzelli, J. and B. Kebbekus, "Collection and Analysis of Selected Volatile Organic Compounds in Ambient Air," paper No. 82-65-2, *Proceedings of the 75th Annual Meeting,* Air Pollution Control Association, Pittsburgh, 1982.

9. Harkov, R., "Toxic Air Pollutants in New Jersey," N.J. Department of Environmental Protection, Trenton, 49 pp., 1983.
10. Bozzelli, J. W. and B. B. Kebbekus, "Volatile Organic Compounds in the Ambient Atmosphere of the New Jersey, New York Area, report No. R806-2710-10 to U.S. Environmental Protection Agency, Research Triangle Park, NC, 1980.
11. Roberts, R., F. C. Feshenfeld, P. C. Liu, and D. Bollinger, "Concentration Ratios of Organic Aromatics to Hydrocarbon Ratios and to Nitric Oxides in the Troposphere," *Atmospheric Environment* **18,** 2421-32 (1984).
12. Arnts, R. and S. Meeks, "Biogenic Hydrocarbon Contribution into Ambient Air of Selected Areas," *Atmos. Environment* **15,** 2173 (1981).
13. Holzer, G., "Collection and Analysis of Trace Organic Emissions from Natural Sources," *J. Chromatography* **142,** 755-64 (1977).
14. "Index of Mass Spectral Data," ASTM No. ADM 11 Phila., Penn. (1969).

Joseph Bozzelli is a professor and principal investigator, **John LaRegina** is a research associate, both are with the New Jersey Institute of Technology Air Pollution Research Laboratories, Chemical Engineering and Chemistry Department.

Ron Harkov is a project director in the Office of Science and Research and **Samuel Gianti, Jr.** is a project officer in the Hazardous Site Mitigation Administration with the New Jersey Department of Environmental Protection.

Modeling the Transport of 2,3,7,8-TCDD and Other Low Volatility Chemicals in Soils

A model has been developed to describe the transport of low volatility organic chemicals in a column of soil. The mathematical model calculates the rate of movement through the soil by solving the dynamic material and energy balances around the soil column. The model is used to make predictions on the transport of 2,3,7,8-tetrachlorodibenzo-p-dioxin (TCDD) at the Eglin Air Force Base Agent Orange biodegradation test plots. The model predicts a vertical movement of TCDD, buried in 1972, through the soil column. Soil column profile data confirm the vertical movement of TCDD.

Raymond A. Freeman and Jerry M. Schroy, Monsanto Co., 800 N. Lindbergh Blvd., St. Louis, Missouri 63167

BACKGROUND

The compound 2,3,7,8-tetrachlorodibenzo-p-dioxin (TCDD) has a very low vapor pressure (2.0×10^{-7} pascals at 25.0 C) [*1*] and a very low water solubility (7.96×10^{-9} g/liter at 22.0 C) [2]. Although the vapor pressure and water solubility of DDT and TCDD are not identical, they are similar. For comparison DDT has a vapor pressure of 1.9×10^{-5} pascals (20 C) and a water solubility of 1.2×10^{-6} g/liter at 20 C [3]. Thus, the environmental mobilty of TCDD should be qualitatively similar to DDT.

Several investigators have shown that DDT is mobile in the environment via vaporization. Guenzi and Beard [*4*] found that the presence of at least a monomolecular layer of water is needed for DDT vaporization to occur. Farmer et al. [*5*] found that DDT will volatilize from soil, and Hee et al. [*6*] found that DDT will volatilize from glass when applied as a film. Beall and Nash [7] demonstrated that DDT will volatilize from soils and can be absorbed from the air by soybean plants.

Freeman and Schroy [*8*] have reviewed the pesticide literature and found that other chemicals such as lindane, dieldrin, heptaclor, and trifluralin are also volatile. From the literature review, the following generalizations were made on the environmental mobility of chemicals with low vapor pressures ($< 10^{-4}$ pascals) and low water solubilities (<2 ppb by weight) such as DDT and TCDD:

1. A chemical with a low water solubility and a low vapor pressure can volatilize with rates that are important to the chemical's ultimate environmental fate.
2. Chemicals with low water solubilities will not migrate in soils at rates which are significant to their ultimate fate due to bulk water flow (rain, irrigation, floods, etc.).
3. Soil temperature variations will have a strong impact on the movement of a chemical in the soil.
4. Low volatility chemicals may bind strongly with dry soil. However, when a monomolecular layer of water is present the chemical can become more mobile.

Thus, TCDD should be mobile via vaporization in the environment. Nash and Beall [9] have demonstrated that TCDD is volatile both in laboratory microcosm and field plot experiments. Figure 1 presents the air concentrations of TCDD measured by Nash in the microcosm experiment.

Liberti et al., [*10*] gathered data on Seveso soil, using deep-tray tests, which showed TCDD losses from the subsurface layers after exposure to the sun. Liberti's explanation for the loss was due to free radical movement into the soil column. A more reasonable explanation is due to the transport of TCDD to the soil surface where it could be photochemically destroyed or vaporized.

Muir [*11*] found that 1,3,6,8-TCDD rapidly disappeared from field soil plots. After 131 days, 44 percent of the labelled ^{14}C-1,3,6,8-TCDD had disappeared from the soil column. The 1,3,6,8-TCDD was found in greatest amounts in the top 5 cm of soil. Trace amounts of 1,3,6,8-TCDD was found in the 5 to 10 cm increment and was attributed to contamination during sampling. Muir reported the half-

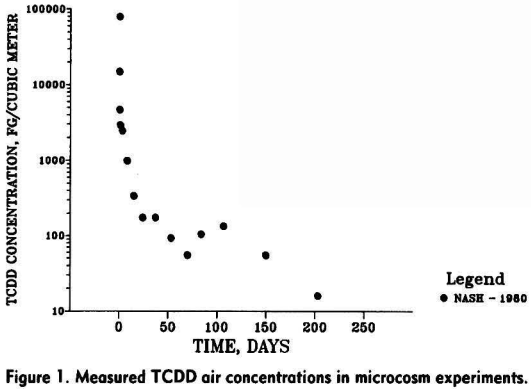

Figure 1. Measured TCDD air concentrations in microcosm experiments.

life under field conditions as between 131 and 321 days. Muir concluded that:

1. Measured losses of 1,3,6,8-TCDD from soil may have been due to vaporization.
2. The reduction in 1,3,6,8-TCDD concentrations in the field soil plots was not due to degradation or movement of the molecule into the soil column below 5 cm. (Authors Note: Muir used a 5 cm depth increment for sampling and analysis. Thus, it was impossible for Muir to detect TCDD movement which may have occurred in the top 5 cm of the soil column).

The conclusion that TCDD volatilizes under field conditions has strong experimental support. Can volatilization of TCDD in a soil column explain the movement of TCDD in the soil column?

THEORY

Previous Models

Many models have been developed to describe the movement of pesticides in the environment. Jury [12] developed an analytical model to describe the movement of pesticides via vaporization. Jury's model makes several simplifications, such as constant soil temperature, and was constructed to allow for "environmental screening" of a new pesticide before development. Mayer [13] has studied the boundary conditions to use with the transport equations that describe the movement of chemicals in a soil column.

Other investigators such as Oddson [14], Leistra [15], Davidson [16], and Lindstrom [17] have studied the movement of chemicals via convective transport in water. These models generally ignore the possibility of vapor phase transport and require constant soil properties and temperatures. These conditions rarely are obtained under actual field conditions.

Material Balance Equations

Freeman and Schroy [8] constructed a model based on a solid and a vapor phase being in contact with each other. The material balance model is essentially the same as that used by Jury [12] and is given as:

$$\frac{\partial C_d}{\partial t} = \frac{2\,\rho_{molar} D_{ab}}{\Phi}\left[\frac{C_a}{M_w\,\rho_{molar}} - \frac{K C_d P^o}{P_t}\right] \frac{M_w a}{\rho_{soil}} = R \qquad (1)$$

$$\frac{\partial C_a}{\partial t} = h\,\frac{\partial}{\partial Z}\left(D_{ab}\,\frac{\partial C_a}{\partial Z}\right) - \frac{R}{\epsilon} \qquad (2)$$

These two partial differential equations must be solved simultaneously and this requires a large amount of computer time.

Numerical and theoretical studies of the material balance equations found that the vapor phase is always in equilibrium with the solid soil phase. An empirical equilibrium partitioning coefficient, K, is defined by the relation between the gas space partial pressure of TCDD and the vapor pressure as:

$$K = P'/(C_d P^o) \qquad (3)$$

Substituting the vapor phase equilibrium expression and collecting terms allows the Freeman-Schroy material balance equations to be re-written as:

$$\frac{\partial C_a}{\partial t} = \frac{(\epsilon^2/\tau)}{\epsilon + P_T/(K\,P^o M_w\,\rho_{molar})}\,\frac{\partial}{\partial Z}\left(D_{ab}\,\frac{\partial C_a}{\partial Z}\right) \qquad (4)$$

The material balance, given as Equation 4, is solved using boundary conditions 1 and 2:

B.C. 1 — Air-Soil Interface Concentration

$$\text{at } Z = O;\ C_a = O \qquad (5)$$

B.C. 2 — Constant Concentration Some Depth in Ground

$$\text{at } Z = L;\ C_d = O \qquad (6)$$

The diffusivity, D_{ab}, the molar density, ρ_{molar}, and the vapor pressure, P^o, are all functions of temperature. Daily high soil surface temperatures of 40 C have been measured during the day with corresponding lows of 20 C during the night [18]. The vapor pressure of TCDD is 8.61×10^{-8} pascals at 20 C and is 2.21×10^{-6} at 40 C. Thus, the daily 20 C temperature change will change the vapor pressure of TCDD by a factor of 25. In addition, the molar density, ρ_{molar}, will decrease 6 percent and the diffusivity, D_{ab}, will increase 10 percent over the same 20 C temperature range. Since the soil temperature will also vary from season to season, an energy balance model is required to correctly estimate the impact of temperature variations on the mass transport process.

Energy Balance Equation

The energy balance equation is the same as previously presented by Tung, Freeman, and Schroy [18]. A brief description is presented below. The one-dimensional transient energy balance equation may be written as:

$$\rho_{soil}\,C_p\,\frac{\partial T}{\partial t} = k\,\frac{\partial^2 T}{\partial Z^2} \qquad (7)$$

To solve this equation for the temperature waves that pass through a soil column, requires two boundary conditions:

B.C. 3 — Surface Energy Flux

$$\text{at } Z = O;\ k\frac{\partial T}{\partial Z} = q_r + q_c + q_b \text{ for all } t \geq O \qquad (8)$$

B.C. 4 — Constant Temperature at Some Depth in Ground

$$\text{at } Z = L;\ T = T_g \text{ for all } t \geq O \qquad (9)$$

The term q_r, represents the radiative solar input into the soil column. The term, q_c, is convective heat transfer between the soil and the air. The term, q_b, represents the black body radiative loss of energy from the soil surface. These soil surface energy fluxes are complex functions of soil temperature, weather conditions, and site location. Schroy [19] has previously presented methods for the computation of q_r, q_c, and q_b. For details of the soil temperature model and the numerical solution, see Tung, Freeman, and Schroy [18].

Essentially the same predicted concentration profiles were found using the energy balance equation and either the simplified or the complex material balance equations for soil cores taken from Times Beach, Missouri. A model, using the simplified material balance equation and energy balance equations, was used to predict the soil TCDD profiles measured at Eglin Air Force Base in Florida.

EGLIN AIR FORCE BASE

In April of 1972, Dr. Alvin Young (USAF) established several biodegradation plots at Eglin AFB [20]. The area selected for the biodegradation plots was clean and had not been sprayed with Agent Orange or other herbicides. Table 1 presents the physical properties of the Eglin AFB soil. Each plot consisted of three replicate trenches. Trenches approximately 10 centimeters (4 to 5 inches) deep were dug into the soil, and Agent Orange containing

TABLE 1. SOIL PHYSICAL PROPERTIES USED FOR EGLIN AIR FORCE BASE SIMULATIONS

Property	Units	Value	Reference No., Page
Sand Content	wt %	91.6	23, 7
Silt Content	wt %	4.0 (1)	23, 7
Clay Content	wt %	4.4	23, 7
Organic Matter Content	wt %	0.5	23, 7
Ph	---	5.6	23, 7
Density	g/cm^3	1.6	22, 351
Heat Capacity	kJ/kg/K	1.67	24, 351
Thermal Conductivity	kJ/m/K/s	2.68×10^{-3}	24, 351
Void Fraction		0.3	25, 15

Note: 1. Silt content includes the organic matter content of 0.5 percent.
2. Eglin AFB soil is classified as a sandy-loam.

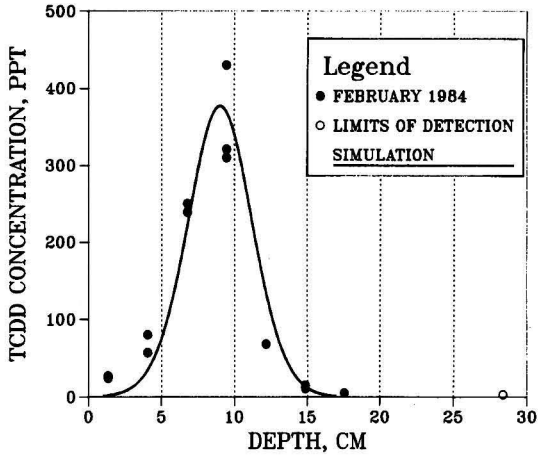

Figure 2. Simulation of Eglin AFB TCDD profile core 4N. NONAMENDED BIODEGRADATION PLOT.

40 ppb of TCDD was applied to the trench bottom. The application loading was 950 ml of Agent Orange on an area of 0.930 square meters (10 square feet) or 0.1 ml Agent Orange/cm^2 [*21*]. After the Agent Orange was applied, the trenches were back filled with clean soil.

Samples were subsequently taken from the plots and analyzed for TCDD by the Air Force. These samples showed an apparent decrease in the total TCDD content of the soil over time, and this is discussed below. In February of 1984, Dr. Young and a team from Monsanto took a set of core samples from the biodegradation plots.

The cores taken by the Monsanto team were segmented into approximately 2 centimeters increments and analyzed for TCDD. The results of these analyses are given in Table 2. Cores 4 N and 5N were taken from two parallel trenches, separated by a distance of 1 meter, in the "Non-amended Biodegradation Plot." The data for cores 4N and 5N are plotted in Figures 2 and 3. As is readily apparent from both Figures 2 and 3, the TCDD has moved upward through the soil layer from the initial depth of approximately 10 centimeters.

Using the transport model previously presented in this paper, a simulation of the TCDD movement was done. The weather data used in this simulation are presented in Table 3. The initial mass of TCDD was estimated by integrating the soil TCDD concentration profile in each core. The total initial TCDD mass was assumed to have been contained in a one centimeter increment of soil buried at a depth of approximately 10 centimeters. The calculated initial TCDD concentration profiles are shown in Figures 4 and 5. The initial peak TCDD concentration of core 4N was computed to be 2100 ppt (by wt) and 7160 ppt (by wt) for core 5N.

The simulation was solved for a time span of 12 years. The final peak concentration of TCDD was adjusted, by varying the empirical equilibrium partition coefficient, K, until the measured value was obtained. The equilibrium partition coefficient, K, is an empirical parameter that describes the concentration relationship between the soil and the adjacent air spaces (Equation 3). The spread of the calculated concentration profile is compared to the measured data in Figures 2 and 3. The model fits the data well.

The good agreement between the model and the data suggests that all of the TCDD originally applied by Dr. Young in 1972 is still contained in the biodegradation plots. However, the TCDD is moving very slowly away from the position where it was initially placed. The near

TABLE 2. MEASUREMENTS OF TCDD CONCENTRATION PROFILES IN EGLIN AFB BIODEGRADATION PLOTS

Core Increment Centimeters	TCDD Concentrations, ppt (wt) Core 4N	Core 5N
0.00-2.54	24, 27	29
2.54-5.08	57, 80	70
5.08-7.62	239, 250	346, 450
7.62-10.16	321, 310, 430	785, 860
10.16-12.70	68	582, 650
12.70-15.24	15, 11	185, 200, 230, 240
15.24-17.78	5	73, 120
17.78-20.32	**	22
20.32-22.86	**	19
22.86-25.40	**	8
25.40-27.94	ND (3)	8
27.94-30.48	ND (3)	3, 3
30.48-33.02		3
33.02-35.56		ND (1)
35.56-38.10		2
>38.10		ND (1)

Notes: 1. ND — None detected at a detection limit given in parenthesis as ppt by wt.
2. Analyses given for compacted sample cores, where:
Core 4N — compaction was 1.91 cm in 31.8 cm
Core 5N — compaction was 11.43 cm in 63.5 cm
**Analytical protocol failed (ie., poor recovery).

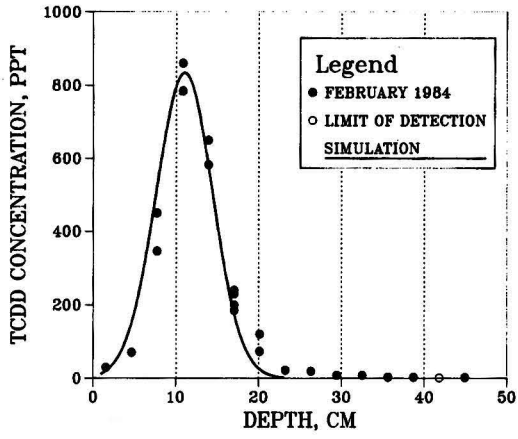

Figure 3. Simulation of Eglin AFB TCDD profile core 5N. Nonamended biodegradation plot.

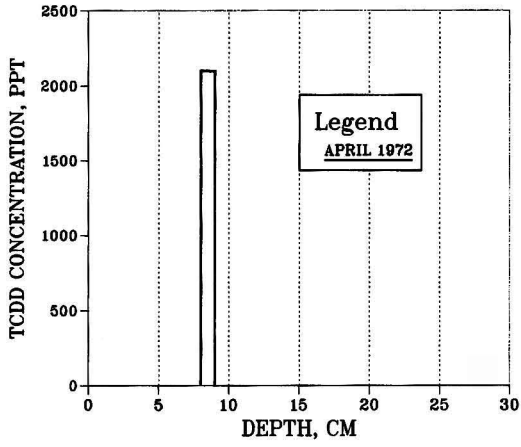

Figure 4. Initial Eglin AFB TCDD profile core 4N. Nonamended biodegradation plot.

symmetry of both the measured and calculated concentration profiles suggests that the rate of downward movement is essentially equal to the rate of upward movement. The good agreement with the data also implies that although vapor transport may not be the only mechanism, the model provides a good structural form to represent all TCDD transport mechanisms.

The results of the Air Force and Monsanto analyses of Eglin AFB soil are compared in Table 4. The analyses by the Air Force shows an apparent decrease of TCDD concentration with time. Young and Arnold [22] have reanalyzed archived Air Force soil samples and found that most of the originally applied TCDD could be recovered using an exhaustive extraction procedure. Therefore, the question of the fate of TCDD remained an open question until the completion of this study.

In addition to the extraction problems found by Young and Arnold, variations in initial TCDD loading are apparent. The Monsanto cores from the same plot show a factor of 3 variation in the average TCDD concentration. When compared to the initial calculated TCDD concentration and area loading, one of the Monsanto cores lies below and one lies above the calculated average. The day 5 and day 414 Air Force data are three to four times greater than the calculated initial TCDD levels. The day 513 and day 707 data are below calculated initial average TCDD concentration and loading.

Some of the variation in the data appears due to the difficulty of spreading 950 milliliters of Agent Orange over 0.93 square meters of surface uniformly. The change in concentration with time noted in the Air Force Data appears due to the variation in loading and to analytical problems, rather than any reduction in the level of TCDD with time.

CONCLUSIONS

Based on the above analysis, the following conclusions about the mobility of TCDD can be reached:

1. All of the TCDD buried in the biodegradation plots is still contained in the soil.
2. The apparent biodegradation of TCDD, previously reported by Young(20), can be explained by the variation in the initial loading of the biodegradation plots and/or by analytical problems.
3. The transport of TCDD in a soil column can be modeled by a temperature-driven diffusion process.
4. The rate of TCDD movement is very slow. The TCDD in the Eglin AFB biodegradation plots has moved only about 10 centimeters in 12 years.

ACKNOWLEDGMENT

The authors wish to thank Dr. Alvin Young for his generous assistance with this work. The authors also thank the

TABLE 3. WEATHER SERVICE DATA FOR EGLIN AIR FORCE BASE, FLORIDA

Month	Temperature, Deg C Maximum	Minimum	Average	Wind Vel., m/sec	Rel. Hum., %(2)	Sky Cover, %	Solar Insolation KJ/day /m²
January	16.2	6.1	11.2	4.07	71	66	9678
February	17.8	7.5	12.7	4.20	66	57	12778
March	20.5	10.4	15.5	4.34	69	63	16728
April	24.9	15.2	20.1	4.25	67	57	21326
May	29.0	18.9	24.0	3.80	67	56	23728
June	31.7	22.3	27.0	3.35	67	53	22677
July	32.1	23.3	27.7	3.09	72	63	20581
August	32.2	23.1	27.7	2.91	74	61	19150
September	30.2	21.2	25.7	3.44	71	55	17426
October	21.6	15.6	21.1	3.62	81	44	15565
November	20.9	9.6	15.3	3.71	83	50	11803
December	17.3	6.8	12.1	4.02	90	61	9280
Average	24.9	15.0	20.0	3.75	84	57	16728

Notes: 1. Based on 1947 to 1970 weather records at the Pensacola Florida Regional Airport
2. At noon

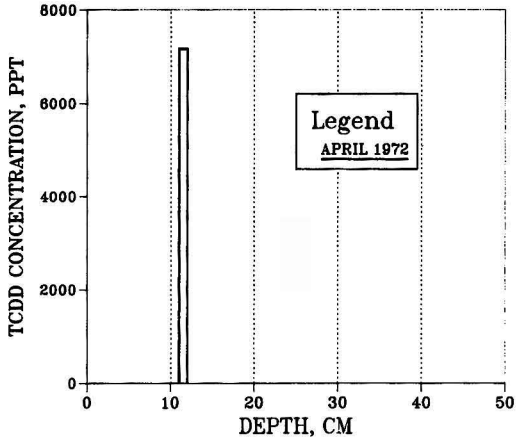

Figure 5. Initial Eglin AFB TCDD profile core 5N. Nonamended biodegradation plot.

United States Air Force for allowing the samples to be taken and Roy Noble, Dr. Fred Hileman, and their staff for the TCDD soil analyses. The authors also thank the peer reviewers for their many useful and valuable suggestions to improve this paper.

NOMENCLATURE

a	= Air-soil interfacial area per unit soil volume
C_a	= Concentration of TCDD in air
C_d	= Concentration of TCDD in soil
C_p	= Heat capacity of soil
D_{ab}	= Diffusivity of TCDD in air
h	= Hindrance factor, $h = \epsilon/\tau$
K	= Empirical equilibrium partitioning coefficient between soil and air
k	= Thermal conductivity of soil
L	= Soil depth where temperature and concentration does not change during a year
M_w	= Molecular weight of TCDD
P^o	= Vapor pressure of TCDD
P'	= Partial pressure of TCDD in gas space
P_T	= Total barometric pressure
q_b	= Black body radiation loss to the sky
q_c	= Convective energy exchange between soil and atmosphere
q_r	= Radiative energy received by soil from the sun
R	= Volumetric rate of volatilization of TCDD into air voids
T_g	= Soil temperature at a depth L
t	= Time
Z	= Depth into the ground

Greek Symbols

ϵ	= Soil void fraction
ρ_{molar}	= Molar density of air in soil void space
ρ_{soil}	= Density of soil
τ	= Tortuosity factor, $\tau = 2$ for an average soil
Φ	= Average diameter of soil particle

LITERATURE CITED

1. Schroy, J. M., F. E. Hileman, and S. C. Cheng, "Physical and Chemical Properties of 2,3,7,8 TCDD, The Key to Transport and Fate Characterization", Paper presented at the 8th ASTM Aquatic Toxicology Symposium held April 15-17, 1984 in Fort Mitchell, Kentucky.
2. Adams, W. J., and D. K. Blaine, "A Water Solubility Determination of 2,3,7,8-TCDD", Presented at the Fifth International Symposium on Chlorinated Dioxins and Related Compounds, Bayreuth, Germany, September 16-19, 1985.

TABLE 4. TOTAL TCDD MASS LOADING IN EGLIN AFB BIODEGRADATION PLOTS

Test Description	Calculated TCDD Loading, grams/sq meter	TCDD Concentration, ppt (wt) (1)
Liquid	5.22×10^{-5}	86 (2)
Air Force Data		
Day 5	22.88×10^{-5}	375 (3)
Day 414	15.25×10^{-5}	250 (3)
Day 513	4.58×10^{-5}	75 (3)
Day 707	2.81×10^{-5}	46 (3)
Monsanto Data (4)		
Core 4N	3.36×10^{-5}	55 (5)
Core 5N	11.46×10^{-5}	188 (5)

Notes: 1. Average TCDD concentration in a 38.1 cm core.
2. Calculated average loading over entire trench.
3. Measured
4. Monsanto samples taken 12 years after initial burial.
5. Calculated based on data in Table 2.

3. Goring, C. A. I., "Physical Aspects of Soil in Relation to the Action of Soil Fungicides", *Annual Rev. Phytopathol.*, pg. 285-318, 1967.
4. Guenzi, W. D. and W. E. Beard, "Volatilization of Lindane and DDT from Soils", *Soil Sci. Soc. Amer. Proc., Vol. 34*, pg. 443-447, 1970.
5. Farmer, W. J., K. Igue, W. F. Spencer, and J. P. Martin, "Volatility of Organochlorine Insecticides From Soil: I. Effect of Concentration, Temperature, Air Flow Rate, and Vapor Pressure", *Soil Sci. Soc. Amer. Proc., Vol. 36*, pg. 443-447, 1972.
6. Hee, S. S. Q., K. S. Mckinlay, and J. G. Saha, "Factors Affecting the Volatility of DDT, Dieldrin, and Dimethylamine Salt of (2,4-dichlorophenoxy) acetic Acid (2,4-D) From Leaf and Glass Surfaces", *Bulletin of Environmental Contamination & Toxicology*, pg. 284-290, 1975.
7. Beall, M. L. and R. G. Nash, "Organochlorine Insecticide Residues in Soybean Plant Tops: Root vs. Vapor Sorption", *Agronomy Journal, Vol. 63*, pg. 460-464, 1971.
8. Freeman, R. A. and Schroy, "Environmental Mobility of Dioxins", Paper presented at the 8th ASTM Aquatic Toxicology Symposium held April 15-17, 1984 in Fort Mitchell, Kentucky. Published after peer review in *Aquatic Toxicology and Hazard Assessment: 8th Symposium*, Edited by R. C. Bahner and D. J. Hansen, ASTM STP 891, American Society of Testing Materials, Philadelphia, December 1985.
9. Nash, R. G. and M. L. Beall, "Distribution of Silvex, 2,4-D, and TCDD Applied to Turf in Chambers and Field Plots", *J. Agric. Food Chem., Vol. 28*, pg. 614-623, 1980.
10. Liberti, A., D. Broco, I. Allergrini, A. Cecinato, and M. Possanzini, "Solar and UV Photodecomposition of 2,3,7,8-Tetrachlorodibenzo-p-Dioxin In The Environment", *The Science of the Total Environment, Vol. 10*, pp. 97-104, 1978.
11. Muir, D. C. G., et al., "Laboratory and Field Studies on the Fate of 1,3,6,8-Tetrachlorodibenzo-p-dioxin in Soil and Sediment", *J. Agric. Food Chem., Vol. 33*, pg. 518-523, 1985.
12. Jury, W. A., W. F. Spencer, and W. J. Farmer, "Behavior Assessment Model for Trace Organics in Soil: I. Model Description", *J. Environ. Qual., Vol. 12*, pg. 558-564, 1983.
13. Mayer, R., J. Letey, and W. J. Farmer, "Models for Predicting Volatilization of Soil-Incorporated Pesticides", *Soil Sci. Soc. Amer. Proc., Vol. 38*, pg. 563-568, 1974.
14. Oddson, J. K., J. Letey, and L. V. Weeks, "Predicted Distribution of Organic Chemicals in Solution and Adsorbed as a Function of Position and Time for Various Chemicals and Soil Properties", *Soil Sci. Soc. Amer. Proc., Vol. 34*, pg. 412-417, 1970.
15. Leistra, M., "Computing the Movement of Ethoprophos in Soil After Application in Spring," *Soil Sci., Vol. 128*, pg. 303-311, 1979.
16. Davidson, J. M. and J. R. McDougal, "Experimental and Predicted Movement of Three Herbicides in a Water-Saturated Soil", *J. Environ. Quality, Vol. 2*, pg. 428-433, 1973.
17. Lindstrom, F. T., L. Boersma, and H. Gardiner, "2,4-D Diffusion in Saturated Soils: A Mathematical Theory", *Soil Sci., Vol. 106*, pg. 107-113, 1968.
18. Tung, L. S., R. A. Freeman, and J. M. Schroy, "Prediction of Soil Temperature Profiles: A Concern in the Assessment of

Transport of Low Volatility Chemicals in the Soil Column", Presented at the AICHE National Meeting in Seattle", Washington, August 25-29, 1985.
19. Schroy, J. M. and J. S. Weiss, "Prediction of Wastewater Basin Temperatures, A Design and Operating Concern", Presented at the AICHE Symposium, Washington, D.C., November 4, 1983.
20. Young, A. L., J. A. Calcagni, C. E. Thalken, and J. W. Tremblay, "The Toxicology, Environmental Fate and Human Risk of Herbicide Orange and Its Associated Dioxin", USAF OEHL - 78 -92, October 1978.
21. Private communication between A. L. Young and J. M. Schroy, June 1984.
22. Young, A. L. and E. L. Arnold, "Environmental Fate of TCDD — Conclusion From Three Long Term Field Studies", paper presented at the September, 1983 ACS meeting in Washington, D.C.
23. Young, A. L., C. E. Thalken, E. L. Arnold, J. M. Cupello, and L. G. Cockerham, "Fate of 2,3,7,8-Tetrachlorodibenzo-p-dioxin in the Environment: Summary and Decontamination Recommendations", Report Number SAFA-TR-76-18, October 1976, Department of Chemistry and Biological Sciences, USAF Academy, Colorado 80840. Available as NTIS Report Number ADA 033491.
24. Thibodeaux, L. J., *Chemodynamics*, John Wiley & Sons, New York, New York, 1979.
25. Muskat, M., *The Flow of Homogeneous Fluids Through Porous Media* J. W. Edwards, Inc., Ann Arbor, Michigan, 1946.

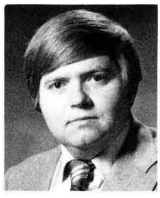

Raymond A. Freeman is an Engineering Specialist in the Engineering Technology Group of Monsanto Corporate Engineering. He serves as a general process consultant to the corporation in the areas of risk assessment and process design. He holds B.S., M.S. and Ph.D. degrees in Chemical Engineering from the University of Missouri—Rolla. He is a registered professional engineer in Missouri, a member of the American Institute of Chemical Engineers, American Chemical Society, the Society for Risk Analysis, American Society for Testing and Materials, and the American Association for the Advancement of Science.

Jerry M. Schroy is presently a Fellow in the Environmental Enginering section of Monsanto Company's Corporate Engineering Department. He holds a Chemical Engineering degree from the University of Cincinnati and has been with Monsanto since graduation. He has held various process engineering and environmental control assignments since joining Monsanto in 1963. At present, his activities center on control of hazardous chemicals in the workplace and wastewater treatment technology.

Dissolution Rate Of Calcium Sulfite Hemihydrate In Flue Gas Desulfurization Processes

The rate of calcium sulfite dissolution in slurry scrubbers and hold tanks for flue gas desulfurization affects SO_2 absorption, limestone utilization and sulfite oxidation. The dissolution rates of calcium sulfite were measured by the pH-state method. A mass transfer model was developed assuming that calcium sulfite particles behave as spheres in an infinite stagnant solution. The model combined with the Bechtel-modified Radian solution equilibrium program successfully predicts calcium sulfite dissolution rates at pH 3.5 − 5.5, 23 and 55 °C, 0.001 − 0.3 M Ca^{++} and 2 − 25 mM dissolved sulfite. The effects of sulfate content in solids and liquids and particle size/shape were also studied.

At conditions typical of flue gas desulfurization processes calcium sulfite dissolution was controlled by mass transfer, not surface reaction kinetics. Dissolution was fast at low pH and slowed near the equilibrium pH determined by dissolved Ca^{++} and $SO_3^{=}$ concentrations in the aqueous solutions, K_{sp} of the $CaSO_3 \cdot 1/2H_2O$ solids, and temperature. The presence of dissolved Mg^{++} increased the equilibrium pH and enhanced the disolution rate. The presence of dissolved sulfate reduced the dissolution rate and the equilibrium pH. The effect of sulfate was not adequately described by the mass transfer model.

Philip C. Tseng and Gary T. Rochelle, Department of Chemical Engineering, The University of Texas at Austin, Austin, TX 78712

INTRODUCTION

The objective of this work is to measure and model the dissolution rate of calcium sulfite in flue gas desulfurization processes which absorb SO_2 by a slurry of lime or limestone with simultaneous calcium sulfite/sulfate crystallization. Calcium sulfite dissolution can be important in these processes because it affects the solution composition and chemical equilibria in the scrubbing solution, and therefore affects SO_2 absorption, sulfite oxidation, and limestone dissolution [*1*]. Rates of both SO_2 absorption and limestone dissolution are usually determined by mass transfer with equilibrium acid/base reactions in the solution [2, 3, 4, 5, 6, 7, 8]. With low excess $CaCO_3$ or $Ca(OH)_2$ solids, as in low pH $CaCO_3$ scrubbing or general $Ca(OH)_2$ scrubbing processes, $CaSO_3 \cdot 1/2H_2O$ will dissolve in the scrubber with the stoichiometry [2]:

$$CaSO_3^{\circ} + SO_2 + H_2O \longleftrightarrow Ca^{++} + 2\,HSO_3^{+} \quad (1)$$

Intentional sulfite oxidation has been used to increase the SO_2 removal efficiency and to oxidize calcium sulfite ($CaSO_3 \cdot 1/2H_2O$) to gypsum ($CaSO_4 \cdot 2H_2O$) which generally consists of larger crystals, has less disposal volume and settles faster [9, 10]. In forced oxidation of a bleed stream, or in a second-stage scrubber loop where calcium sulfite/calcium sulfate has crystallized, sulfite oxidation can be limited by calcium sulfite dissolution. Such operations require low pH to get calcium sulfite dissolution and subsequent oxidation. Erwin *et al*, [*11*] and Nurmi *et al*, [*12*] modelled the oxidation of calcium sulfite slurries in aqueous solutions and indicated that $CaSO_3 \cdot 1/2H_2O$ dissolution is controlled by mass transfer whereas sulfite oxidation is controlled by solution reaction kinetics.

The dissolution of ionic solids may be controlled either by surface kinetics or by diffusion of ions [*1, 13, 14, 15*]. Chan [*16*] measured $CaCO_3$ dissolution of flue gas desulfurization conditions using the pH-stat method, and modeled the experimental data by a stagnant mass transfer model with equilibrium acid/base reactions. That work was extended by Toprac and Rochelle [*17*] who accounted for the dependence of dissolution rates on particle size and shape. Calcium sulfite dissolution is basically similar to calcite dissolution, but the solids composition is usually a mixture of calcium sulfite and calcium sulfate instead of pure calcium sulfite, and the particles can be aggregates of many small crystals. The shape of the crystals also varies from platelet to rosette. Jones *et al.* [*18*] used X-ray, DSC, and IR to confirm the formation of a solid solution of calcium sulfate in $CaSO_3 \cdot 1/2H_2O$. Setoyama *et al.* [*19*] found that the solubility of calcium sulfate in $CaSO_3 \cdot 1/2H_2O$ is a function of temperature.

The reported solubility (mg/l) of $CaSO_3 \cdot 1/2H_2O$ in water is 43 (18°C, [20]) and 46.3 (30°C, [21;]). *Lowell et al.* [22] reported in the Radian solution equilibrium program a measured thermodynamic solubility product of $CaSO_3 \cdot 1/2H_2O$ as 8.4×10^{-8} M^2, and indicated that there is little change in solubility with temperature. Bechtel increased the K_{sp} to 4.498×10^{-7} M^2 to match field data [23]. Recently Faist *et al.*, [24] give an expression of $CaSO_3 \cdot 1/2H_2O$ solubility as a function of temperature:

$$\text{Log } K_{sp} = 838.3/T - 9.7572 \quad (2)$$

Discrepancies in these results may have resulted from the difficulties in controlling the dissolved sulfate concentration and the variation in solid sulfate content of the $CaSO_3 \cdot 1/2H_2O$ samples used in these experiments.

In this paper, the dissolution rates of $CaSO_3 \cdot 1/2H_2O$ at conditions typical of flue gas desulfurization processes were measured using the pH-stat method introduced by Chan [16] and Prada [25]. A model was developed by using mass transfer with equilibrium acid/base reactions similar to Chan and Rochelle's work for $CaCO_3$ dissolution [1]. This work is a part of an effort for overall scrubber modeling which includes rate models for SO_2 absorption, $CaCO_3$ dissolution, sulfite oxidation, and calcium sulfite dissolution and crystallization [26, 27].

The calcium sulfite dissolution experiments were conducted at pH 3.5 – 6, 0.001 – 0.3 M Ca^{++}, 1 - 10 mM dissolved sulfite, 23 and 55°C, 0.3 - 0.9 eq/l ionic strength, and 0 - 200% gypsum saturation. Three batches of $CaSO_3 \cdot 1/2H_2O$ seed crystals were used to study the effects of particle size and shape. The effects of pH, sulfite, sulfate, temperature and ionic strength were investigated and the solubility product of $CaSO_3 \cdot 1/2H_2O$ was found to be a function of temperature and the sulfate content in the solids.

THEORY

Limestone and calcium sulfite dissolution can both be modeled as steady-state mass transfer between the solid surface and the bulk solution [1, 11, 26]. A steady-state solution of the mass transfer model is obtained by assuming spherical calcium sulfite particles in an infinite stagnant solution, corresponding to a mass transfer coefficient equal to the ratio of diffusivity to particle radius (D/r).

Effects of Solution Composition

The main feature of the mass transfer model is that chemical equilibrium is maintained throughout the diffusion path for all chemical species. H^+ diffuses through the boundary layer from the bulk solution to the calcium sulfite particle surface and the dissolved $SO_3^=/HSO_3^-$ or $CaSO_3^o$ diffuses from the sulfite particle surface to the bulk solution. The boundary conditions are the calcium sulfite solubility product at the particle surface and the specified composition of the bulk solution. Chemical equilibria, ionic electroneutrality, and material balances are then used to determine the concentrations of all chemical and ionic species in the boundary layer.

This model utilizes pseudo-equilibrium constants derived from the Bechtel-modified Radian solution equilibrium program, so that the equilibrium program needs to be called only once during the calcium sulfite dissolution modeling work. The effects of ion pairs are accounted for by the pseudo-equilibrium constants, and there are no direct ion pair equilibria. Therefore, solution of the mass diffusion equations is greatly simplified.

(i) Solution Equilibria

In this work, the important solution equilibria for calcium sulfite dissolution were:

$$HSO_3^- \longleftrightarrow H^+ + SO_3^= \quad (3)$$

$$HSO_4^- \longleftrightarrow H^+ + SO_4^= \quad (4)$$

$$H_2O \longleftrightarrow H^+ + OH^- \quad (5)$$

Additional equilibria would need to be added to simulate the effects of other buffers such as organic acids and CO_2/HCO_3^-.

Using the Bechtel-modified Radian equilibrium program, the concentrations of various chemical species were calculated. In order to perform the mass transfer calculation without manipulating ion pair equilibria, the following pseudo-concentrations were defined:

(ii) Pseudo-Concentrations

$$[Ca^{++}]' = [Ca^{++}] + [CaOH^+] + [CaSO_3^o] + [CaSO_4^o] \quad (6)$$

$$[SO_3^=]' = [SO_3^=] + [CaSO_3^o] + [MgSO_3^o] \quad (7)$$

$$[SO_4^=]' = [SO_4^=] + [CaSO_4^o] + [MgSO_4^o] + [NaSO_4^-] \quad (8)$$

$$[OH^-]' = [OH^-] + [CaOH^+] + [MgOH^+] \quad (9)$$

The pseudo-concentrations for HSO_3^-, HSO_4^-, and H^+ are equal to their true concentrations due to the absence or the insignificance of ion pairs including these species.

(iii) Diffusion Coefficients:

Values of diffusion coefficients used in the model are given in Table 1 [1, 23]. At 25°C and infinite dilution, ionic diffusivities were calculated by:

$$D = RT\lambda_o/n_j(Fa)^2 \quad (10)$$

where Fa is the Faraday number, n_j is the charge on the j_{th} ion, and λ_o is the equivalent ionic conductivity.

Diffusivities at 55°C were estimated by the Stokes-Einstein relationship:

$$D_1\eta_1/T_1 = D_2\eta_2/T_2 \quad (11)$$

(iv) Pseudo-Diffusivities:

To use the pseudo-concentrations in the solution equilibrium program, pseudo-diffusivities have been defined for all the pseudo chemical species defined above:

$$D_j' = (\Sigma\ D_iC_i)/\Sigma\ C_i \quad (12)$$

which is summed over all species i containing component j. For example, to calculate the pseudo-diffusivity for the pseudo-species, Ca^{++}, let j = Ca^{++} and i = Ca^{++}, $CaOH^+$, $CaSO_3^o$, $CaSO_4^o$. The pseudo-diffusivities for HSO_3^-, HSO_4^-, and H^+ are set equal to their true diffusivities.

(v) Pseudo-Equilibrium Constants:

Based on the above pseudo-concentrations, the pseudo-equilibrium constants were calculated as follows:

$$K_w = [H^+]\,[OH^-]' \quad (13)$$

$$K_{HSO_4^-} = ([H^+[\,[SO_4^=]')/[HSO_4^-] \quad (14)$$

$$K_{HSO_3^-} = [H^+]\,[SO_3^=]')/[HSO_3^-] \quad (15)$$

$$SK_{sp} = (K_{sp}\,[Ca^{++}]'\,[SO_3^=]')/([Ca^{+2}]\,[SO_3^{-2}]) \quad (16)$$

(vi) Diffusion Balances:

In general the flux of a component is given by:

$$\text{Flux}_j = \Sigma\ D_j\,([J_j]_i - [J_j]_b)/\delta \quad (17)$$

TABLE 1. DIFFUSIVITIES AT 25°C

Species	D × 10^{-5} (cm^2/sec)
HSO_4^-	1.33
$SO_4^=$	1.06
Ca^{++}	0.79
$SO_3^=$	0.96
HSO_3^-	1.33
OH^-	5.24
H^+	9.31
$CaSO_3^o$	0.53
$MgSO_3^{-o}$	0.53

The calcium sulfite dissolution flux is defined as the sum of sulfite flux and bisulfite flux:

$$\text{Dissolution Flux} = D'_{SO_3^{=}}([SO_3^{=}]'_i - [SO_3^{=}]'_b)/\delta + D_{HSO_3^-}([HSO_3^-]_i - [HSO_3^-]_b)/\delta \quad (18)$$

where the subscripts i and b denote solid-liquid interface and bulk solution respectively, and δ is the boundary layer thickness.

By the principle of electroneutrality, the net flux of electric charge in the boundary layer is equal to zero:

$$2\,Ca^{++}\text{ flux} + H^+\text{ flux} - 2\,SO_3^{=}\text{ flux} - 2\,SO_4^{=}\text{ flux} - HSO_3^-\text{ flux} - HSO_4^-\text{ flux} - OH^-\text{ flux} = 0 \quad (19)$$

By stoichiometry the calcium flux must be equal to the total flux of sulfite and sulfate from the solid:

$$Ca^{++}\text{ flux} = SO_3^{=}\text{ flux} + HSO_3^-\text{ flux} + SO_4^{=}\text{ flux} + HSO_4^-\text{ flux} \quad (20)$$

By stoichiometry the ratio of the fluxes of total sulfite and total sulfate must be the same as the composition of the solid:

$$(SO_3^{=}\text{ flux} + HSO_3^-\text{ flux})/(1 - Y_{SO_4}) = (SO_4^{=}\text{ flux} + HSO_4^-\text{ flux})/Y_{SO_4} \quad (21)$$

where Y_{SO_4} is the mole fraction of sulfate in the calcium sulfite solids.

(vii) Solution of the surface diffusion balances and equilibria:

In the mass transfer model, there are eight unknowns in the solution boundary layer surrounding the $CaSO_3$ particle: $[Ca^{++}]'$, $[SO_3^{=}]'$, $[SO_4^{=}]'$, $[OH^-]'$, $[HSO_4^-]$, $[HSO_3^-]$, $[H^+]$ and the $CaSO_3$ dissolution flux. Material and charge balances (Equations 18 to 21) and chemical equilibria (Equations 13 to 15) were solved by iteration on pH at the particle surface. Bulk pH was used as an initial guess. The boundary condition from solubility was used to check for convergence:

$$\text{B. C. } [Ca^+]'\,[SO_3^{=}]' = SK_{sp} \quad (22)$$

The product of the calculated pseudo-concentrations of Ca^{++} and $SO_3^{=}$ at the particle surface was compared with the boundary condition. The guessed surface H^+ concentration was then reduced by a factor of 2 each time until the difference changed sign. After bracketing the H^+ concentration, a half-interval method was used to find the surface H^+ concentration that satisfied the boundary condition. Equation 18 was then used to calculate the product of boundary layer thickness and calcium sulfite dissolution flux. This quantity ($D\Delta C$) is used in the next section to give an effective product of the diffusion coefficient and driving force.

Effect of Particle Size Distribution

The rate of dissolution of a single spherical particle can be represented by the proportionality (Chan and Rochelle, 1981):

$$-dV/dt = Sh\,\pi\,d_p\,(D\Delta C)/\rho_m \quad (23)$$

where $Sh = k_c d_p/D$. For small spherical particles in stagnant solution, assuming Sh is independent of d_p and is approximately equal to 2 (Toprac, 1981), integrating the above equation gives:

$$f = \text{fraction remaining} = V/V_o = (1 - kt/d_p^2)^{1.5} \quad (24)$$

where $k = 4\,Sh\,D\,\Delta C/\rho_m \simeq 8\,D\,\Delta C/\rho_m$. The molar density of calcium sulfite hemihydrate was taken to be 0.0194 gmol/cm³.

For polydisperse solids, the total fraction remaining, F, can be determined by summing over the differential size distribution ϕ where ϕ_j is the fraction of total particle volume with initial diameter from d_j to d_{j+1}:

$$F = V/V_o = \Sigma\,\phi_j\,(1 - kt/d_j d_{j+1})^{1.5} \quad (25)$$

EXPERIMENTAL

Dissolution Rate Measurement

The calcium sulfite dissolution rate was determined by the pH-stat method in an agitated reactor. The pH-stat apparatus was the same as that used previously for measurement of $CaCO_3$ dissolution [1] and sulfite oxidation [28]. The agitator speed was set at 720 rpm. The reactor was sparged with N_2 before adding the calcium sulfite solids and was blanketed with N_2 during the rate measurement. The pH was automatically controlled to ± 0.02 units by titrating with 0.04 to 0.2 N HCl. Calcium sulfite dissolution rate was related to the titration rate by the stoichiometry:

$$CaSO_3 \cdot 1/2H_2O + H^+ \rightarrow Ca^{++} + HSO_3^- + 1/2\,H_2O \quad (26)$$

The dissolution rate at high pH was corrected by a calibration of the $SO_3^{=}/HSO_3^-$ equilibrium.

The compositions of the aqueous solution simulate the operating conditions of actual scrubber systems. Two millimoles of $CaSO_3 \cdot 1/2H_2O$ solids were put in one liter of solution at the beginning of each dissolution experiment. Calcium sulfite sample 1 was used in most of the dissolution experiments. Samples 3 and 5 were used in some experimental runs to study the effect of solids variation. During a batch experiment the pH was constant, and both Ca^{++} and total dissolved sulfite concentration increased slightly. After the addition of Na_2SO_3, the gas dispersion tube was lifted to avoid stripping of SO_2. Most of the experiments were performed at room temperature, but some runs were at 55°C to study the effect of temperature.

Synthesis and Characterization of Calcium Sulfite Samples

Three batches of $CaSO_3 \cdot 1/2H_2O$ samples were synthesized in the laboratory by reacting solutions of $CaCl_2$ with Na_2SO_3/Na_2SO_4. The solids were characterized by iodometric titration, differential scanning calorimetry, X-ray powder diffraction, infrared spectroscopy, scanning electron microscopy, BET surface area measurement, and particle size analysis (Coulter Counter). Table 2 gives the particle size distributions. The sulfate content of the particles was found by IR analysis to be 3.4, 10.7, and 1.0 mole% for samples 1, 3, and 5, respectively. The samples were agglomerates of crystallites typified by sample 1 (Figure 1). Additional detailed results are given in Tseng [29] and Tseng and Rochelle [30].

Experimental Rate Constant Determination

A typical dissolution experiment is shown in Figure 2. The total fraction remaining, F, calculated from the volume of HCl added is given as a function of dimensionless time, t/t_{50}, where t_{50} is the time required to dissolve 50% of the $CaSO_3 \cdot 1/2H_2O$ solids. A calculated curve is also given using the stagnant mass transfer model with the polydisperse particle size distribution. As shown in Figure 2, the shape of the polydisperse stagnant mass transfer model fits the experimental data very well.

The experimental rate constant, k, was determined by using Equation 24 with the calculated and measured values of F at kt_{55} and kt_{45}. For the typical experimental run at pH 4.3, t_{55} = 10.1 minutes, t_{45} = 7.35 minutes. From Equation 26 and the initial calcium sulfite particle size distribution, the calculated $kt_{55} = 160.6 \times 10^{-8}$ cm², and $kt_{45} = 112.3 \times 10^{-8}$ Therefore,

$$k = (kt_{55} - kt_{45})/(t_{55} - t_{45}) = 2.93 \times 10^{-9}\ \text{cm}^2/\text{sec} \quad (27)$$

TABLE 2. $CaSO_3 \cdot 1/2H_2O$ PARTICLE SIZE DISTRIBUTIONS

Effective Diameter (μm)	Volume % Between The Two Diameters Sample 1	Sample 3	Sample 5
1.59	0	0	0
2.00	0.6	0.8	0
2.52	0.7	1.5	0
3.17	0.6	0.7	0
4.00	0.8	1.3	0
5.04	1.6	3.2	0
6.35	2.6	6.8	0
8.00	4.4	12.2	0.2
10.08	6.6	17.4	0.9
12.7	10.3	18.0	4.3
16.0	15.4	14.7	17.9
20.2	23.6	10.5	38.2
25.4	20.2	5.7	27.2
32.0	8.0	4.3	8.7
40.3	2.5	1.5	2.3
50.8	2.1	1.4	0.3
64.0			

RESULTS AND DISCUSSION

The $CaSO_3 \cdot 1/2H_2O$ dissolution rates were measured with various solution compositions, ionic strength, temperature, gypsum saturation and seed crystals. The mass transfer model accurately predicts the effects of all variables except for inhibition by dissolved sulfate.

The curves given in Figures 3 through 9 were calculated by the mass transfer model with adjustment of the Sherwood number and K_{sp} for each seed crystal (Table 3). The observed values of Sh (3.4 to 4.0) are expected with the particle size and shape observed. There is no evidence of any effect of surface kinetics, even at conditions near equilibrium pH, except in the presence of dissolved sulfate.

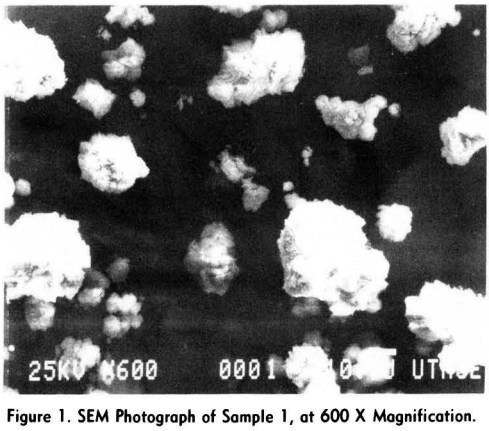

Figure 1. SEM Photograph of Sample 1, at 600 X Magnification.

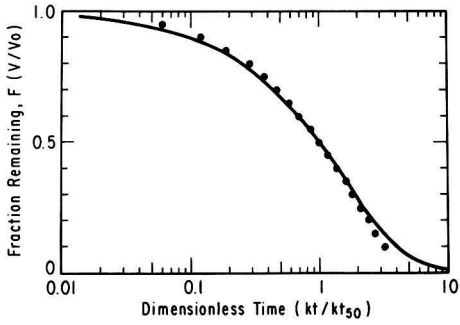

Figure 2. Experimental Rate Constant Determination.

Effects of Particle Size/Shape and Sulfate Content in Solids

Three batches of $CaSO_3 \cdot 1/2H_2O$ samples with different sulfate content and particle size/shape were used in a series of dissolution experiments. As shown in Figure 3 the experimental data were best represented using a Sherwood number of 3.4 with seed 1, 3.8 with seed 3, and 4.0 with seed 5. The stagnant mass transfer model with a Sherwood number of 2 underpredicted the dissolution rates due to the deviation of the calcium sulfite particle size/shape from small diameter and smooth spheres. Values of the Sherwood number calculated from Toprac's correlation [17] with limestone particles using average particle sizes are 3.42, 2.78, and 3.61, respectively. Solids with lower $CaSO_4$ content tend to have lower dissolution rates with decreased equilibrium pH. The experimental data were best represented by letting K_{sp} vary with sulfate content (Table 3). The deduced values of K_{sp} are between those used by Radian [22] and Bechtel [23].

Effects of Temperature

Higher temperature affects $CaSO_3 \cdot 1/2H_2O$ dissolution rate by increasing diffusion coefficients and reducing $CaSO_3 \cdot 1/2H_2O$ solubility (K_{sp}). Figure 4 shows that at low pH, mass transfer is important and calcium sulfite dissolves faster because of higher diffusivities. At high pH,

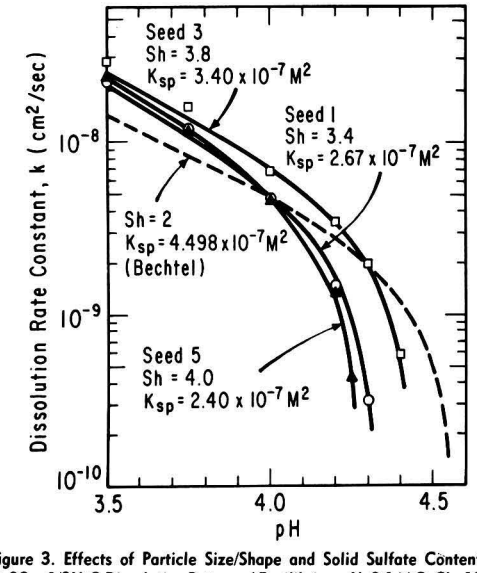

Figure 3. Effects of Particle Size/Shape and Solid Sulfate Content on $CaSO_3 \cdot 1/2H_2O$ Dissolution Rates and Equilibrium pH, 0.1 M $CaCl_2$, 10mM S^{+4}, 23°C, Curves Calculated by The Mass Transfer Model.

TABLE 3. ADJUSTED SH AND K_{sp} OF $CaSO_3 \cdot 1/2H_2O$ AS A FUNCTION OF SOLID SULFATE CONTENT AND TEMPERATURE

$CaSO_3 \cdot 1/2H_2O$ Seed Crystal	Sample 1	Sample 2	Sample 3
Mole% $CaSO_4$	3.4	10.7	1.0
K_{sp} at 23°C (M^2)	2.67×10^{-7}	3.40×10^{-7}	2.40×10^{-7}
K_{sp} at 55°C (M^2)	1.12×10^{-7}	1.44×10^{-7}	1.01×10^{-7}
Sherwood No.	3.4	3.8	4.0

chemical equilibrium is important and the effect of the solubility product dominates, so that calcium sulfite has a lower dissolution rate. The value of K_{sp} at 55°C for seed 1 was implied to be only 42% of that at 23°C, corresponding to a heat of solution of −2.6 kcal/gmol (Table 3).

Effects of pH and Dissolved Sulfite

The effects of pH and total dissolved sulfite (S^{+4}) on calcium sulfite dissolution rate are shown in Figure 5. At low pH, the pH has a strong and almost linear effect on dissolution rate, suggesting that H^+ diffusion determines the dissolution rate of calcium sulfite. At high pH, however, the dissolved sulfite is significant because chemical equilibrium becomes important. The mass transfer model with adjusted K_{sp} values predicts the dissolution rates very well.

Effects of Dissolved Sulfate

The presence of sulfate in the aqueous solution reduces the $CaSO_3 \cdot 1/2H_2O$ dissolution rate. Figure 6 is a plot of the experimental rate constant k versus sulfate concentration at pH 4.2, in a solution of 0.1 M $CaCl_2$ and 10 mM S^{+4}. It shows that the presence of dissolved sulfate strongly inhibits the calcium sulfite dissolution rate.

In terms of the mass transfer model, dissolved sulfate appears to reduce the Sherwood number (Figure 6). Dissolved sulfate could shift Sh by essentially stopping dissolution on certain crystal faces without affecting dissolution of the other faces. Therefore the effective area is reduced, but the dissolution rate is still controlled by mass transfer.

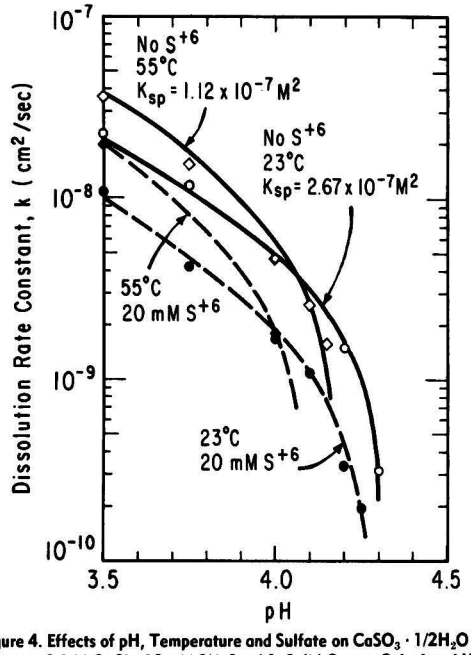

Figure 4. Effects of pH, Temperature and Sulfate on $CaSO_3 \cdot 1/2H_2O$ Dissolution, 0.1 M $CaCl_2$, 10 mM S^{+4}, Seed 1, Solid Curves Calculated Using Sh = 3.4.

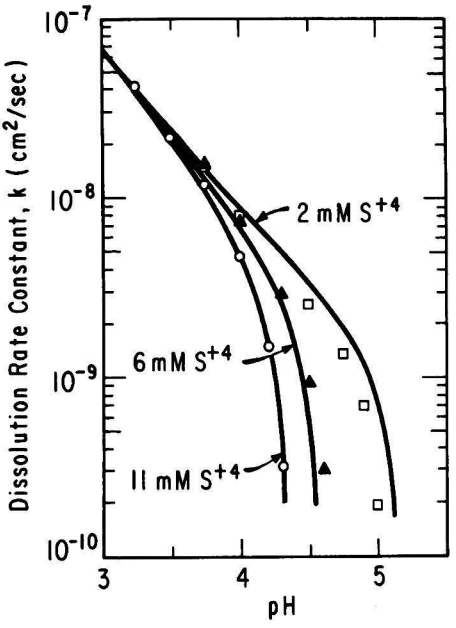

Figure 5. Effects of pH and S^{+4} on $CaSO_3 \cdot 1/2H_2O$ Dissolution, 0.1 M $CaCl_2$, 23°C, Seed 1, Curves Calculated Using $K_{sp} = 2.67 \times 10^{-7}$ M^2, Sh = 3.4.

Figure 7 represents the experimental rate constant k as a function of pH and dissolved sulfate concentration. The presence of dissolved sulfate reduced calcium sulfite dissolution rate at both high pH and low pH. As shown previously in Figure 8, the presence of dissolved sulfate at high temperature reduces $CaSO_3 \cdot 1/2H_2O$ dissolution rate in the same manner as it does at room temperature. Therefore the role of dissolved sulfate in calcium sulfite dissolution is not strongly affected by the temperature change.

Effects of Ionic Environment and Solution Composition

As shown in Figure 8, the dissolution rate of calcium sulfite was measured in five different solution compositions of the same ionic strength (0.3 eq/l). Dissolved Ca^{++} has a strong effect on dissolution rate and equilibrium pH because it directly determines the solubility product of calcium sulfite in the aqueous solution. However, dissolved Mg^{++} makes $CaSO_3 \cdot 1/2H_2O$ dissolve faster because it forms an ion pair with $SO_3^=$. The mass transfer model accounts for this effect. The agreement of experimental and

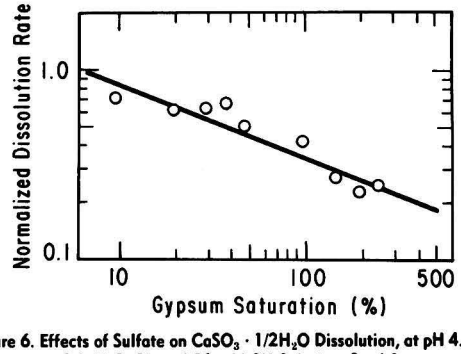

Figure 6. Effects of Sulfate on $CaSO_3 \cdot 1/2H_2O$ Dissolution, at pH 4.2, in 0.1 M $CaCl_2$ and 10 mM S^{+4} Solution, Seed 1.

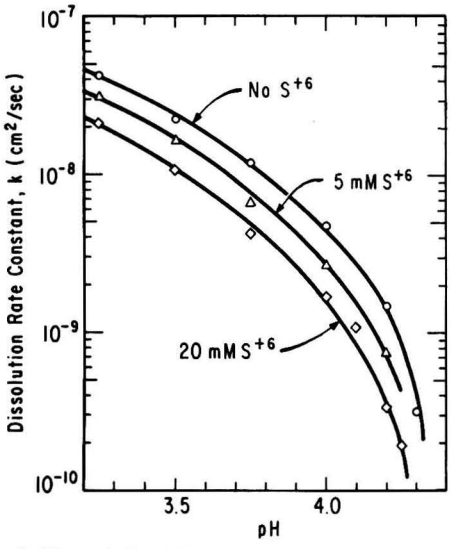

Figure 7. Effects of pH and Sulfate on $CaSO_3 \cdot 1/2H_2O$ Dissolution, at 23°C, in 0.1 M $CaCl_2$ and 10 mM S^{+4} Solution, Seed 1.

calculated results indicates that Mg^{++} does not have additional effects on calcium sulfite dissolution, such as reducing the rate of surface reaction by adsorption.

In Figure 9, the $CaSO_3 \cdot 1/2H_2O$ dissolution rates were measured at a higher ionic strength (0.9 eq/l). The same effects of the dissolved Ca^{++} and Mg^{++} were observed. The mass transfer model predicts the dissolution rates fairly well but the deviation of Mg^{++} data suggests that some correction or modification of the diffusivities or equilibrium constants in the solution equilibrium program may be necessary at higher ionic strength.

NOMENCLATURE

C = concentration (M)
D = diffusivity (cm^2/sec)
D′ = pseudo-diffusivity (cm^2/sec)

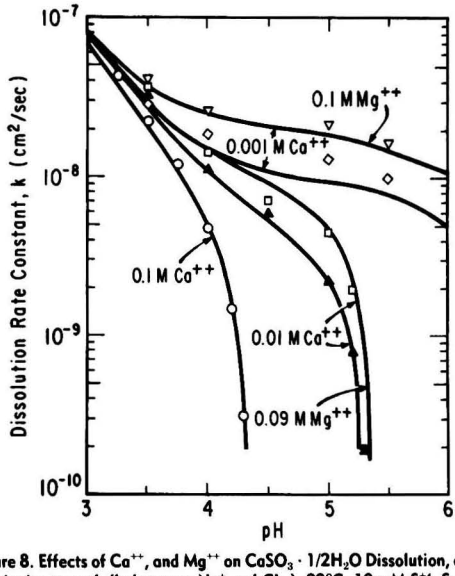

Figure 8. Effects of Ca^{++}, and Mg^{++} on $CaSO_3 \cdot 1/2H_2O$ Dissolution, at 0.3 eq/l ionic strength (balance as Na^+ and Cl^-), 23°C, 10 mM S^{+4}, Seed 1, Curves Calculated Using $K_{sp} = 2.67 \times 10^{-7}$ M^2, Sh = 3.4.

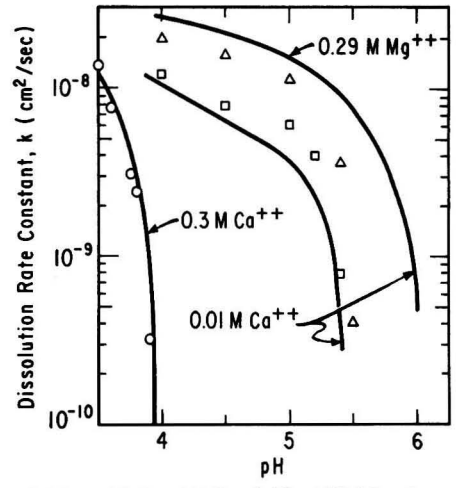

Figure 9. Effects of Ca^{++}, and Mg^{++} on $CaSO_3 \cdot 1/2H_2O$ Dissolution, at 0.9 eq/l ionic strength (balance as Na^+ and Cl^-), 23°C, 10 mM S^{+4}, Seed 1, Curves Calculated Using $K_{sp} = 2.67 \times 10^{-7}$ M^2, Sh = 3.4.

Fa = Faraday constant = 23,062 (cal/volt-equiv)
K = equilibrium constant
K_{sp} = solubility product (M^2)
M = molarity (gmol/liter)
R = gas constant = 1.987 (cal/gmole-°K)
Sh = Sherwood number ($k_c d_p/D$)
SK_{sp} = pseudo-solubility product (M^2)
T = temperature (°K)
V = volume of particle (cm^3)
Y_{SO4} = mole fraction of sulfate content
a = activity (gmole/liter)
d_p = particle diameter (cm)
k = rate constant (cm^2/sec)
k_c = mass transfer coefficient (cm/sec)
r = radius (cm)
t = time (sec)
λ_o = equivalent ionic conductivity at infinite dilution (cm^2/ gmole-ohm)
η = viscosity (poise)
ρ = density (gram/cm^3)
ρ_m = molar density (gmol/cm^3)
ϕ = volume fraction
[ ] = concentration (M)
[ ]′ = pseudo-concentration (M)

Superscripts

+ = positive charge
− = negative charge
o = ion pair, degrees

Subscripts

b = bulk solution
i = solid-liquid interface
o = initial state

LITERATURE CITED

1. Chan, P. K. and G. T. Rochelle, "Limestone Dissolution: Effects of pH, CO_2, and Buffers Modelled by Mass Transfer", *ACS Symp. Ser.*, **188**, 75-97 (1982).
2. Rochelle, G. T. and C. J. King, "The Effects of Additives on Mass Transfer in CaO/$CaCO_3$ Slurry Scrubbing of SO_2 From Waste Gases", *Ind. Eng. Chem. Fundam.*, **16**, 67-75 (1977).
3. Chang, C. S. and G. T. Rochelle, "Mass Transfer Enhanced by Equilibrium Reactions", *Ind. Eng. Chem. Fundam.*, **21**, 379-385 (1982).
4. Chang, C. S. and G. T. Rochelle, "SO_2 Absorption Into Aqueous Solutions", *AIChE J.*, **27**, 292-298 (1981).

5. Chang, C. S. and G. T. Rochelle, "Effect of Organic Acid Additives on SO_2 Absorption into $CaO/CaCO_3$ Slurries", *AIChE J.*, **28**, 261-266 (1982).
6. Weems, W. T., "Enhanced Absorption of SO_2 by Sulfite and Other Buffers", M. S. Thesis, University of Texas, Austin, Texas (1981).
7. Sada, E., H. Kumazawa and M. A. Butt, "Absorption of Sulfur Dioxide into Aqueous Slurries of Sparingly Soluble Fine Particles", *Chem. Eng. Sci.*, **35**, 771-777 (1980).
8. Sada, E., H. Kumazawa and H. Nishimura, "Absorption of Sulfur Dioxide into Aqueous Double Slurries Containing Limestone and Magnesium Hydroxide", *AIChE J.*, **29**, 60-65 (1983).
9. Borgwardt, R. H., Proceedings: Symposium on Flue Gas Desulfurization, EPA-600/2-76-136a, 117-144 (1976).
10. Borgwardt, R. H., Proceedings: Symposium on Flue Gas Desulfurization, EPA-600/7-78-058a (1977).
11. Erwin, J., C. C. Wang and J. L. Hudson, "A Model of Oxidation in Calcium Sulfite Slurries", *ACS Symp. Ser.*, **188**, 191-200 (1982).
12. Nurmi, D. B., J. W. Overman, J. Erwin and J. L. Hudson, *ACS Symp. Ser.*, **188**, 173-189 (1982).
13. Garside, J., J. W. Mullin and S. N. Das, "Growth and Dissolution Kinetics of Potassium Sulfate Crystals in An Agitated Vessel", *Ind. Eng. Chem. Fundam.*, **13**, 299-305 (1974).
14. Plummer, L. N., T. M. L. Wigley and D. L. Parkhurst, "The Kinetics of Calcite Dissolution in CO_2-Water Systems", *Am. J. Sci.*, **278**, 179-216 (1978).
15. Meserole, F. B., R. L. Glover and D. A. Stewart, "Studies of The Major Factors Affecting Magnesium Limestone Dissolution", *ACS Symp. Ser.*, **188**, 99-111 (1982).
16. Chan, P. K. "$CaCO_3$ Dissolution in SO_2 Scrubbing Solution, Mass Transfer Enhanced by Chemical Reactions", M. S. Thesis, University of Texas, Austin, Texas (1981).
17. Toprac, A. J. and G. T. Rochelle, "Limestone Dissolution in Stack Gas Desulfurization", *Environ. Prog.*, **1**, 52-58 (1982).
18. Jones, B. F., P. S. Lowell and F. B. Meserole, "Experimental and Theoretical Studies of Solid Solution Formation in Lime and Limestone SO_2 Scrubbers.", EPA-600/2-76-273a (1976).
19. Setoyama, K. and S. Takahashi, "Solid Solution of Calcium Sulfite Hemihydrate and Calcium Sulfate", *Yogyo-Kyokai-Shi*, **86**, 56-62 (1978).
20. Weisberg, J., *Bl. Soc. Chim.*, **3**, (15) 1247-1250 (1896).
21. Linden, T. van der., *J. Soc. Chem. Ind.*, **36**, 96 (1917).
22. Lowell, P. S., D. M. Ottmers, T. I. Strange, K. Schwitzgebel and D. W. DeBerry, "A Theoretical Description of The Limestone Injection - Wet Scrubbing Process", Radian, Contract No. CPA-22-69-138 (1970).
23. Epstein, M., "EPA Alkali Scrubbing Test Facility: Summary of Testing Through October 1974", EPA-650/2-75-047 (1975).
24. Faist, M. B., C. E. Riese and L. Gevirtzman, "Species Distribution Model: A General Computer Program to Calculate The Distribution of Chemical Species Among Several Multicomponent Phases", DOE Contract No. DE-AC21-80MC14549, Radian (1981).
25. Prada, R. E., M. S. Thesis, University of Texas, Austin, Texas (1981).
26. Mehta, R. R., "Modeling of SO_2 Removal and Limestone Utilization in Slurry Scrubbing with Forced Oxidation", M. S. Thesis, University of Texas, Austin, Texas (1982).
27. Chan, P. K. and G. T. Rochelle, "Modeling of SO_2 Removal by Limestone Slurry Scrubbing: Effects of Chlorides", Presented at EPA/EPRI Symposium on Flue Gas Desulfurization, New Orleans, November 1-4, 1983.
28. Ulrich, R. K., G. T. Rochelle and R. E. Prada, "Enhanced Oxygen Absorption into Bisulfite Solutions Containing Transition Metal Ion Catalysts", Submitted to *Chem. Eng. Sci.*, (1984).
29. Tseng, P. C., "Calcium Sulfite Hemihydrate Dissolution and Crystallization", Ph.D. Dissertation, University of Texas, Austin, Texas (1984).
30. Tseng, P. C. and G. T. Rochelle, "Calcium Sulfite Hemihydrate: Crystal Growth Rate and Crystal Habit", *Env. Prog.*, **5**, 5-11 (1986).

Philip C. H. Tseng received his B.S. Ch.E. from National Taiwan University, M.S. from National Tsing Hua University, and Ph.D. from the University of Texas at Austin. He was previously employed as a research chemical engineer for Chinese Petroleum Corporation in Taiwan. He is currently employed by Exxon Research and Engineering Company as a post-doctoral fellow in the Corporate Research Center at Clinton, New Jersey. His areas of research and experience have been in polymers, catalysis, flue gas desulfurization, crystallization, gas treating, and membrane separations.

Gary T. Rochelle is an Associate Professor of Chemical Engineering and holds the Frank A. Liddell, Jr. Centennial Teaching Fellowship at the University of Texas at Austin. He received degrees in chemical engineering from the Massachusetts Institute of Technology (BS/MS, 1971) and the University of California at Berkeley (Ph.D., 1977). He was employed by the U.S. EPA at Durham, NC from 1971 to 1973 and has been at the University of Texas since 1977. His research interest has been focused on flue gas desulfurization technology with over 20 publications in that field.

Biological Treatment of a Landfill Leachate in Sequencing Batch Reactors

A landfill leachate is treated, after mixing with chemical manufacturing wastewaters, by activated carbon adsorption. Biotreatment of the combined wastewater in sequencing batch reactors (SBRs) reduced the carbon requirement by 90%. Excellent treatment efficiency was consistently achieved under a variety of operating conditions: wastewater TOC, feed rate, hydraulic retention time, MLSS, organic loading, temperature, and cycle time. The SBR performance was unaffected when wastewater feeding was suspended during weekends and holidays. Results obtained in 1-L SBRs were reproduced in 12-L and 500-L units. The experimental data served as the basis for design of a full-scale SBR-adsorption system. The integrated wastewater treatment system would produce a better quality effluent at a lower overall cost. Biodegradation rates for some of the more persistent wastewater constituents were enhanced in batch bioreactors which were supplemented with strains of bacteria isolated from the landfill site.

Wei-chi Ying, Robert R. Bonk, Vernon J. Lloyd, Stanley A. Sojka, Occidental Chemical Corporation, Grand Island, NY 14072

The Hyde Park Landfill site is located in an industrial complex in the extreme northwest corner of the Town of Niagara, New York (Figure 1). The site is roughly triangular in shape and occupies approximately 6.1 hectares. The Hyde Park Landfill was used from 1953 to 1975 as a disposal site for an estimated 73000 metric tons of chemical waste, including chlorinated organics. A compacted clay cover was placed over the landfill in 1978, and a tile leachate collection system was installed around the perimeter in 1979.

The leachate is collected in a sump, at the end of the tile system, and is then pumped to a two-compartment lagoon.

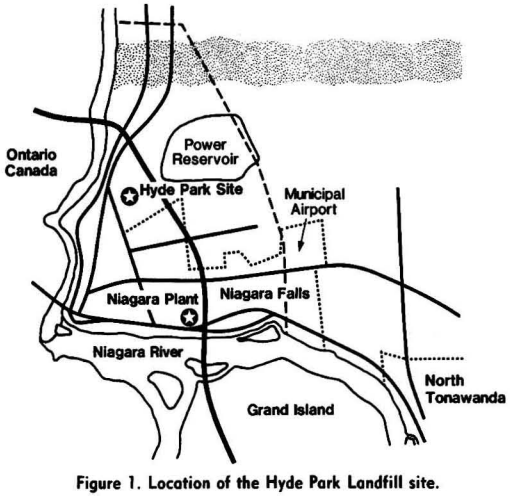

Figure 1. Location of the Hyde Park Landfill site.

The contents of the first lagoon compartment are allowed to separate, and the supernatant overflows by gravity into the second compartment. From here it is trucked to the treatment facility at the nearby Niagara Plant. The leachate production rate for the last three years averaged about 230 cubic meters per week. Additional leachate collection systems at Hyde Park and other sites will be constructed in the near future, and the total volume of wastewaters to be treated will increase substantially.

At the treatment site, the trucked leachate is mixed with plant wastewaters and is stored in four storage tanks, each about 90 cubic meters in capacity. After pH adjustment, sometimes necessary to insure that the pH of the plant discharge is between 5.0 and 10.0, and settling of suspended solids, the combined wastewater is pumped through an on-line 50-micron bag filter, and the filtrate then is treated in a two-stage activated carbon adsorption system. In the first stage of treatment, the wastewater downflows through two smaller adsorbers (900 kg of Calgon F-300 each) in series for removal of carry-over organic liquids. Dissolved organic compounds are removed in the second stage adsorption system consisting of three larger serial adsorbers (9000 kg of Calgon Service carbon each). The effluent, which meets the treatment criteria, is discharged to a municipal sewer.

The present wastewater treatment by the conventional adsorption technology, although producing a suitable quality effluent, is not the best long-term solution. The adsorption system would have to be substantially expanded to handle the expected increase in wastewater flowrate. The future carbon consumption rate would rise accordingly; the cost forecast for carbon adsorption service alone is about 21 million dollars over the next ten years. Clearly there is a strong economic incentive to explore other treatment technologies. The technical impetus derives from the fact that the adsorptive capacity of carbon for

any specific compound of concern is under-utilized due to simultaneous adsorption of other compounds. Table 1 shows that cumulative loadings of five major leachate organic constituents at the end of an adsorption cycle were far less than those estimated from the adsorptions isotherms for the same compounds in pure water. The fact that the TOC and o-chlorobenzoic acid loadings were almost the same as the adsorptive capacities predicted by the leachate isotherms indicates that the low bed utilization rates were primarily the result of competitive adsorption rather than poor adsorber design and/or operational problems. Any treatment technology capable of reducing this competition could extend the adsorption service cycle and would thus be worthwhile to pursue. Biodegradation in sequencing batch reactors (SBRs) was selected as the appropriate waste treatment process to reduce the future carbon consumption rate of an expanded adsorption system.

EXPERIMENTAL SECTION

Analytical Methods:

Extensive efforts were made in this investigation for the identification of constituents in, and analysis of, raw, pretreated, SBR-treated, and carbon-adsorbed wastewater samples. Measurements for parameters commonly used for characterization of wastewater were made in accordance with the methods given in the *Standard Methods* [1]. These parameters include: pH (Section 423), total organic carbon (TOC, Section 505), biological oxygen demand (BOD, 507), chemical oxygen demand (COD, 508 A), total dissolved solids (TDS, 209 C), suspended solids (SS, 209 D), volatile suspended solids (VSS, 209 E), orthophosphate phosphorus (P-PO_4, 424 F), acid-hydrolyzable phosphorus (acid-P, 424 B), total phosphorus (total-P, 424 C), ammonia nitrogen (N-NH_4, 417 B), nitrate nitrogen (N-NO_3, 418 B), nitrite nitrogen (N-NO_2, 419), total kjeldahl nitrogen (TKN, 420 B), dissolved oxygen (DO, 421 F), oxygen consumption rate (213 A), turbidity (214 A), and settled sludge volume (213 B). Total organic halide (TOX) was analyzed by a Dohrmann DX-20 TOX analyzer using EPA Method 450.1. Concentrations for chlorendic acid (HET acid), phenol, benzoic acid, and o-, m-, p-chlorobenzoic acids (CBAs) were estimated by a high performance liquid chromatography (HPLC) method, with a Perkin-Elmer Model 3B, adapted for analysis of the wastewater samples. The sample aliquot was acidified to pH < 2 and then successively extracted three times with methyl-t-butyl ether. The specific compounds in the extract were determined by HPLC on a C_{18} column (30 cm × 4.6 mm) using a 2 cc/min gradient elution solution initially composed of 18% CH_3CN in water containing 0.01% acetic acid. Using a program gradient curve of 3 over a 40-minute span, the solvent was changed to a final composition of 60% CH_3CN in water also containing 0.01% acetic acid. Detection was made at 214 nm, and the concentration was estimated against a standardization curve prepared under the same conditions.

Concentration of pollutants in raw leachate, and thus the combined wastewater, fluctuated widely over the study period; TOC had a range from 800 to 10000 mg/L, and SS from 200 to 2000 mg/L. Table 1 presents the composition, in terms of gross organic parameters (TOC and TOX) and their major components, of various samples — raw leachate, combined wastewater feed, and adsorber effluent taken during a carbon adsorption column study. Characteristics of typical raw and pretreated (neutralization, aeration, and sedimentation) leachates are shown in Table 2.

Activated Carbon Adsorption Isotherms:

Adsorption isotherm experiments were frequently conducted for testing the adsorptive capacity of carbon for TOC, TOX, and their major components. The conventional EPA procedure [2] for carbon isotherm was employed. The Freundlich adsorption isotherm model was utilized to correlate the adsorptive capacity (X/M, mg adsorbed/g carbon) with the residual concentration (C_f,

TABLE 2. CHARACTERISTICS OF TYPICAL RAW AND PRETREATED HYDE PARK LEACHATES

Parameter[a]	Raw leachate	Pretreated leachate[b]
pH	4.3	7.5
TOC	3500	3200
COD	10040	9200
BOD	7500	7200
SS	900	80
VSS	300	40
TDS	25700	22400
P-PO_4	<1	<1
Acid-P	3	3
Total-P	131	92
N-NH_4	150	130
TKN	180	160
N-NO_3	20	20
N-NO_2	<5	<5

a. All values, except pH, are given in mg/L.
b. Pretreatment consisted of neutralization with NaOH to a pH of 7.5, two hours of aeration, and two hours or longer of settling.

TABLE 1. ADSORPTIVE CAPACITIES OF CARBON FOR MAJOR LEACHATE CONSTITUENTS

	Concentration (mg/L)			Adsorptive capacity (mg adsorbed/g carbon)		
Concentration parameter	raw leachate	combined[a] waste feed	adsorber[b] effluent	carbon[c] loading	leachate[d] isotherm	pure[e] compound isotherm
pH	5.3	5.5-6.4	5.5-6.4	5.5-6.4	4.9-5.5	5.0-6.0
Phenol	981	780	$ND_{0.1}$[f]	41.0	74.9	166
Benzoic acid	830	910	0.8	48.0	74.1	171
o-chlorobenzoic acid	562	372	7.4	19.6	22.9	109
m-chlorobenzoic acid	61	120	$ND_{0.5}$	6.4	23.0	160
p-chlorobenzoic acid	40	80	$ND_{0.1}$	4.2	15.7	171
TOC	3080	2618	318	137	143	
TOX	264	299	2.7	15.8	11.7	

a. Average concentrations for the adsorber feed during an adsorption service cycle.
b. Concentrations were measured at the end of an adsorption cycle.
c. Total removal of the compound at the end of an adsorption cycle.
d. Capacities were estimated at the feed concentration from the raw leachate isotherms.
e. Capacities were estimated at the feed concentration from the pure compound isotherms.
f. ND_x = not detected at a detection limit of x mg/L.

mg/L) for the purpose of estimating the treatment capacity of the adsorber at a given feed concentration. The isotherm has the following form:

$$X/M = k \times C_f^{1/n}$$

where k, and 1/n are constants characterizing the adsorption isotherm [3].

Feasibility Study:

Soon after the existing adsorption system was installed, large populations of bacteria were found in the treated effluent. Similar observations of bacterial growth in the carbon adsorbers were reported [4]. The TOC, COD and concentrations for some of their major components of a refrigerated raw leachate sample were found to decrease over time. The rate of concentration reduction increased when the sample was stored at room temperature. The BOD to TOC ratios for several leachate and the combined wastewater samples were all greater than 2, indicating that the organic compounds in these samples were readily biodegradable. Experiments on bio-utilization of specific organic compounds by bacteria isolated from the Hyde Park Landfill site were conducted at the University of Michigan [5] and Battelle Columbus Laboratories [6]. Table 3 shows that several strains of bacteria present in the landfill site were capable of metabolizing many of the more persistent leachate constituents. Biological processes were therefore evaluated for treating the combined wastewater before entering the carbon adsorption system.

Figure 2 depicts the five sequential steps of the SBR biotreatment process. The wastewater is fed, during FILL, to a tank, which contains acclimated activated sludge from the previous cycle. Aeration and mechanical mixing are provided while feeding, or subsequently during REACT, to enhance the rate of aerobic biodegradation. After the mixed liquor is biologically stabilized, air and mixing are stopped, and clarification takes place in the SETTLE step. During DRAW, the clear supernatant is withdrawn from the reactor for discharge or, if needed, additional treatment. The IDLE period finally completes the SBR cycle. The five SBR steps are often overlapped, and one or two steps may be omitted in a particular treatment cycle. The withdrawal of effluent may start as soon as a clear zone of supernatant is formed, and the wastewater feeding may begin immediately after the completion of the DRAW step of the last SBR cycle [7]. Many combinations of feeding, aeration, and mixing strategies are possible. The required nutrients are either supplemented to the feed or added directly to the bioreactor. The sludge wasting is accomplished by removing a portion of the settled sludge in the DRAW or IDLE step. The optimum SBR operating and

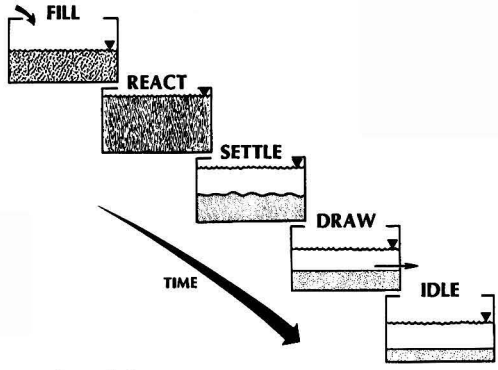

Figure 2. Illustration of SBR biotreatment technology.

cycle schedules must be experimentally established for a wastewater to achieve the specific treatment objectives. Examples of the SBR schedules employed in this investigation are given in Table 4.

The SBR biotreatment is essentially a fill-and-draw activated sludge process. Its operation and control for bench-scale experiments are simple, and the requirements for laboratory space and wastewater volumes are small. Relative to the continuous activated sludge process, better comparative study is possible since more parallel SBR units can be operated simultaneously using smaller tanks. It is therefore often the process of choice for study of wastewater treatability [8, 9]. The advantages of more complete treatment [10], greater operational flexibility to accommodate changing feed characteristics, intermittent treatment [11], and single tank for biodegradation and sludge separation make the SBR process an attractive technology for treating municipal and industrial wastewaters [12-16].

Preliminary Biotreatment Results:

Initial study on SBR treatment of leachate was conducted at the University of Notre Dame. The results (Table 5) show that Hyde Park leachate was well treated in the small (working volume = 2 L) SBRs. About 90% TOC reduction was achieved under a 24-hr cycle and 10-d hydraulic retention time (HRT) schedule. Supplementation of a strain of bacteria (SS3) isolated from the landfill site had improved the treatment efficiency [17]. Nitrogen and phosphate nutrients were not supplemented. The operating and cycle schedules are given in Table 4 (SBRs I thru IV).

TABLE 3. NUTRITIONAL VERSATILITY OF OCC BACTERIA ISOLATED FROM THE HYDE PARK LANDFILL SITE[a]

Organic carbon source	H1	H2	H3	H4	H5	H7	SS1	SS3
o-chlorotoluene	+++[b]	+++	+++	+++	+++	++	+++	+++
m-chlorotoluene	+++	+++	+++	+++	+++	--[c]	+++	+++
3,4-dichlorotoluene	+++	+++	+++	+++	+++	--	+++	+++
2,6-dichlorotoluene	+++	+++	+++	+++	+++	++	+++	+++
Xylenes	+	+	+	+	+	+	+	+
Benzoic acid	++++	--	++++	++++	++++	--	++++	++++
p-chlorobenzoic acid	+++	++	+++	+++	+++	+	+++	+++
2,4-dichlorobenzoic acid	+++	+++	+++	+++	+++	--	+++	+++
2,4-dichlorophenoxyacetic acid	+++	++	+++	+++	+++	+	+++	+++
2,4-dichlorophenol	+	+	--	--	+	+	+	+
2,4,5-trichlorophenoxyacetic acid	++	+	++	++	++	+	++	++

a. Observations were made after incubation at 25°C for 1 week. The bacteria were inoculated onto agar plates containing 300 mg/L of the specific compound as the sole source of organic carbon.
b. Growth relative to that found in an agar plate containing glucose (++++) as the organic carbon source.
c. No growth.

TABLE 4. EXAMPLES OF SBR OPERATING AND CYCLE SCHEDULES

Operating schedule	Sequencing batch reactor I	II	III	IV	A	B	C
Leachate feed	(	diluted	raw[a]	)	(	pretreated[b]	)
Sterilization of feed	no	no	yes	yes	(	no	)
Bacterial supplementation	n	SS3[c]	no	SS3	(	no	)
SBR cycle time, h	(		24	)	(	24	)
Working volume, L	(		2	)	(	.300	)
Feeding, % working volume	(		10	)	20	20	50
HRT, d	(		10	)	5	5	2
MLSS, mg/L	(	not controlled		)	5000	10000	10000
Time per SBR cycle, h							
FILL (air & mixing)	(	10		)	(	6	)
REACT (air & mixing)	(	12		)	(	10	)
SETTLE	(	1		)	(	2	)
DRAW	(	0.5		)	(	5	)
IDLE	(	0.5		)	(	1	)

a. The raw leachate was neutralized to pH of 7.5, filtered, and diluted to TOC about 2300 mg/L. Nutrients (ammonia and phosphate) were not supplemented.
b. The raw leachate was neutralized to pH of 7.5, aerated for two hours, and then settled for at least two hours. No dilution was made. Ammonia and phosphate were supplemented to a TOC/N-NH_4/P-PO_4 ratio of 150/10/2.
c. The nutritional versatility of the OCC bacteria is given in Table 3.

Treatability Study:

Although good biotreatment results were obtained in the Notre Dame study, long term SBR performance data under a variety of conditions were necessary to design a full-size SBR system. A comprehensive treatability study was later conducted to: 1) Establish the best start-up procedure 2) Identify the nutrient requirements 3) Treat the combined wastewater 4) Define the optimum strategies for achieving the maximum TOC reduction under various SBR operating and cycle schedules 5) Develop a procedure for improving the performance of an upset SBR 6) Qualify the sludge production rate and select a method for its disposal 7) Verify the carbon saving due to biotreatment of wastewater 8) Study the benefits of bacterial supplementation. The treatability study was undertaken in several experimental programs, from December 1982 through March 1984, utilizing three sets of bioreactors: four 1-L, four 12-L, and three 500-L. Table 6 presents the treatability study programs and the associated specific objectives. Table 7 outlines the routine maintenance, sampling, and monitoring schedule for the SBRs.

RESULTS AND DISCUSSION

Start-Up Procedure:

The return activated sludge from a nearby POTW (Wheatfield, NY) was used to seed the bioreactors for treating Hyde Park leachate and the combined waste-

TABLE 5. PRELIMINARY RESULTS OF BIOTREATMENT OF HYDE PARK LEACHATE[a]

SBR[b] sample	MLSS (mg/L)	OUR[c] unspiked (mg O_2/g	OUR[c] spiked[d] MLVSS-h)	TOC feed (mg/L)	TOC effluent (mg/L)
I	3600 (31)	4.9 (25)	26 (25)	2300	260 (29)
II (SS3)	3700 (31)	4.6 (22)	21 (26)	2300	200 (31)
III	2800 (50)	5.1 (40)	48 (40)	2400	220 (48)
IV (SS3)	2700 (52)	5.7 (43)	52 (44)	2400	180 (48)

a. Values shown are average of the number of measurements indicated in the parenthesis.
b. The experimental conditions are described in Table 4.
c. OUR = oxygen consumption rate in mg O_2/L-h divided by the MLVSS of the test sample.
d. OURs were measured two minutes after 20 μl of diluted leachate (2000 mg TOC/L) was spiked to the 2.0 mm Gilson Oxygraph cell.

TABLE 6. EXPERIMENTAL PROGRAMS FOR THE SBR TREATABILITY STUDY

Program	Objectives	Tank/adsorber used
A	determine the nutrient (N and P) requirements, compare methods for wastewater feed preparation, obtain performance data for replicate units, and study the effect of feeding period	four 1-L and four 12-L SBRs
B	compare performance in treating full strength leachate with the combined waste, simulate full size SBR operation, and develop procedure for improving the performance of upset SBR	three 500-L and four 12-L SBRs
C	verify carbon savings, correlate carbon saving to biotreatment performance, select the best carbon, and perform bioassay on raw and treated leachates	three 500-L SBRs, two 2.5-cm and two 7.5-cm adsorbers
D	determine the fate of volatile constituents establish aeration requirement for air-stripping, and test air pollution control device	two feed tanks, three 500-L SBRs, one vapor adsorber
E	quantify sludge production rate, characterize the precipitation and biological sludges, test sludge digestion, compaction, and dewatering	two feed tanks, three 500-L SBRs, one 500-L digester
F	obtain performance data at 1-d, 1.7-d, 2-d, 5-d, and 10-d HRT under the 24-h cycle; operate the SBRs without weekend feedings	three 500-L, four 12-L, and four 1-L SBRs
G	obtain performance data under 12-h and 24-h cycles; establish the optimum SBR schedule	four 12-L SBRs
H	obtain performance data at temperatures of 9, 12, 15, and 20°C, determine the maximum organic loading for winter operation	four 1-L SBRs
I	study effects of bacterial supplementation	four 12-L and four 1-L SBRs

TABLE 7. ROUTINE MAINTENANCE, SAMPLING, AND MONITORING SCHEDULE FOR SBRs

	Monday	Tuesday	Wednesday	Thursday	Friday
pH[a]	x	x	x	x	x
Turbidity	x		x		x
TOC	x	x	x	x	x
Settled sludge volume	x			x	
Mixed liquor SS/VSS	x/x			x	
Sludge wasting[b]		x			x
Effluent SS/VSS		x/x			x
$N\text{-}NH_4$		x			x
$N\text{-}NO_2/N\text{-}NO_3$		x			x
$P\text{-}PO_4$		x			x

a. Acid or base was used to maintain pH within 7.0-7.5 after REACT
b. The volume of the settled sludge to be wasted each time, VW (L):

$$VW = VT \times (MLSS1 - MLSS2)/(MLSS1 \times TMV/SV)$$

where, VT – working volume (L), after FILL,
TMV – the sample volume used in measuring the settled sludge volume,
SV – settled sludge volume after two hours of settling,
MLSS1 – mixed liquor suspended solids (mg/L) before wasting,
MLSS2 – the MLSS to be maintained in the reactor.
Tapwater was used for making up the settled sludge volume wasted.

water. The SBRs, with more than half of the desired working volume filled with dilute POTW sludge (to MLSS = 6000 mg/L), were fed, over four days, at an increasing per cycle volume of wastewater to 10% of the reactor working volume (after FILL), i.e. 10-d HRT. The amount of effluent discharged was about 50% of the feeding until the full SBR working volume was attained. When treating a 3000 mg TOC/L leachate using a 10-d HRT and 24-hr cycle schedule, the effluent TOC was found to increase gradually to about 180 mg/L. No mass die-off of the seed sludge was observed, and the effluent SS was consistently less than 100 mg/L. Successful start-ups were accomplished without the use of any supplementary sources of organic carbon.

SBR Feed Preparation:

The feed preparation procedure was established in a series of experiments to compare the performance in treating two types of leachate feed — one prepared by neutralization (to pH = 7.5) and filtration, as practiced in the Notre Dame study, and the other by neutralization, oxidation by aeration (2 hr), and sedimentation (2 hr or longer). More complete reductions in TOC and its components, as well as greater MLVSS/MLSS ratios were achieved in the 1-L SBRs receiving the oxidized feed. The pretreatment procedure of neutralization, aeration, and sedimentation was employed to provide feed for the SBRs in all treatability programs. The wastewater feeds for the 1-L SBRs were prepared in 4-L beakers, and the feeds for the 12-L and 500-L SBRs were prepared in two large tanks (500 and 2000 L).

SBR Performances:

The nutrient requirements were determined utilizing the smaller (1-L and 12-L) SBRs operating at a 24-hr cycle schedule. The effects of nitrogen supplementation in the forms of $N\text{-}NH_4$ and $N\text{-}NO_3$ [*18*] can be seen from the results given in Table 8. The leachate feeds to SBRs II and III were respectively supplemented with sodium nitrate and ammonium hydroxide to a TOC/$N\text{-}NH_4$ or $N\text{-}NO_3$ ratio of 15, as established in a separate series of experiments. Since Hyde Park leachate is deficient in orthophosphate (Table 2), phosphoric acid was added to all feeds to provide a 30 mg/L of $P\text{-}PO_4$ for bacterial growth [*19*]. A 75-ml aliquot of pretreated leachate was fed to the SBRs four times in six hours; aeration and mixing were provided between the batch feedings. The results obtained from the 2.5-d HRT SBRs showed that both forms of nitrogen addition had improved the treatment efficiency. Although nitrate was an effective nitrogen source, ammonia was used in the subsequent treatability programs since it also neutralized the naturally acidic leachate and the combined wastewater. Results for SBR IV, which was operated similarly as SBR III but at 9°C, showed that excellent treatment was also accomplished at a lower temperature expected for the winter operation.

The optimum nutrient supplementation for the leachate was validated by the results of the 12-L SBRs, as shown in Table 9. SBR IV, with a nitrogen and phosphate supplemented feed (TOC/$N\text{-}NH_4$/$P\text{-}PO_4$ ratio of 150/10/2), accomplished the best treatment of the high TOC (8135 mg/L) leachate. Supplementing only N produced almost the same results as adding both N and P, indicating that the total-P in the leachate (Table 2) was available for bacterial synthesis. It is important to note that the high TOC leachate was very well treated in these SBRs. Aeration and mixing were provided during the 4-hr FILL period to accelerate the biodegradation process. The high MLSS of 10000 mg/L was at least partially responsible for the excellent SBR performances. A reactor with a MLSS of 5000 mg/L had failed early in this study program. All SBRs operated at a MLSS from 8000 to 13000 mg/L achieved at least 90% reduction in TOC and COD. Another important advantage of having established a wide range of acceptable MLSS is that the excess biological sludge can be wasted periodically at the operator's convenience.

Nitrification and denitrification were observed in a single SBR with no aeration during the last two hours of REACT. The SBR treatment can thus accomplish nitrogen removal as well [*20*]. The treatment efficiency was not adversely affected with up to 150 mg/L of $N\text{-}NH_4$ in the mixed liquor at the end of REACT.

TABLE 8. RESULTS OF BIOTREATMENT OF LEACHATE IN 1-L SBRs[a]

SBR[b] sample	TOC	TOX	HET acid	Phenol	Benzoic acid	o-CBA	m-CBA	p-CBA
	(			mg/L				)
Feed	1800	205	110	436	708	227	62	74
I effluent (no nitrogen)	283	126	84	13	28	98	26	21
II effluent (nitrate)	164	91	80	3	12	3	6	15
III effluent (ammonia, 20°C)	152	95	76	4	12	1	5	17
IV effluent (ammonia, 9°C)	155	88	69	3	11	1	<3	13

a. Samples were taken at the end of the program.
b. 24-h SBR cycle, HRT = 2.5 d (four 10% batch feedings in 6-h aerated FILL), MLSS = 10000 mg/L, working volume = 750 ml.

The second portion of Table 9 data show results obtained at much higher hydraulic loadings; SBR B was operated at a 1.7-d HRT (24-hr cycle and 60% feeding) and SBR III at a 1-d HRT (12-hr cycle and 50% feeding). Good performances were achieved, using again the high MLSS for reducing the food to biomass ratio, the F/M, in the SBRs and a lower feed rate for distributing the organic loading evenly over the 6-hr FILL period. Aeration and mixing were also provided to these highly loaded SBRs during FILL.

The 500-L SBRs were utilized for simulating full scale treatment of leachate alone, and of the combined wastewater. They provided data on long-term treatment performance, under various operating conditions, fate of volatile compounds, and production and disposal of sludges. The feed was prepared by neutralization, aeration, nitrogen supplementation, and sedimentation in a 2000-L tank. Table 10 presents the results of the pilot-scale SBR biotreatment with two HRTs (2 and 5 d) and two MLSSs (5000 and 10000 mg/L). The better performance of SBR B relative to SBR A demonstrated again the advantage of the high MLSS. The low quality of the effluent from SBR C indicated that it was overloaded at a HRT of 2 days. After reducing the per cycle volume of feeding to 20%, the SBR C performance gradually improved, and in two weeks its effluent was almost the same as SBR B. Table 10 also shows that aquatic toxicity of the leachate feed, as measured by the Beckman Microtox bioassay method, was virtually all removed after the SBR treatment and that the toxicity reduction was consistent with the effluent quality [21].

The following observations were made during the treatability study:

- Up to 15% variations in the effluent TOC, COD and SS were observed for the replicated SBRs. Hyde Park leachate was well treated either alone or combined with other Niagara Plant wastewaters. The treatment performances were almost identical for the three sizes of SBRs when they were operated under the same conditions. It thus established the validity of using the smaller (1-L and 12-L) units for treatability study. Virtually the same performances were obtained for SBRs with several FILL periods — batch feed, 2, 4, and 6 hr. The complex nature of the high TOC wastewater had diminished the effects of FILL period [22, 23].

- Insufficient dissolved oxygen in the mixed liquor was the major cause of low (<85%) TOC removal. To treat a 2000 mg TOC/L wastewater, about 150 mg DO/L-h of oxygen transfer capability should be provided to the SBR operating at a HRT of 1.5 d and a MLSS of 10000 mg/L. The oxygenation rate may be gradually reduced during the REACT period to satisfy only the cell respiration oxygen utilization rate (OUR) of less than 4 mg DO/g MLVSS-h. With at least 1 mg/L of DO during the REACT period, TOC and COD reductions were more than 90% for the

TABLE 9. RESULTS OF BIOTREATMENT OF LEACHATE IN 12-L SBRs[a]

SBR[b] sample	TOC	TOX	HET acid	Phenol	Benzoic acid	o-CBA	m-CBA	p-CBA
	(			mg/L				)
Feed	8135	780	435	1650	2475	840	240	285
I effluent (no N & P)	603	320	240	16	43	158	<9	23
II effluent (ammonia)	393	270	239	<2	21	3	<4	33
III effluent (phosphate)	595	330	273	16	47	127	<4	45
IV effluent (N & P)	409	240	238	<1	7	3	<2	6
SBR sample[c]								
Feed	1784	210	135	390	590	220	60	70
B effluent (24-h, 60% feed)	219	98	115	6	11	2	9	14
III effluent (12-h, 50% feed)	256	98	90	7	8	34	7	12

a. Samples were taken at the end of the program.
b. 24-h SBR cycle, HRT = 10 d (10% feeding over 4-h FILL), MLSS = 10000 mg/L, working volume = 10 L.
c. MLSS = 10000 mg/L, FILL period = 6 h, working volume = 10 L.

TABLE 10. RESULTS OF BIOTREATMENT OF LEACHATE IN 500-L SBRs[a]

SBR[b] sample	TOC	COD	TOX	SS	HET acid	Phenol	Benzoic acid	o-CBA	m-CBA	p-CBA	Microtox[c] toxicity (EC20)
	(			mg/L						)	
Feed	2000	5300	325		260	530	730	350	110	110	1.7%
A effluent	140	510	110	114	170	6	6	12	25	3	41.9%
B effluent	120	400	105	100	150	1	2	2	3	2	68.0%
C effluent	536	1700	235	400	175	12	6	20	25	3	9.3%

a. Samples were taken at the end of the program.
b. The experimental conditions are described in Table 4.
c. Average of three observations. EC20s (% dilution of test sample which would cause 20% corrected light reduction) are shown, since EC50s for the effluent samples (A, B and C) cannot be calculated as a result of SBR biotreatment.

SBRs operated at a F/M as high as 0.2 mg TOC/mg MLSS-d (MLSS = 10000 mg/L).

- Cloudy effluents (SS > 250 mg/L), due to large populations of dispersed and/or filamentous bacteria, were observed several times during this study. They were caused by excessive organic loading, short REACT period, low DO, nutrient deficiency, and accumulation of toxic compounds [22-26]. After correcting these causes, the SBR treatment performance slowly improved. Effluent SS was less than 100 mg/L except when the feed TOC was higher than 3000 mg/L.
- The SBR performance was nearly unchanged when the feeding was suspended on holidays, Saturday and/or Sunday. The REACT period for the four 1-L SBRs was extended over the weekend, with either continuous or intermittent aeration and mixing during the extra time period. This resulted in slightly lower effluent TOC, more complete nitrification and/or denitrification. Normal cyclic operation was resumed from Monday through Friday, and the same performance as the 7 days-a-week SBRs was then observed. The ability to operate the SBRs in this manner is significant since the existing adsorption system is operated five days a week.

Volatile Compounds:

Many aromatic and straight-chain chlorinated hydrocarbons were present in leachate and the combined wastewater. Their concentrations were typically less than 5 mg/L, except for chlorotoluenes which occasionally approached 40 mg/L. Air stripping was found to be the predominant mechanism for their removals in the aerobic SBR treatment system [27]. About 99% of the volatile constituents, which altogether accounted for about 5% of wastewater TOC, were air-stripped from the feed tank during pretreatment, and the rest were removed from the SBRs during aerated FILL and/or REACT. These compounds were easily separated from the air by carbon adsorption. With a vapor phase carbon adsorber installed for treating the exhaust gases, no air pollution would result from the SBR biotreatment system.

Sludge Disposal:

Depending on the wastewater characteristics, 200 to 2000 mg of pretreatment sludge per liter of feed were produced by neutralization, aeration, and sedimentation. It was mainly ferric hydroxide which included adsorbed organic compounds. As much as 62% of HET acid in the raw wastewater was removed by iron precipitation; other constituents were removed to lesser extents. The sludge was well compacted in the feed tank, to 7% solids, and easily dewatered by either vacuum or press filtration, to more than 30% solids. It was periodically removed from the feed tank.

Biomass yield was estimated at 0.64 mg/mg feed TOC for SBR A of Table 4. At a higher MLSS, biological yield was smaller [28]. For example, the apparent yield for the 1-L SBRs (feed TOC = 3000 mg/L, MLSS = 10000 mg/L, HRT = 10 d, working volume = 750 ml) was about 0.2. The initial MLSS settling rate was estimated at 3 cm/min. The wasted biological sludge from the high MLSS SBRs was already aerobically stabilized, and no significant volume reduction was observed after 10 days of aerobic digestion. The settled sludge contained about 3.5% solids, and the dewatered sludge had about 30% solids.

Carbon Saving:

Figure 3 shows the capacity for the persistent HET acid was significantly increased after the leachate was biologically treated in the SBRs. The improvement was actually higher than that indicated by the isotherms, as shown by

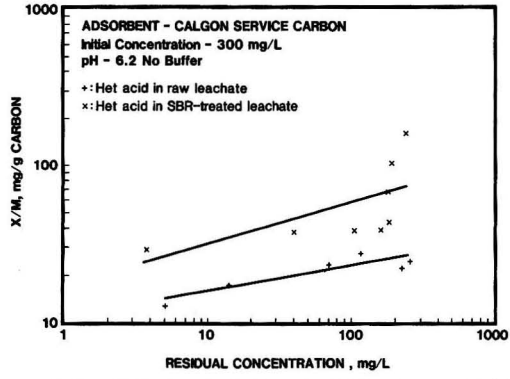

Figure 3. Freundlich adsorption isotherms for HET acid in raw and SBR-treated leachate samples.

the fast-rising X/Ms measured at higher residual concentrations (C_fs). The carbon capacity for HET acid (pk_as = 2.6 and 4.8) was higher at an acidic pH. In the unbuffered isotherm experiment, pH was found to increase with the carbon dose, and thus resulted in reduced observed capacity at the lower C_fs [29]. Table 11 demonstrates that the carbon capacity for TOC in the SBR-treated leachate was about the same as in the raw leachate and that the capacity for TOX was much greater after biotreatment. The results are shown for five different types of activated carbon — three virgin and two reactivated carbons. Since the SBR biotreatment could easily accomplish 90% reduction of TOC in the combined wastewater, the carbon exhaustion rate of the existing adsorber would be reduced by at least 90% if the SBR system is installed before the adsorption system. Table 12 presents the expected saving in the future wastewater treatment cost with the SBR biotreatment; Figure 4 depicts the process schematic for the integrated SBR-adsorption treatment of the combined wastewater. Including the anticipated wastewaters from other sources, substantially greater cost saving would be possible.

Bacterial Supplementation:

Twice a week for three months, two strains of OCC bacteria (H4 and SS3) and two commercial bacterial cultures were supplemented to the 1-L and 12-L SBRs, operated at a F/M from 0.05 to 0.2 mg TOC/mg MLSS-d. No significant differences were observed in the performances of these units compared to that of the control (no supplemen-

TABLE 11. ADSORPTIVE CAPACITIES OF CARBON FOR TOC AND TOX IN RAW AND SBR-TREATED LEACHATE SAMPLES[a]

Activated carbon type	Raw leachate[b] TOC (mg adsorbed/g carbon)	Raw leachate[b] TOX (mg adsorbed/g carbon)	SBR-treated leachate[c] TOC (mg adsorbed/g carbon)	SBR-treated leachate[c] TOX (mg adsorbed/g carbon)
Calgon F-300	133	11.7	152	127
Calgon Service carbon	97.9	8.8	113	75.9
Carborundum 30	173	19.6	268	172
ICI Hydrodarco 3000	103	11.5	87.8	83.8
Laboratory reactivated spent Calgon Service carbon	148	18.3	115	91.6

a. Adsorptive capacities were estimated from the Freundlich adsorption isotherms.
b. Raw leachate: TOC = 3080 mg/L, TOX = 264 mg/L, pH = 5.3. The TOC capacities were estimated at TOC = 1500 mg/L, and the TOX capacities were estimated at TOX = 125 mg/L.
c. SBR-treated leachate: TOC = 400 mg/L, TOX = 334 mg/L, pH = 6.8. (The raw leachate had a TOC of 8100 mg/L and a TOX of 780 mg/L). The TOC capacities were estimated at TOC = 300 mg/L, and the TOX capacities were estimated at TOX = 125 mg/L.

TABLE 12. SAVING IN WASTEWATER TREATMENT COST WITH SBR BIOTREATMENT

Time Period	Flowrate (m^3/d)	TOC[a] loading (	Carbon[b] usage kg/d	Carbon[c] saving)	Cost Saving[d] $/d	$1000/yr
Jan. 1985	95	142	991	892	1475	538
July 1985	295	215	1442	1298	2146	783
Jan. 1986	250	202	1361	1225	2025	739
July 1986	144	170	1170	1053	1742	636
Jan. 1987	144	170	1170	1053	1742	636
July 1987	144	170	1170	1053	1742	636
Jan. 1988 to 1995	144	170	1170	1053	1742	636
			10-year Average Saving			$643,600/year

a. The first 68 m^3/d at 1700 mg TOC/L; the next 45 m^3/d at 1000 mg TOC/L; the rest at 300 mg TOC/L.
b. 12 g/L for the first 68 m^3/d; 6.6 g/L for the next 45 m^3/d; 1.8 g/L for the rest.
c. 90% reduction in carbon exhaustion rate after biotreatment.
d. $1.65/kg carbon. All costs are in 1984 U.S. dollars.

SBR treatment system — design TOC loading = 181 kg/d
average TOC loading = 173 kg/d

	$/year
1. Carbon saving	643,600
2. Operating labor, misc. costs[a]	(0)
3. Maintenance[a]	(50,000)
4. Electrical power[b]	(18,000)
5. Sludge disposal[c]	(21,300)
6. Analytical[a]	(23,000)
7. Nutrients and chemicals[d]	(4,600)
Net Saving	$526,700/year

a. Cost over the expanded adsorption operation required in the near future.
b. $0.06/kWh.
c. Total sludge production rate — 1.02 g/g TOC; dewatered sludge — 30% solid, disposal costs — $0.10/kg.
d. Supplementing NH_3 and H_3PO_4 to a TOC/N-NH_4/P-PO_4 ratio of 150/10/2.

tation [30]. It was possible that the excellent treatment performance obtained in all units had already included benefits found in the preliminary study [17], since the wastewater feed contained many strains of bacteria shown in Table 3. Five OCC mutant bacteria, derived from the H5 isolate by chemical mutagenesis using nitric acid [31], were later supplemented to 1-L electrolytical respirometer (O-I E/BOD Model 2-302) bottles. Using these automated batch reactors, improvements due to bacterial supplementation were observed as evidenced by the cumulative oxygen uptake curve [32] (Figure 5), and the composition of samples taken two weeks after the test run (Table 13). Supplementation of the right kinds of bacteria was shown to have enhanced biodegradation rates for many of the more persistent wastewater constituents. Its potential in improving the performance of an over-loaded biological treatment system is thus indicated.

SUMMARY

Approximately 73000 metric tons of chemical waste are contained in the Hyde Park Landfill site. Leachate is collected, trucked to a nearby chemical manufacturing plant, and then treated with plant wastewaters by activated carbon adsorption. The leachate which accounts for about

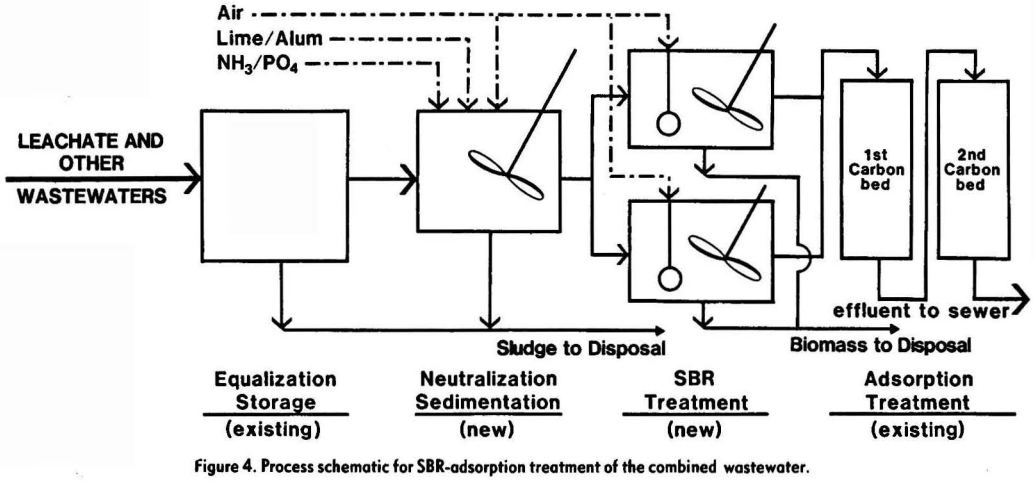

Figure 4. Process schematic for SBR-adsorption treatment of the combined wastewater.

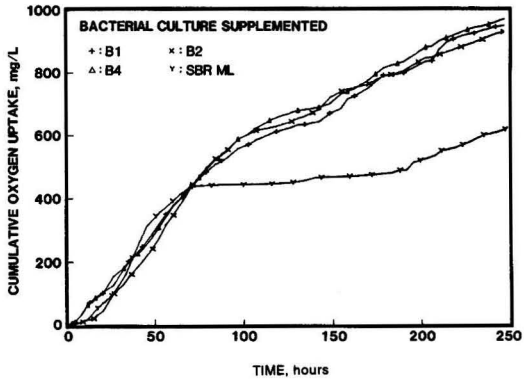

Figure 5. Cumulative oxygen uptake curves for E/BOD reactors.

60% of the combined wastewater volume but more than 80% of the total organic loading to the existing adsorption system, was found to be easily biodegraded. Excellent treatment of leachate and the combined wastewater was consistently accomplished in sequencing batch reactors (SBRs) which were operated under a variety of operating conditions: wastewater TOC, feed rate, variations of aeration and mixing strategies, hydraulic retention time, mixed liquor suspended solids concentration, organic loading, temperature, and cycle time. The SBR treatment performance was unaffected when wastewater feeding was suspended during weekends and holidays. Results obtained in the small bench-scale SBRs were reproduced in the pilot-scale units. An analysis of process economics indicated that significant cost saving was possible, in meeting the future wastewater treatment requirements, if SBR biotreatment is implemented before the carbon adsorption. The integrated wastewater treatment system would produce a better quality effluent at a lower overall cost. A full scale SBR-adsorption system has been designed for treating the combined wastewater. Biodegradation rates for some of the more persistent wastewater constituents were enhanced in batch reactors which were supplemented with strains of bacteria isolated from the landfill site.

ACKNOWLEDGMENTS

D. E. Ernst assisted in the planning and coordination; M. H. Wendell supervised the construction and operation of the pilot-scale SBR-adsorption treatment system. G. E. Moscoto carried out the experimental programs involving the 12-L and 500-L SBRs; G. D. LaLiberty supplied wastewaters for this study. E. A. Dietz developed the analytical methods for identifying and quantifying the major wastewater constituents. This paper was presented at the 57th Annual Water Pollution Control Federation Conference in New Orleans, La., October 1-4, 1984.

LITERATURE CITED

1. *Standard Methods for the Examination of Water and Wastewater,* 15th edition, American Public Health Association, Washington, D.C. (1980).
2. Dobbs, R. A., and Cohen, J. M., *Carbon Adsorption Isotherms for Toxic Organics,* EPA-600/8-80-023, U. S. EPA, Cincinnati, Ohio, 309 (1980).
3. Weber, W. J., Jr., *Physicochemical Processes for Water Quality Control,* Wiley-Interscience, New York, 210 (1972).
4. Weber, W. J., Jr., and Ying, W., "Integrated Biological and Physicochemical Treatment for Reclamation of Wastewater," *Proc. International Conference on Advanced Treatment and Reclamation of Wastewater,* IAWPR, Johannesburgh, South Africa, S. 131 (1977).
5. Vandenbergh, P.A., *et al.*, "Isolation and Genetic Characterization of Bacteria That Degrade Chloroaromatic Compounds," *Appl. Environ. Microbiol.*, **42**, 737 (1981).
6. Pierce, G. E., *et al.*, "Substrate Diversity of *Pseudomonas* Species containing Chlorotoluene Degradative Plasmids," *Del. Ind. Microbiol.*, **24**, 499 (1983).
7. Irvine, R. L., and Busch, A. W., "Sequencing Batch Biological Reactors — An Overview," *Jour. Water Pollu. Control Fed.*, **51**, 235 (1979).
8. "Standard Test Method for Biodegradability of Alkylbenzene Sulfonates," Method D2667-82, ASTM, Philadelphia, Pa. (April 1982).
9. Sack, W. A., and Bokey, W. R., "Biological Treatment of Coal Gasification Wastewater," *Proc. 33rd Annual Purdue Industrial Waste Conference,* 278 (1979).
10. O'Shaughnessy, F. R., "The Physical Aspects of Sewage Disposal," *Journal Soc. Chem. Ind.*, **42**, 359T (1923).
11. Goronszy, M. C., "Intermittent Operation of the Extended Aeration Process for Small Systems," *Jour. Water Pollu. Control Fed.*, **51**, 274 (1979).
12. Ardern E., "The Activated Sludge Process of Sewage Purification," *Jour. Soc. Chem. Ind.*, **36**, 822 (1917).

TABLE 13. RESULTS OF BACTERIAL SUPPLEMENTATION IN E/BOD REACTORS[a]

Reactor content:		
	SBR mixed liquor (MLSS = 10000 mg/L)	10.0 ml
	leachate	190.0 ml
	inoculated growth broth[b]	2.0 ml
	nutrient (10 mg N-NH_4 and 2 mg P-PO_4/ml)	2.5 ml
	aerated tapwater	796.0 ml

Sample	TOC	COD	TOX	HET acid	Phenol	Benzoic acid	o-CBA	m-CBA	p-CBA
	(				mg/L				)
Leachate[c]	2100	8000	420	167	1000	1400	500	80	150
B1 (H5 N-1 TN)[d]	105	210	36	31	<1	1	1	ND	3
B2 (H5 N-17 TN)	92	250	44	34	<1	<1	1	ND	4
B3 (MT-2 NA)	163	340	64	39	3	2	58	5	5
B4 (TC-21 TN)	81	210	38	36	<1	<1	<1	ND	4
B5 (TC-17 TN)	222	450	70	37	3	1	70	4	27
SBR ML (control)	200	300	60	34	2	1	53	2	4

a. The cumulative oxygen uptake curves for the E/BOD reactors are shown in Figure 5. Samples were taken two weeks after the beginning of the test run.

b. Growth broth — tryptone 10 gm; yeast extract 5 gm; NaCl 10 gm; pretreated leachate 30 ml; distilled water 970 ml

Inoculated by culture transferred from the agar plate (2 gm agar per 100 ml of the growth broth); incubated at 25°C for 48 hours.

c. Parameter values measured at the beginning of the test run.

d. Type of OCC mutant bacteria supplemented to the E/BOD reactor. The nutritional versatility of the parent bacteria (H5) is given in Table 3.

13. "Innovation Technology: The Sequencing Batch Reactor," *Technology Transfer*, EPA-600/D-82-331, U. S. EPA, Cincinnati, Ohio (October 1982).
14. Hoover, S. R., "Biochemical Oxidation of Dairy Wastes," *Sew. & Ind. Wastes*, **25**, 201 (1953).
15. Rea, J. E., Jr., "Single Cell Activated Sludge Using Fill and Draw Combined Industrial/Domestic Waste Treatment Plant," *Proc. 32nd Annual Purdue Industrial Waste Conference*, 611 (1978).
16. Downes, M., "SBR Treatment of Food Processing Wastewaters," Doxsee Food Corp., Baltimore, Maryland (1984).
17. Irvine, R. L., *et al.*, "Enhanced Biological Treatment of Leachates from Industrial Landfills," *Hazard, Waste*, **1**, 123 (1984).
18. Emerson, S. L., and Sherrard, J. S., "Aerobic Biological Treatment of Nitrogen-deficient Organic Wastewaters," *Jour. Water Pollu. Control Fed.*, **55**, 467 (1983).
19. McKinney, R. E., *Microbiology for Sanitary Engineers*, McGraw-Hill, New York, 32 (1962).
20. Silverstein, J., and Schroeder, E. D., "Performance of SBR Activated Sludge Processes with Nitrification/Denitrification," *Jour. Water Pollu. Control Fed.*, **55**, 377 (1983).
21. Casseri, N. A., *et al.*, "Use of a Rapid Bioassay for Assessment of Industrial Wastewater Treatment Effectiveness," *Proc. 38th Annual Purdue Industrial Waste Conference*, 867 (1984).
22. Dennis, R. W., and Irvine, R. L., "Effect of FILL/REACT ratio on Sequencing Batch Biological Reactors," *Jour. Water Pollu. Control Fed.*, **51**, 255 (1979).
23. Hoepker, E. C., and Schroeder, E. D., "The Effect of Loading Rate on Batch Activated Sludge Effluent Quality," *Jour. Water Pollu. Control Fed.*, **51**, 264 (1979).
24. Palm, J. C., *et al.*, "Relationship Between Organic Loading, Dissolved Oxygen Concentration, and Sludge Settleability in the Completely-mixed Activated Sludge Process," *Jour. Water Pollu. Control Fed.*, **52**, 2485 (1980).
25. Jenkins, D., and Richard, M. G., "Factors Affecting the Selection of Filamentous Organisms in Activated Sludge," *Proc. Symposium on Impact of Applied Genetics in Pollution Control*, Univ. of Notre Dame Press, 63 (1982).
26. Gude, H., "Interactions Between Floc-Forming and Nonfloc-Forming Bacterial Populations from Activated Sludge," *Current Microbiology*, **7**, 347 (1982).
27. Lurker, P. A., *et al.*, "Worker Exposure to Chlorinated Organic Compounds from the Activated-sludge Wastewater Treatment Process," *Am. Ind. Hyg. Assoc. J.*, **44**, 109 (Feb. 1983).
28. Schultz, J. R., *et al.*, "Realistic Sludge Production for Activated Sludge Plants Without Primary Clarifiers," *Jour. Water Pollu. Control Fed.*, **54**, 1355 (1982).
29. Ying, W., *Investigation and Modeling of Bio-physicochemical Processes in Activated Carbon Columns*, Ph.D. Dissertation, Univ. of Michigan, 70 (1978).
30. Qasim, S. R., and Stinehelfer, M. L., "Effect of a Bacterial Culture Product on Biological Kinetics," *Jour. Water Pollu. Control Fed.*, **54**, 255 (1982).
31. Calton, B. C., and Brown, B. J., In *Manual of Methods for General Bacteriology*, Gerhardt, P., (Ed.), American Society for Microbiology, Washington, D.C., 227 (1981).
32. Young, J. C., and Baumann, E. R., "The Electrolytic Respirometer — I. Factors Affecting Oxygen Uptake Measurements," *Water Research*, **10**, 1031 (1976).

Wei-chi Ying is an associate scientist for Occidental Chemical Corporation and an adjunct associate professor of Environmental Engineering at State University of New York at Buffalo. He was a visiting professor at East China Institute of Chemical Technology in 1983. His work on modelling and application of biological carbon adsorption process won the 1979 Nalco Award for significant research in water and wastewater treatment. He earned a B.S. in Chemical Engineering from Tunghai University (Taiwan), an M.S. in Chemical Engineering from the University of Toledo, an M.S.E. and a Ph.D. in Environmental Engineering from the University of Michigan.

Robert R. Bonk is an associate chemist of Environmental Technology at the Grand Island Research Center, New York, of Occidental Chemical Corporation. He has participated in a variety of environmental control research and development projects including biological, chemical, and physical processes for treating industrial wastewaters. He earned a B.S. in Chemistry from Rochester Institute of Technology and an M.B.A. from Canisius College. He is enrolled in the graduate Water Resources and Environmental Engineering program at State University of New York at Buffalo.

Vernon J. Lloyd is the technical manager of the Niagara Falls, New York, plant of Occidental Chemical Corporation. In that role, he is responsible for process improvement, environmental control, and the analytical laboratory for the Niagara Plant, which is a multi-product operation, producing over thirty inorganic and organic chemical products in a wide range of capacities. He has a B.S. and an M.S. in Chemical Engineering from Clarkson University and an M.B.A. from State University of New York at Buffalo.

Stanley A. Sojka is the manager of Special Environmental Programs for Occidental Chemical Corporation. He is in charge of waste landfill site remediation activities including the selection of appropriate technologies for treating liquid and solid wastes. He continues to play a major role in the R&D projects on the use of genetically engineered bacteria for pollution control purposes. He has received numerous awards for outstanding research and for professional service. He has a B.S. in Chemistry from Canisius College and a Ph.D. in Organic Chemistry from Indiana University. He conducted post doctoral research at University of Basel (Switzerland) and served on the Chemistry faculty at Trinity College in Washington, D.C.

An Alternative RBC Design-Second Order Kinetics

An alternative design method was used employing 2nd order kinetics and good engineering practice to specify a RBC process for secondary treatment.

The kinetics of the RBC process had previously been shown to follow a second order rate expression when the disappearance of soluble biochemical oxygen demand (sBOD) is correlated with time (2). This relationship was combined with other RBC process limitations to design an RBC system based on achieving final effluent sBOD requirements of less than 10 mg/L of soluble BOD (sBOD). This alternative design approach can be used to determine:

- **The number of shafts**
- **The number of stages**
- **The shafts in each stage**
- **The sBOD in each stage**
- **The effect on performance by diurnal variations in flow from 50 to 200% of design flow**
- **When oxygen transfer governs the kinetics**

This paper demonstrates the technique employed to design the RBC plant using second order kinetics and the rationale behind each step in the design process.

Edward J. Opatken, Land Pollution Control Division, U.S. E.P.A. Office of Research & Development, Hazardous Waste Engineering Research Laboratory, Cincinnati, Ohio

INTRODUCTION

The design of rotating biological contactor (RBC) systems for municipal wastewater treatment is normally based on empirical curves developed by the various manufacturers. The user communities have relied heavily upon the RBC manufacturers to provide design assistance and to specify the number of RBC units required, as well as their arrangement into stages and trains. The users normally include a performance clause in their specifications to provide the necessary insurance that the process will produce the desired effluent quality at the specified design flow. A manufacturer's empirical curves were used to predict both interstage and final effluent quality at 10 RBC facilities, and the predicted results were considerably different from the actual results. A second order kinetic evaluation was also performed and the predicted results were in close agreement with the actual results. This paper presents an alternative design method using second order kinetics and good engineering practices to specify a RBC process for secondary treatment.

The kinetics of the RBC process have been shown to follow a second order rate expression when the disappearance of soluble biochemical oxygen demand (sBOD) is correlated with time [2]. This relationship can then be combined with other RBC process limitations to design RBC systems based on achieving final effluent sBOD requirements. This alternative design approach can be used to determine:

- The number of shafts
- The number of stages
- The shafts in each stage
- The sBOD in each stage
- The effect on performance by diurnal variations in flow from 50 to 200% of design flow
- When oxygen transfer governs the kinetics

This paper will demonstrate the technique employed to design an RBC plant using second order kinetics and the rationale behind each step in the design process.

PLANT CONDITIONS—ASSUMED

Design flow = 10 million gallons per day (mgd) (38,000 m^3/d)
Diurnal variation = 50 to 20% of design flow
Influent characteristics
TBOD = 120 mg/L
sBOD = 60 mg/L
TSS = 120 mg/L
VSS = 72 mg/L
k = 0.083 L/mg · h [from reference 2]
Requirements: Final effluent = 12 mg/L sBOD ≈ 24 mg/L TBOD

Step 1 Determine the Number of Shafts in the First Stage

To avoid organic overloads and possible nuisance growths and/or shaft overloads a design limitation of 2.5 lbs sBOD/1000 sq ft (12 g sBOD/m²) [3] is a recommended condition in the Design Information Document. By applying this limitation the number of shafts required in the first stage can be estimated.

60 mg sBOD/L ≈ 60 lbs/10^6 lbs × 8.3 lbs/gal × 10^7 gal/d = 5000 lbs sBOD/d
(60 mg sBOD/L × g/1000 mg × kg/1000g × 1000 L/m³ × 38,000 m³/d = 2300 kg sBOD/d)

Since the standard first stage shafts usually have 100,000 sq ft (9300 m²) each shaft can handle

100,000 sq ft × 2.5 lbs/d · k sq ft = 250 lbs sBOD/d · shaft
(9300 m² × 12 g sBOD/d · m² = 110 kg sBOD/d · shaft)

5000 lbs sBOD/d ÷ 250 lbs sBOD/d · shafts = 20 shafts in first stage
(2300 kg sBOD/d ÷ 110 kg sBOd/d · shaft = 20 shafts)

A RBC design standard set by the manufacturers is a volume to surface ratio of 0.12 gal/sq ft (4.9 L/m²) or a 12000 gal (45 m³) volume for a 100,000 sq ft (9300 m²) RBC. Based on this design standard, the residence time in the first stage is calculated as follows:

10 MGD ≈ 420,000 gal/h
(38,000 m³/d = 1600 m³/h)

12000 gal/shaft × 20 shafts/first stage ÷ 420,000 gal/h = 0.57h in first stage ≈ 34 min
(45 m³/shaft × 20 shafts/first stage ÷ 1600 m³/h = 0.57 h in first stage = 34 min)

To simulate a completely mixed condition, each stage should have an assumed minimum residence time of 15 minutes. The 34 minutes of residence time calculated for the first stage is considerably greater than the 15 minute limitation and is satisfactory for this application.

Step 2 Determine the Concentration of sBOD in the First Stage

The Levenspiel equation [4] is used to determine the concentration of sBOD in the first stage and is represented by the following equation for second order kinetics.

$$C_1 = \frac{-1 + \sqrt{1 + 4\,kt\,C_{inf}}}{2\,kt}$$

where

C_1 = concentration of sBOD in the first stage
k = second order reaction rate constant, 0.083 L/mg · h
t = residence time in first stage, 0.57h
C_{inf} = concentration of sBOD entering the first stage, 60 mg/L

$$C_1 = \frac{-1 + \sqrt{1 + 4\,(.083\ L/mg)\,(.57h)\,(60\ mg/L)}}{2\,(.083\ L/mg \cdot h)\,(.57h)}$$

C_1 = 26 mg/L sBOD

Check the adequacy of oxygen transfer in the first stage using 40 mg O_2/h · sq ft (0.43 g O_2/h · m²) [3] as the maximum oxygen transfer rate for a RBC containing 100,000 sq ft (9300 m²) of plastic media and rotating at 1.6 rpm.

ΔC = 60-26 = 34 mg sBOD/L removed ≈ 34 mgO_2/L transferred

Q = 10,000,000 gal/d × 3.8 L/gal ÷ 24h/d = 1,600,000 L/h

1,600,000 L/h · ÷ 20 shafts = 80,000 L/h · shaft

34 mg sBOD/L × 80,000 L/h · shaft ÷ 100,000 sq ft/shaft (9300 m²/shaft) = 27 mg O_2/h · sq ft (0.29 gO_2/h · m²)

27 mg O_2/h · sq ft < 40 mgO_2/h · sq ft
(0.29 gO_2/h · m² < 0.43 gO_2/h · m²)

Therefore the first stage can adequately transfer the oxygen, and the system is reaction rate limited. If the oxygen transfer rate is greater than 40 mg/O_2h · sq ft (0.43 gO_2/h · m²) then the concentration is determined by the oxygen transfer rate. An example of an oxygen limiting condition, that is used to determine the stage concentration, is shown on pages 53 and 54.

Step 3 Determine the Number of Shafts in the Second Stage

Again applying the 2.5 lbs sBOD/1000 sq ft (12 g sBOD/m²) limitation, determine the minimum number of shafts required in the second stage.

26 mg sBOD/L ≈ 26 lbs/10^6 lbs × 8.3 lbs/gal × 10^7 gal/d = 2200 lbs sBOD/d
(26 mg sBOD/L × 38 × 10^6 L/d × kg/10^6 mg = 1000 kg sBOD/d)

Therefore, the number of shafts required are:

2200 lbs sBOD/d ÷ 250 lbs sBOD/d · shaft = 8.8 ≈ 9 shafts
(1000 kg sBOD/d ÷ 110 kg sBOD/d · shaft ≈ 9 shafts)

Another design feature endorsed by the Design Information on Rotating Biological Contactors [3] is positive flow control to each contractor for proper distribution of primary effluent to each RBC. If nine RBC are used in the second stage another series of flow monitors and controls will be required to again control the flow to each of the 9 shafts to insure equal distribution. By adding another shaft, thus employing 10 shafts in the second stage, the flow from 2 RBC in the first stage can be directed to each RBC in the second thus eliminating the need to monitor and control the flow into the second stage. Therefore 10 contactors will be employed in the second stage.

Check retention time in the second stage using 10 RBC's to determine if 15 minutes residence time is provided to simulate a completely mixed system.

V = 12000 gal/shaft × 10 shafts = 120,000 gal
(V = 45 m³/shaft × 10 shafts = 450 m³)

t = V/Q = 120,000 gal/420,000 gal/h = 0.29h ≈ 17 min
(t = V/Q = 450 m³ ÷ 1600 m³/h = 0.29h)

The hydraulic residence time in the second stage exceeds the 15 minutes limitation by 2 minutes, thus 10 shafts are adequate for treatment in the second stage.

Step 4 Determine the concentration of SBOD in the Second Stage

$$C_2 = \frac{-1 + \sqrt{1 + 4\,(.083\ L/mg \cdot h)\,(.29h)\,(26\ mg/L)}}{2\,(.083\ L/mg \cdot h)\,(.29h)}$$

C_2 = 18 mg/L sBOD

Check adequacy of O_2 transfer in second stage

ΔC = 26-18 = 8 mg/L of sBOD ≈ 8 mgO_2/L transferred

Q = 10^7 gal/d ≈ 1.6 × 10^6 L/h · 10 shafts ≈ 160,000 L/h · shaft to second stage
(Q = 1600 m³/h ÷ 10 shafts = 160 m³/h · shaft in second stage)

8 mg O_2/L × 160,000 L/h · shaft ÷ 100,000 sq ft (9300 m²/shaft) = 13 mg O_2/h · sq ft (0.14 g O_2/h · m²)

13 mg O_2/h · sq ft < 40 mg O_2/h · sq ft
(0.14 mg O_2/h · m² < 0.43 g O_2/h · m²)

therefore the oxygen transfer is well within the capability of the 10 contactors and the second stage is reaction rate limited.

Step 5 Determine the Number of Shafts in the Third Stage

Since the residence time in the second stage is 17 minutes, or only 2 minutes more than the minimum 15 minutes, then the third stage will also consist of 10 shafts which will again allow us to omit flow control equipment. The flow from each RBC in the second stage will be directed to a RBC in the third stage, thus maintaining proper flow distribution in the third stage.

Step 6 Determine the Concentration in the Third Stage

Calculate the concentration of sBOD in the third stage. Employ 10 shafts in the third stage with a residence time of 0.29 h and an influent of 18 mg/L of sBOD.

$$C_3 = \frac{-1 + \sqrt{1 + 4\,(.083\ \text{L/mg} \cdot \text{h})\,(.29\text{h})\,(18\ \text{mg/L})}}{2\,(.083\ \text{L/mg} \cdot \text{h})\,(.29\text{h})}$$

C_3 = 14 mg/L of sBOD

Check oxygen transfer in the third stage

ΔC = 18-14 = 4 mg/L O_2 transferred

4 mg O_2/L × 160,000 L/h · shaft ÷ shaft/100,000 sq ft (9300 m^2) = 6.4 mg O_2/h · sq ft (0.069 g O_2/h · m^2)

6.4 mg O_2/h · sq ft << 40 mg O_2/h · sq ft (0.069 g O_2/h · m^2 << 0.43 g O_2/h · m^2)

The capability of the contactor to transfer oxygen is more than six times its requirement in the third stage. To offset this excess oxygen transfer capability, it is proposed that the effluent from every two contactors in stage two be combined and directed to one contactor in stage three that is modified to contain the same volume as two standard RBC tanks. That is, a contactor with 100,000 sq ft (9300 m^2) is set in a 24000 gal (90 m^3) tank in lieu of two contactors with 100,000 sq ft (9300 m^2) each set in two tanks which contain 12000 gallons (45 m^3) each. This approach will reduce the contactors in stage three from 10 to 5. Savings will be achieved in capital expenditures by eliminating 5 contactors valued at $40,000 each or $200,000. Further operating savings will be obtained by cutting the power requirements in half for the third stage by eliminating half the contactors that would normally be specified and saving more than $9,000/yr in electrical power costs.

Step 7 Determine the Number of Shafts in Stage Four

Only 5 shafts will be specified for stage four. The same analyses that was used to specify 5 contactors in stage three also applies to stage four. Each contactor sets inside a tank that contains twice the standard volume [24000 gal (90 m^3) in lieu of 12,000 gal (45 m^3)] to maintain an adequate mix time of 0.29h or 17 minutes and a controlled flow by directing the flow from each RBC in stage three to an RBC in stage four.

Step 8 Calculate the Concentration of Stage Four

The calculation of the concentration in stage four again uses a residence time of 0.29h with an influent concentration of 14 mg/L.

$$C_4 = \frac{-1 + \sqrt{1 + 4\,(.083\ \text{L/mg/h})\,(.29\text{h})\,(14\ \text{mg/L})}}{2\,(.083\ \text{L/mg} \cdot \text{h})\,(.29\text{h})}$$

C_4 = 11 mg/L of sBOD

The final effluent concentration is estimated at 11 mg/L of sBOD or an assumed TBOD level of 22 mg/L. Forty shafts are required to treat 10 MGD (38,000 m^3/d) to a level below 25 mg/L of TBOD. The arrangement consists of 20 shafts in the first stage, followed by 10 shafts in the second stage and 5 shafts each in the third and fourth stages. However the tankage in the third and fourth stages equal the tankage in the second stage as well as the same hydraulic residence time.

Diurnal Variation

The effect of changing conditions, such as flow can be analyzed by the second order rate expression or by oxygen transfer if this factor becomes the limiting condition. We assumed an increase in flow of about twice the design flow for diurnal variation and, vice versa, we assumed a drop in the flow of half design flow because of diurnal variation. This differential increase or decrease in flow can be taken into consideration by a kinetic analyses. The overall daily effluent is calculated to determine if the final effluent quality is being compromised by relying upon average conditions to specify equipment requirements without any consideration for diurnal variations.

The analysis for determining the effect of a diurnal flow variation between 50 and 200% of design flow is based on a second order rate expression to calculate the effluent quality.

With a 200% increase in flow, the reaction time will be reduced to 50% of the residence time at design flow. Conversely the reduction of flow at 50% of design will double the residence time in each stage. The diurnal effects of flow variation on residence time are shown in Table 1.

The reaction times are then inserted into the 2nd order rate expression to determine the concentrations in each of the four stages for both low flow and high flow conditions. The reaction rate constant remains at 0.083 L/mg · h and the initial concentration is assumed at the same level, 60 mg/L of sBOD.

An example for determining the concentration of sBOD in stage one with a flow of 200% of design flow is shown below

$$C_1 = \frac{-1 + \sqrt{1 + 4\,ktCo}}{2\,kt}$$

where

k = 0.083 L/mg · h
C_0 = 60 mg sBOD/L
t = .28h at 200% design flow

$$C_1 = \frac{-1 + \sqrt{1 + 4\,(.083)\,(.28)\,(60)}}{2\,(.083)\,(.28)}$$

C_1 = 34 mg/L of sBOD

Past work has shown that the RBC are capable of transferring a maximum of 40 mg O_2/h · sq ft (0.43 g O_2/h · m^2). This limitation on oxygen transfer needs to be assessed to insure that the process remains only kinetically limited during the periods of high diurnal flow.

An example of the calculation to determine whether the process is kinetically limited or oxygen transfer limited is again illustrated below:

(60 mg/L − 34 mg/L) = 26 mg/L of sBOD removed or O_2 transferred

26 mg/L × 3.8 L/gal × 12000 gal/0.28h ÷ 100,000 sq ft = 42 mgO_2/h · sq ft
(26 g/m^3 × 45 m^3/0.28h ÷ 9300 m^2 = 0.45 g O_2/h · m^2)

TABLE 1. EFFECT OF DIURNAL FLOW ON RESIDENCE TIME

Time in Stage	Design flow	50% Design	200% Design
t_1, h	.57	1.14	.28
t_2, h	.28	.57	.14
t_3, h	.28	.57	.14
t_4, h	.28	.57	.14

Since the oxygen requirement is 42 mg/h · sq ft (0.45 g O_2/h · m^2) and a RBC can only transfer 40 mg O_2/h · sq ft (0.43 g O_2/h · m^2) the process is assumed to be oxygen transfer limited and the concentration in the first stage is calculated as follows:

40 mg/h · sq ft × 100,000 sq ft × .28h/12000 gal × gal/3.8L = 24 mg/L of O_2

60 mg/L − 24 mg/L = 36 mg/L of sBOD which is the estimated concentration in the first stage which is controlled by oxygen transfer.

Using the concentration in stage one as the influent to stage two, calculate the concentration in stage two using the 2nd order rate equation.

$$C_2 = \frac{-1 + \sqrt{1 + 4\,kt_2C_1}}{2\,kt_2}$$

$$C_2 = \frac{-1 + \sqrt{1 + 4\,(.083)\,(.14)\,(36)}}{2\,(.083)\,(.14)}$$

C_2 = 27 mg/L

ΔC = 36-27 = 9 mg/L of sBOD removed or O_2 transferred

Since the residence time in stage two is only half the residence time in stage one, a recheck of the O_2 transfer limitation is required.

9 mgO_2/L × 3.8 L/gal × 12000 gal/.14h ÷ 100,000 sq ft = 29 mgO_2/h · sq ft
(9 g O_2/L × 45 m^3/0.14h ÷ 9300 m^2 = 0.31 g O_2/h · m^2)

which is below the 40 mg O_2/h · sq ft (0.43 g O_2/h · m^2) that the contactor is capable of transferring; therefore the second stage is reaction rate limited and the concentration is calculated by the second order rate expression.

Since the residence time in stages three and four equals the residnce time in stage two and the concentration in stage two is greater than the concentrations in stages three and four, the oxygen transfer rate or the sBOD removal rate in stages three and four will be less than stage two and will be chemical reaction rate limited. The concentrations for stages three and four can be calculated by the 2nd order rate expression and it will not be necessary to check for oxygen transfer limitation because the influent concentration in stages three and four are less than stage two.

The results are shown in Table 2 for the 50% and 200% of design flow and also for the combined analyses involving both O_2 transfer and kinetics as the limiting factor.

If these results are weighted over 24 hours, the mean sBOD of final effluent is conservatively estimated by assuming that both high and low flows occurs for 6 hours and design flow occurs for 12 hours.

$$C_{eff} = \frac{(12 \times 11) + (6 \times 6.5) + (6 \times 18)}{24}$$

$$= 12 \text{ mg/L sBOD} \approx 24 \text{ mg/L of TBOD}$$

TABLE 2. CONCENTRATIONS AT DIURNAL FLOW CONDITIONS

	Design	50% Design	200% Design (kinetically limited)	200% Design* O_2 & kinetically limited
C_0, mg/L	60	60	60	60
C_1, mg/L	26	20	34	36
C_2, mg/L	18	12	26	27
C_3, mg/L	14	8.5	21	22
C_4, mg/L	11	6.5	17	18

* Predicted concentrations

The overall effect of diurnal variation is to increase the final effluent quality from 11 to 12 mg sBOD/L or from 22 to 24 mg TBOD/L which remains below the desired level of 25 mg/L of TBOD.

SUMMARY

The 2nd order design method specified a total of 40 contactors arranged into 20 contactors in the first stage, followed by 10 contactors in the second stage and 5 contactors with twice the hydraulic volume in the third and fourth stage.

The 2nd order approach for designing RBC systems employs chemical kinetics good engineering practice and operational simplicity to design a cost effective RBC process.

- The kinetics governed the number of contactors and stages.
- The organic loading limitation governed the number of contactors in the first stage.
- Good engineering practice was applied by designing below the recommended organic loading of 2.5 lbs/d · k sq ft (12 g/d · m^2) to avoid nuisance growths; and by employing a minimum 15 minute hydraulic residence time in each stage to achieve completely mixed conditions.
- Operational simplicity was applied by using controlled flows into the first stage and then specifying the number of contactors in succeeding stages to insure equal hydraulic residence time without using flow monitors and controllers.
- Cost effectiveness was achieved by removing half the contactors in the final two stages, while maintaining the tankage and hydraulic residence time to achieve the required reaction kinetics.

MANUFACTURERS DESIGN METHOD

The design of the RBC facility using second order kinetics can be compared with a method outlined in a Design Manual [5]. A RBC facility was designed with the Design Manual using the identical plant conditions that were specified for the illustrative example using second order kinetics.

The design curve displayed in Figure C-1b showing the effluent soluble BOD at various hydralic loadings was used to determine the surface area requirements. To achieve a sBOD level of 12 mg/L with an influent containing 60 mg/L requires a hydraulic loading below 3.5 gpd/sq ft (140 L/d · m^2).

10,000,000 gal/d ÷ 3.5 gal/d · sq ft = 2,900,000 sq ft
(38 × 10^6 L/d ÷ 140 L/d · m^2 = 270,000 m^2)

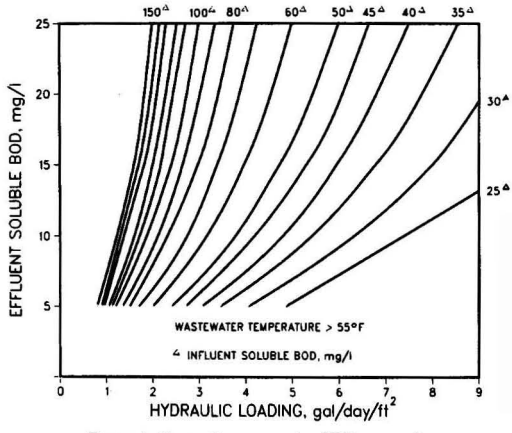

Figure 1. Domestic wastewater BOD removal.

Since there are 100,000 sq ft (9300 m²) per contactor, the total number of contactors required to treat 10 MGD (38,000 m³/d is obtained as follows:

2,900,000 sq ft ÷ 100,000 sq ft/contactor = 29 contactors
(270,000 m² ÷ 9300 m²/shaft = 29 shafts)

The shafts required in the first stage are determined by using the Design Manual's recommended loading rate of 4 lbs sBOD/d · k sq ft (20 g sBOD/d · m²) (5)

60 mg/L ≈ 60 lbs sBOD/10^6 lbs × 8.3 lbs/gal × 10^6 gal/d = 5000 lbs/d
(60 mg/L = 60 g/m³ × 38,000 m³/d = 2300 kg/d)

5000 lbs/d ÷ 4 lbs/d · k sq ft = 1,250 k sq ft ≈ 13 contactors
(2300 kg/d × 1000 g/kg ÷ 20 g sBOD/d · m² ÷ 9300 m²/shaft = 13 shafts)

Table C-2 in the Design Manual recommends two or three stages when the design effluent lies between 10 and 15 mg/L of sBOD.

The use of 13 shafts in the first stage leaves 16 shafts for the following two stages. The second stage limitation specified by the Design Manual required that the surface area be at least 50% of the surface area of the first stage. This condition is met if the remaining 16 contactors are equally divided between the second and third stage.

Overall the Design Manual would specify 13 contactors in the first stage followed by 8 contactors each in the second and third stages.

Diurnal Variation

The daily effluent quality that must be produced by the RBC process is governed by the diurnal variation that was specified for this illustrative example. The low flow condition produces an effluent with a concentration that is below the lower limit on the design curve in Figure C-1B. The lowest concentration is 5 mg/L and this value used to calculate the daily effluent quality.

At 200% of design flow the hydraulic loading rises to 7.0 gal/d · sq ft (280 L/d · m²). The effluent concentration at this hydraulic loading is beyond the limits of the design curve displayed in C-1B. The maximum hydraulic loading that can be used with an influent of 60 mg/L is 5.0 gal/d · sq ft (200 L/d · m²) At this hydraulic loading the effluent concentration is 25 mg/L. Assuming the hydraulic loading rate at 200% of design flow is 5.0 gal/d · sq ft (200 L/d · m²) then the hydraulic loading at design flow is 2.5 gal/d · sq ft (100 L/d · m²). At 2.5 gal/d · sq ft (100 L/d · m²) the effluent concentration is 7 mg/L. The hydraulic loading at low flow conditions is 1.2 gal/d · sq ft (49 L/d · m²); the predicted effluent remains at the minimum level of 5 mg/L which corresponds to the lower limit displayed in curve C-1B.

The daily effluent quality is calculated by assuming 6 hours of operation at 50% and 200% of design flow and 12 hours at design flow. The daily effluent quality based on these conditions is calculated as follows:

$$C_{eff} = (6h \times 5\ mg/L) + (12h \times 7\ mg/L) + (6h \times 25\ mg/L)/24h = 11\ mg/L$$

TABLE C-2 (5)
RECOMMENDED PROCESS STAGING FOR MAXIMUM SURFACE AREA EFFECTIVENESS

Design Effluent sBOD, mg/L	Recommended Minimum No. of Stages
<10	3 or 4
10-15	2 or 3
15-25	1 or 2
>25	1

The surface area, or the number of contactors required to achieve this level of treatment is then calculated by using the hydraulic loading of 2.5 gal/d · sq ft at design flow.

10,000,000 gal/d ÷ 2.5 gal/d · sq ft = 4,000,000 sq ft ≈ 40 contactors
(38 × 10^6 L/d ÷ 100 L/d · m² = 380,000 m² ≈ 40 contactors)

Forty contactors are required to achieve a final effluent quality of 11 mg/L of sBOD with diurnal flow variation that range from 50 to 200% of design flow by using the Design Manual and keeping the conditions within the limits shown on the design curve (Figure C-1B). The results on the total number of contactors yield the same outcome regardless if 2nd order kinetics or the Design Manual is used to specify the number of contactors.

The first stage surface area requirements can be estimated by using the curve displayed in Figure C-2B of the Design Manual. The overall soluble BOD loading is calculated as follows:

60 mg/L ≈ 60 lbs/10^6 lbs × 8.3/gal × 10^6 gal/d ÷ 4,000k sq ft = 1.2 lbs sBOD/d · k sq ft
(60 mg/L × 38 × 10^6 L/d × m³/1000L ÷ 380,000 m² = 6 g sBOD/d · m²)

A minimum of 30% of the total media area is needed in the first stage or at least 12 contactors. Table C-2 in the Design Manual recommended that two or three stages be used to achieve a final effluent between 10 and 15 mg/L. In this case two stages would be specified with 20 shafts/stage to provide positive flow control and keep the number of contactors at a minimum.

A comparison of two design methods is displayed in Table 3.

TABLE 3. COMPARISON OF DESIGN METHODS

	Second Order	Envirex
Flow, mgd	10	10
Diurnal flow variation, %	50-200	50-200
Influent sBOD, mg/L	60	60
Contactors	40	40
Stages, no.	4	2
Hydraulic loading, gpd/sf (L/d · m²)	2.5 (100)	2.5 (100)
1st stage organic loading, lbs/d · ksf (g/d · m²)	2.5 (12)	2.5 (12)
Effluent at design flow, mg/L	11	7
Effluent at 50% flow, mg/L	6.5	<5
Effluent at 200% flow, mg/L	18	25
Daily effluent, mg/L	12	11
Overall residence time, h (min)	1.44(86)	1.44(86)
1st stage residence time, h (min)	.57(34)	.57(34)
2nd stage residence time, h (min)	.29(17)	.57(34)
3rd stage residence time, h (min)	.29(17)	—
4th stage residence time, h (min)	.29(17)	—
Average flow operation		
Influent, mg/L	60	60
1st stage concentration, mg/L	26	25
2nd stage concentration, mg/L	18	7
3rd stage concentration, mg/L	14	
4th stage concentration, mg/L	11	
50% flow operation		
Influent	60	60
1st stage concentration, mg/L	20	7
2nd stage concentration, mg/L	12	<5
3rd stage concentration, mg/L	8.5	
4th stage concentration, mg/L	6.5	
200% flow operation		
Influent	60	60
1st stage concentration, mg/L	36	indeterminate
2nd stage concentration, mg/L	27	25
3rd stage concentration, mg/L	22	
4th stage concentration, mg/L	18	

SUMMARY

The 2nd order kinetic design method was used to illustrate a design approach for specifying and arranging RBC. It provides the designer with a comprehensive analyses of the RBC process. By analyzing the average conditions and the expected overloads, such as the effect of effluent quality by diurnal flow variation, the designer has a better understanding of the capability of the process. These analyses can then be incorporated into the operating document which will enable operators to better understand the limits of the process and to seek remedies whenever conditions fall outside the limits.

LITERATURE CITED

1. Opatken, E. J., Rotating Biological Contactors — Second Order Kinetics In: Proceedings of First International Conference on Fixed Film Biological Processes, King's Island, Ohio, April, 1982.
2. Opatken, E. J., Rotating Biological Contactors — Reaction Kinetics In: Proceedings of Second World Congress of Chemical Engineering, Montreal, Canada, October, 1981.
3. Brenner, R. C., J. A. Heidman, E. J. Opatken, A. C. Petrasek, *Design Information on Rotating Biological Contactors*, EPA-600/2-84-106, June, 1984.
4. Levenspiel, O., *Chemical Reaction Engineering*, John Wiley & Sons, Second Edition, 1972, Chapter 6.
5. Autotrol Wastewater Treatment Systems Design Manual. Autotrol Corporation, Bio Systems Division, Milwaukee, WI, 1978.

Edward J. Opatken is with the Hazardous Waste Engineering Research Laboratory of the U.S. Environmental Protection Agency in Cincinnati, OH.

The Effect of Magnesium-Based Additives on Particulate Emissions from Oil-Fired Power Plants

Detailed experimental results of a wide research program carried out at the University of Seville, Spain.

L. Salvador-Martinez, V. Cortés-Galeano, E. Sánchez-Peña, and P. Garcia-Caballero, University of Seville, Spain

The lack of information regarding the characteristics of particulate emissions from heavy fuel-oil combustion in large boilers has, in the last few years, sparked off an investigation into their genesis and nature. Moreover, particulate regulations are being imposed in many countries, restricting emissions from oil units which usually lack air-pollution control devices [*1*]. The need to understand the factors influencing the load and composition of particulates in flue gases is of the utmost importance if we are to comply with emissions standards.

Research has mainly been directed to determining compound forms [*2, 3, 4*], to investigating the distribution and mean diameter of particles [*5, 6*], to assessing the effect of combustion modification [*7*], and to identifying relevant fuel-oil properties [*8, 9, 10, 11*] etc. . . . To summarize, particulates produced by heavy fuel-oil combustion belong to three types: smoke (submicron carbon particles), cenospheres (non-volatile carbonaceous residue of spray droplets), and ash residue (mostly sulfates in the soluble phase and oxides in the insoluble one). Combustion conditions (excess air, flue-gas recirculation) mostly affect the first two categories, while the third is related to ash content in the fuel. Asphaltenes, Conradson carbon residue, and sulfur seem to be the main characteristics of residual fuel oil which affect total particulate emissions. There has been a growing tendency in the last few years to use magnesium-based additives in oil-fired boilers for a number of reasons: to control high-temperature corrosion of metal surfaces; to reduce acid-smut emissions; to protect the "cold end" of the boiler; and to permit reduced flue-gas exit temperature. Both "front-end" additives (injected with the fuel or as slurries in the combustion chamber) and "back-end" additives (powder which is usually, although not always, injected upstream of the air heaters) have an effect on the amount and composition of particulate-matter emissions. This effect is derived not only from the increased amount of un-converted and converted additives present, but also from the possible interaction with other conversions taking place in the boiler. In any case, the importance of evaluating the influence of magnesium-oxide treatment in emission is evident.

To improve present knowledge of characteristics of particulate emissions from large-size boilers, in particular the role played by magnesium-oxide slurries, research was carried out with the following main objectives in mind:

- To identify the elementary chemical composition of emissions from a large boiler burning heavy fuel-oil
- To define the differences caused by the use of MgO slurries regarding both quantity and characteristics of emissions
- To study the boiler's transient response to sudden changes in additive dosage

The use of different fuel-oil during the experiments has given cause to discuss the following aspects:

- The joint presence of carbon and sulfur in particulate matter
- The influence of certain characteristics of fuel-oil in emissions

EXPERIMENTAL

Test Boiler

The oil-fired power plant used in this study was of the pressurized type, built in 1972 and initially rated at 778 t/h of steam continuous duty at a pressure of 170 kg/cm² and temperature of 540°C (1004°F) with rotary air preheaters. During this research study, maximum load levels were kept constant and excess oxygen ranged from 1 to 1.5% volume.

Emissions tests were carried out in unusual blowing conditions designed to continuously sweep the whole boiler. Thus, results obtained concerning flue-gas particulate loading are not representative of normal operating blowing intensity.

Additive

A magnesium oxide-based additive (minimum 92% wt. MgO, mean diameter 10 μm, specific surface 20 g/m²) was injected as a water slurry (9% wt.) into the combustion chamber of the boiler. Two dosages were tested: 20 kg/h and 53 kg/h.

The history of additive use, which is important as regards our conclusions as to transient responses, was as follows:

- An additive injection several months prior to cases 1 and 2 (see Table 2).
- 2.5 months without any additive injections between cases 3-4 and case 5.
- Seven days of additive use between cases 6 and 7.

Particulate Sampling

Flue-gas particulate sampling was carried out isokinetically in the circular stack of the boiler using two 10-cm (4 in.) ports at 90°. According to the Environmental

Protection Agency's published methodology, ten points were located in the same circular section. They were used to establish velocity and temperature profiles and also to collect samples. A modified EPA method 17 sampling train was used; an in-stack stainless steel filter holder, suitable for a 55-mm ultrapure Whatman QM-A quartz filter, was placed after a standard hook-type stainless steel nozzle with a diameter which was chosen according to stream conditions. Time was allowed for the filter holder to heat up to stack temperature before sampling.

Differences in stack velocity and particulate loading were observed in both sampling diameters in preliminary tests. In order to minimize total sampling times, which is particularly interesting in transient-response research, simultaneous particulate collecting was done by means of two identical units running independently. The weighing for total particulate and analytical determinations was done separately for the material on each filter, and average values for these were calculated.

Analytical Procedures

The elementary analysis of particulates. The samples were analyzed following a procedure used by the Brookhaven National Laboratory [*10*] which carries out species separation on the basis of water solubility. However, only four elements, Mg, V, Fe, and Na, were deemed necessary for this study. Concentrations in both soluble and insoluble phases were determined. According to previous studies made by Henry and Knapp [2], water-soluble compounds of the above mentioned elements have been assumed to be sulfates, while those in the insoluble phase have been considered to be oxides. Insoluble carbon and insoluble sulfur were determined by means of a LECO unit, model CS-244.

The microscopic examination of particles. An HITACHI HHS-2R scanning electron microscope was used to observe the samples. This device was provided with an EDAX dispersive energy X-ray analyzer.

Fuel Analysis. Fuel samples were taken during the test periods. Sulfur was measured by combustion analysis according to ASTM D. 1552; asphaltenes were determined following IP 143; and Conradson carbon was determined from Ramsbottom (ASTM D. 524). Metals of interest were analyzed by atomic absorption spectrometry. Figure 1 shows the values obtained for sulfur, asphaltenes, carbon and vanadium; Table 1 lists the concentrations of Na, Mg, Fe, and V in the fuels burned.

RESULTS AND DISCUSSION

Additive Effects

Tables 2 and 3 show the chemical composition of particles emitted in two groups of four cases; the main differences are due to the various fuel oils burned and to the use or not of the additive in different dosages. Less attention, however, was paid to excess combustion air and fuel-oil atomization temperature in relation to other operating conditions. Cases 3, 4, 6, and 8 correspond to situations that are practically permanent after changes have been made in additive injections. In all the cases, the data shown are taken from an average of at least four samples.

Due to the above-mentioned reasons, the results showed a marked difference between the experiments in Tables 2 and 3. For type A fuel oils without additive (cases 3 and 4), emissions are reduced by 17% when excess oxygen is increased by 0.5%. Using 20 kg/h of additive (cases 1 and 3), total emissions are increased by about 24%. The insoluble fraction, which is more than 70% of the total, is made up mainly of unburned carbon (up to 85%), the rest being almost completely sulfur. The carbon content is very sensitive to the amount of excess oxygen. The soluble fraction presents greater differences in composition in cases with and without additives. In particular, in those cases with additive injection, magnesium sulfate takes up about 32% of the water soluble phase. Vanadium compounds, taken to be $VOSO_4$, are also important in this phase, reaching 15% without the use of the additive.

When type A and type C fuel oils are burned and there is a large additive dosage (53 kg/h), higher emissions which always exceed 400 kg/h are observed (see Table 3).

This increase between cases 7 and 6 is almost com-

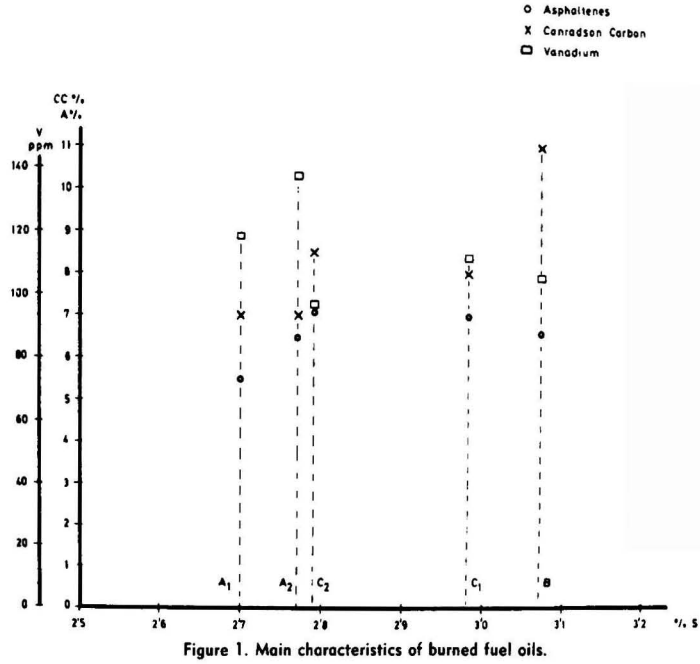

Figure 1. Main characteristics of burned fuel oils.

TABLE 1. METALS IN FUEL OILS BURNED

Fuel Oil Type	A_1	A_2	B	C_1	C_2
Na, ppm	46.6	42.3	67.0	56.6	43.6
Mg, ppm	5.0	4.9	3.3	3.0	2.0
Fe, ppm	14.0	10.7	1.4	2.3	1.6
V, ppm	118	136	98	110	104

pletely due to unburned carbon and cannot be explained only by the changing of fuel oils. We should consider the possible influence of an undetected operating problem during the experiments.

The insoluble fraction (70% without additives) goes up by 10% when MgO is introduced. As pointed out before, there exists a very high percentage of unburned material: 90% with additive and 85% without.

This reduction, which is caused by the presence of MgO and other unidentified compounds in the insoluble phase, is not real in absolute terms. For the same fuel oil, the amount of unburned carbon is slightly higher when the additive is injected. From the above result, therefore, it could be seen that there might be some type of interference between the combustion process and the additive.

Nevertheless, it may not be concluded that this substantial increase in the soluble fraction is a result of the additive injection (53 kg MgO/hr), which is partially converted into sulfate inside the plant. This salt does exceed 40% of the soluble phase (cases 6 and 7), but it is obvious that the suppression of the additive does indeed favor the emission of unidentified soluble compounds, and in noticeable proportions, too.

In short, the additive gives rise to an increase (of about 20%) in emission levels in the cases of fuel oil A-20 kg/hr and fuel oils B/C-53 kg/hr. This amount results from several opposed effects:

- Higher emissions of soluble and insoluble magnesium derivatives.
- Higher emissions of unburned material.
- Lower emissions of other soluble compounds.

These effects are illustrated in Table 4, where case 5′ corresponds to a sample taken four hours after starting additive injection and case 7′ corresponds to a sample collected 6.5 hours after cut-off.

Observations made with the scanning electron microscope have shown the almost exclusive presence of cenospheres with diameters between 10 and 100μ (Figure 2). Their aspect is normal, i.e., a solid skeletal particle, full of void spaces, resulting from the vaporization of volatile components and incomplete burning of highly carbonaceous residue. The elementary composition, as given by the EDAX, shows the presence of carbon, sulfur, and, to a lesser extent, vanadium in the cenospheres.

Samples obtained during additive periods show a very small number of additive particles (of a mean diameter of 15-20μ), whose outer layers are composed of magnesium sulfate. These particles (Figures 3 and 4) show a compact surface of reaction product. Should this layer develop controlling diffusional resistance, the resulting shrinking-core reaction model might explain the observed conversion levels (see next paragraph).

Transient Response to Step Changes in Additive Injection

The results considered in preceding paragraphs were obtained while the boiler was kept in steady operating conditions, especially regarding additive injection in the combustion chamber. In order to evaluate the effects produced on the quantity and characteristics of emissions by a sudden disturbance of additive conditions, the evolutions of several relevant parameters were studied in two experiments of step changes in dose from 0 to 53 kg MgO per hour and vice versa.

Curve 1 in Figure 5 shows the evolution of total magnesium (as soluble sulfate and insoluble oxide) emissions in particulate form after the step input, which is equivalent to 31.8 kg Mg per hour.

The additive injection took place 2.5 months after the last cut-off. Curve 2 in Figure 5 represents the response of soluble magnesium (magnesium sulfate produced by reaction between the additive and SO_3) expressed as a percentage of total particulates.

The additive effects concerning conversion into $MgSO_4$ are fast. The mean residence time for this compound is about 2 hours, while for total magnesium it is 5 hours. The steeper slope of curve 1, compared with that of curve 2 particularly after $t = 6 \div 8$ hours, shows a relative reduction in the conversion degree with proximity to steady state. This fact may be explained by an initial accumulation of the additive in the boiler's surface which is later swept out by blowing, thus having longer permanence times. Near steady state, the additive accumulation rate is stabilized and the mean residence time in the boiler reaches a minimum. The values for steady state show that about a third of the magnesium injected as additive (31.8 kg/h) remains in the boiler; the rest is emitted in particulate form. The conversion observed is 33% (mol).

Curve 1 and 2 in Figure 6 show the evolution of both parameters (total as soluble magnesium) after the cut-off of additive injection, for $t = 0$ after a 7-day additive period. The mean residence times for total magnesium are now shorter (down to 1.5 hours) and the response curve for soluble magnesium is much more damped. The faster response for total magnesium could be explained by boiler accumulation; indeed, this fact should produce a damping effect in start-ups and the opposite in shut-downs. The slow evolution of the soluble fraction would be caused by a sequential out-flow (by means of blowing operations) of magnesium coming from the boiler's surfaces which are exposed to flue gases; in this case, residence times should be longer, thus allowing a higher conversion into sulfate.

As a direct result, it must be admitted that the effects of SO_3 on the flue gases by the retained additive last for several days, and the internal layers of additive will go on protecting the surfaces against corrosion for even longer periods (probably months).

Figure 7 shows the boiler's response regarding total particulate emission to additive cut-off at $t = 0$ after a 7-day additive period. Concentrations have been referred in relation to their initial value, C_0, before the disturbance input. Continuous blowing of the boiler (over a period of about two hours) produces fluctuations in the emissions level. The boiler's response time, with reference to this variable, may be estimated about 20 and 22 hours; from this value, therefore, an important degree of back-mixing and accumulation in the plant may be concluded.

As stated, the additive contributes up to 20% of total emissions. The direct responsibility for converted and unconverted derivatives may be calculated at 50% of this figure.

TABLE 2. CHEMICAL COMPOSITION OF PARTICULATE EMISSIONS

Case	1		2		3		4	
Fuel Oil Type	A_1		A_2		A_2		A_2	
Load	Full		Full		Full		Full	
F. O. Temp., °C	120		130		130		130	
Oxygen, % vol.	1.5		1		1		1.5	
Additive	Yes (1)		Yes (1)		No		No	
	Kg/h	%	Kg/h	%	Kg/h	%	Kg/h	%
Particulate Emissions	351	100.0	434	100.0	350	100.0	290	100.0
Water Insoluble	224.7	64.0	309.9	71.4	245.8	70.2	168.4	58.1
C	179.0	51.0	250.7	57.8	206.2	58.9	151.4	52.2
S	12.5	3.6	15.8	3.6	13.4	3.8	10.3	3.5
Mg as MgO	2.0	0.6	5.9	1.4	0.8	0.2	0.4	0.1
V as V_2O_5	—	—	7.6	1.7	3.0	0.9	—	—
Fe as FeO	—	—	2.6	0.6	1.5	0.4	—	—
Na as Na_2O	—	—	0.1	0.0	0.1	0.0	—	—
Others	31.2	8.8	27.2	6.3	20.8	6.0	6.3	2.3
Water Soluble	126.7	36.0	124.1	28.6	104.2	29.8	121.6	41.9
Mg as $MgSO_4$	38.3	10.9	40.1	9.2	8.9	2.5	8.7	3.0
V as $VOSO_4$	—	—	14.2	3.3	15.3	4.4	—	—
Fe as $FeSO_4$	—	—	3.1	0.7	2.2	0.6	—	—
Na as Na_2SO_4	—	—	1.6	0.4	1.5	0.4	—	—
Others	88.5	25.1	65.1	15.0	76.3	21.9	112.9	38.9

(1) 20 Kg/h MgO
— No data available

TABLE 3. CHEMICAL COMPOSITION OF PARTICULATE EMISSIONS

Case	5		6		7		8	
Fuel Oil Type	B		B		C_1		C_2	
Load	Full		Full		Full		Full	
F. O. Temp., °C	120		120		120		120	
Oxygen, % vol.	1.5		1.5		1.5		1.5	
Additive	No		Yes (1)		Yes (1)		No	
	Kg/h	%	Kg/h	%	Kg/h	%	Kg/h	%
Particulate Emissions	500	100.0	570	100.0	696	100.0	428	100.0
Water Insoluble	351.7	70.3	444.3	78.0	560.2	80.5	289.3	69.7
C	325.7	65.1	381.5	66.9	472.7	67.9	269.8	63.0
S	19.1	3.8	23.6	4.1	28.9	4.2	17.1	4.0
Mg as MgO	0.8	0.2	16.2	2.8	13.9	2.0	0.6	0.1
V as V_2O_5	4.2	0.8	8.3	1.5	4.7	0.7	0.3	0.1
Fe as FeO	1.1	0.2	1.1	0.2	0.8	0.1	0.1	0.0
Na as Na_2O	0.1	0.0	0.1	0.0	1.0	0.1	0.1	0.0
Others	0.7	0.2	13.5	2.5	38.2	5.5	10.3	2.5
Water Soluble	148.3	29.7	125.7	22.0	135.8	19.5	129.7	30.3
Mg as $MgSO_4$	1.8	0.4	49.8	8.7	62.9	9.0	8.6	2.0
V as $VOSO_4$	15.6	3.1	18.5	3.2	19.7	2.8	20.9	4.9
Fe as $FeSO_4$	4.7	0.9	3.5	0.6	2.7	0.4	2.4	0.6
Na as Na_2SO_4	0.3	0.1	0.6	0.1	6.0	0.9	11.4	2.7
Others	125.9	25.2	53.3	9.4	44.5	6.4	86.4	20.1

(1) 53 Kg/h MgO

TABLE 4. EFFECTS OF ADDITIVE INJECTION ON PARTICULATE EMISSIONS

Case	5		5′		7		7′	
Additive	No		Yes (1)		Yes		No (2)	
	Kg/h		Kg/h		Kg/h		Kg/h	
Particulate Emissions	500		586		696		607	
Water Insoluble	351.7		454.5		560.2		495.3	
C		325.7		397.4		472.7		463.6
S		19.1		23.1		28.9		27.5
Mg as MgO		0.8		8.4		13.9		1.4
Others		6.1		25.6		44.7		2.8
Water Soluble	148.3		121.5		135.8		101.4	
Mg as $MgSo_4$		1.8		38.1		62.9		20.0
Others		146.5		83.4		72.9		81.4

(1) 4 hrs after starting up
(2) 6.5 hrs after cutting off

The Carbon/Insoluble Sulfur Ratio

Table 5 lists the mean values of the unburned carbon/insoluble sulfur ratio (w/w) in particulates. The figures for cases 5-8 are slightly higher than those for experiments 1-4. Within the latter group, testing with 1.5% excess oxygen gives the smallest values; this could show a differential increase in the combustion rate of carbon with respect to sulfur. With available data, it cannot be concluded that additive injection produces a substantial modification in the ratio.

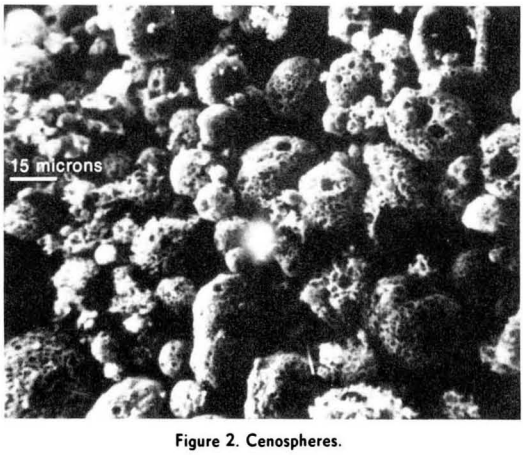

Figure 2. Cenospheres.

The Effects of the Fuel Oil

Figure 8 shows total emissions (kg/hr) *vs.* asphaltenes plus Conradson carbon residue for fuel oils burned (with the exception of case 7), for the previously mentioned reasons. Our research was directed mainly to investigating additive effects, so no special attention was paid to the fuel oils used. This explains why only limited conclusions can be reached. According to Goldstein and Siegmund [9], a relative proportionality between total emissions and both fuel parameters may be observed for the experiments done without additive and with 1.5% excess oxygen.

From the above-mentioned graph, one may also deduce that it becomes necessary to reduce the asphaltenes + Conradson content in the fuel by at least 1% to keep the emissions constant when using additive (20 kg MgO/hr). This is true only if the excess oxygen is increased simulta-

Figure 3. Additive particles whose outer layers are composed of magnesium sulfate.

Figure 4. Additive particles.

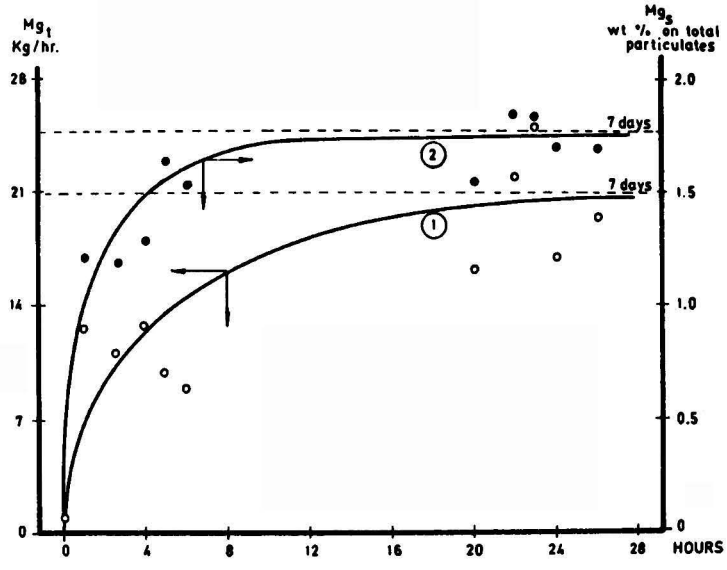

Figure 5. Transient response of magnesium emissions to additive input.

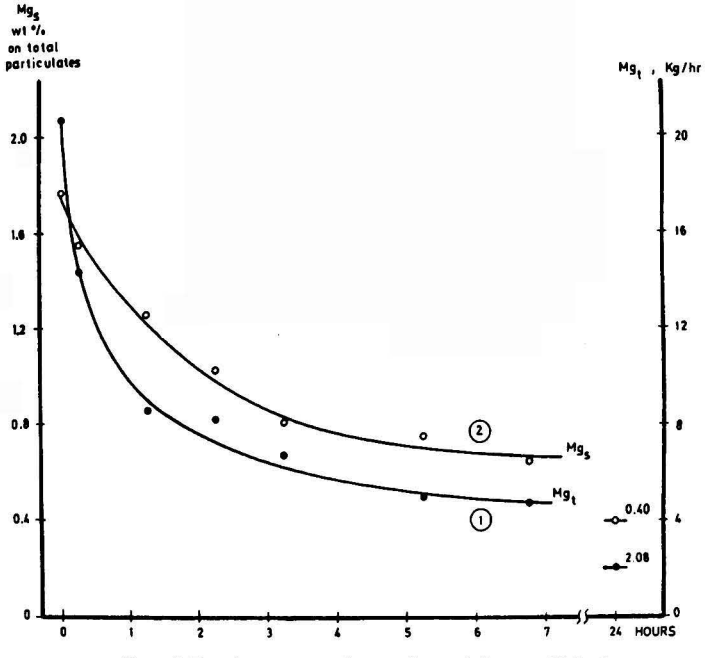

Figure 6. Transient response of magnesium emissions to additive input.

neously by 0.5% (A_2-1% without additive as against A_1-1.5% with additive). If the excess oxygen is to be reduced from 1.5% to 1.0% and the emissions are to be kept constant after using the additive, then the asphaltenes + Conradson content must be decreased by 2% (C_2-1.5% without additive as against A_2-1% with additive).

The C/S correlation for particulates is shown against asphaltenes + Conradson/sulfur (wt./wt.) in fuel oil. This is, to a certain extent, inexact, as it would be more correct to use the amount of sulfur that is really present in the asphaltenes + Conradson; the rest, in the volatile fractions, is easily transformed into SO_2 and SO_3. In spite of what has been said above, the slope of the graph is about 3. Precise knowledge of the sulfur distribution might allow conclusions to be reached concerning preferential enrichments derived from the combustion process.

Bachman and Siegmund's correlation [*10*] gives values for the fuel oils burned that differ from those obtained

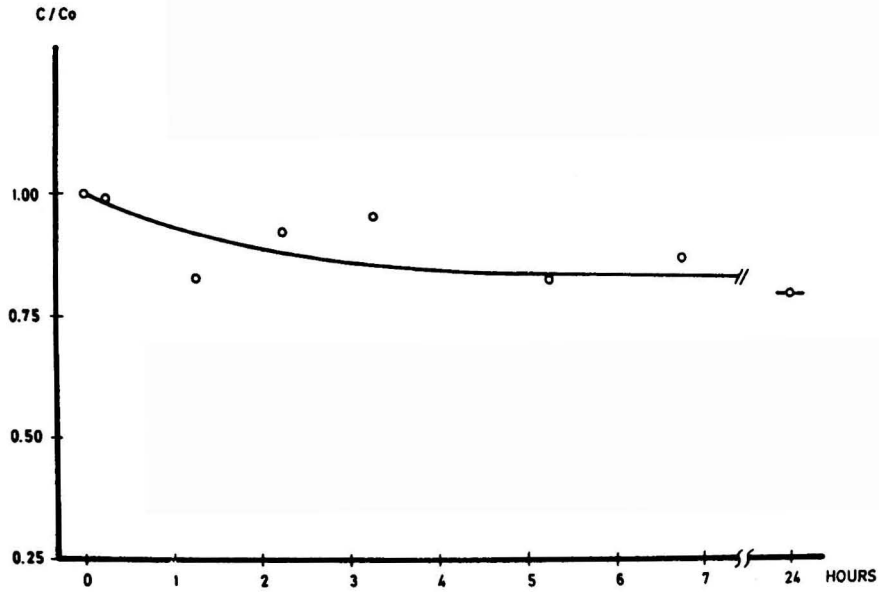

Figure 7. Transient response of total emissions to additive cut off.

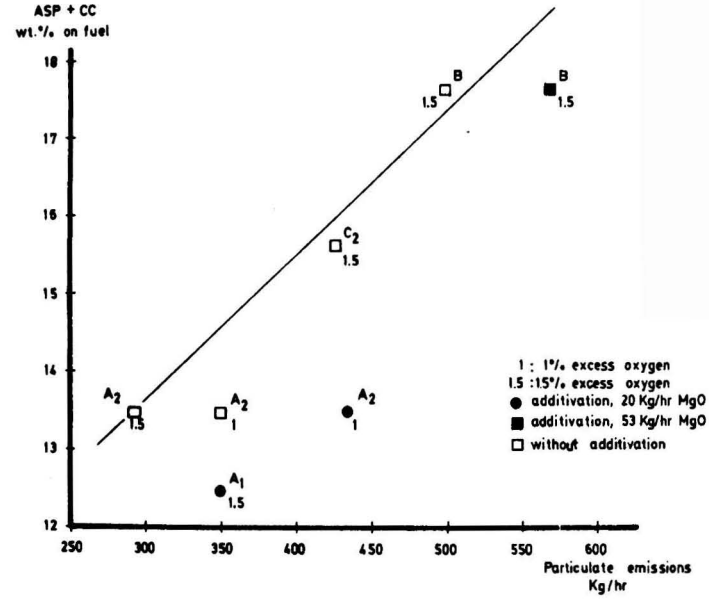

Figure 8. Particulate emissions as function of fuel asphaltenes plus Conradson carbon contents.

through experiments. It must be realized that the interference caused by the additives in the mechanisms generating sulfur derivatives (second term in the correlation) and unburned carbon (third term) are of a type that require stipulating new parameters if the principles inspiring this correlation are deemed valid.

Research is currently being carried out along these lines at the Dept. of Chemical Engineering of the University of Seville.

CONCLUSIONS

1. The injection of MgO water slurries into the combustion chamber of a boiler causes an increase in emission lev-

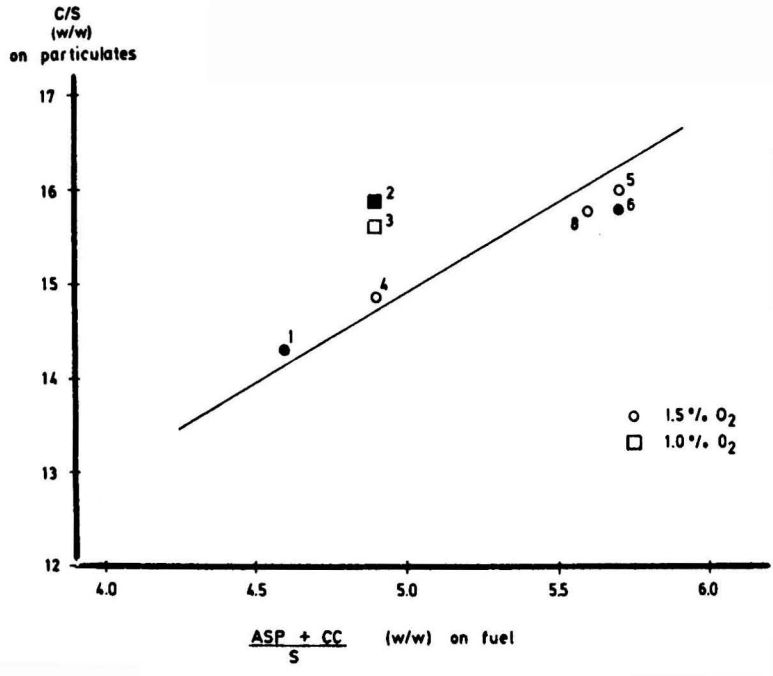

Figure 9. Fuel characteristics vs. ratio c/s.

els of about 20% when the additive rate is 53 kg MgO/hr and the fuel oil burned is 3.0% sulfur, and 17% asphaltenes + Conradson. The same value was found for 20 kg MgO/hr and 2.8% sulfur, 13% asphaltenes + Conradson fuel oil.

2. Additive use produces:
- Higher emissions of soluble and insoluble magnesium derivatives
- Slightly higher emissions of unburned material
- Lower emissions of other soluble compounds

3. Should the outer layer of magnesium sulfur in additive particles develop a controlling diffusional resistance to further reaction, the resulting shrinking-core reaction model might explain the observed conversion levels.

4. The study of the boiler's transient response to step changes in additive dosage shows that, after starting injection, accumulation of the additive takes place on the boiler's surface, thus giving a damped response to input.

This accumulation produces a faster response after the additive is cut off.

5. The values for steady state show that about one third of the magnesium injected as additive (31.8 kg/h) remains in the boiler; the rest being emitted in particulate form.

For those fuel oils tested (with the exception of type B), with or without the use of additive, the following correlation may be applied to carbon (C) and insoluble sulfur (S) in particulates:

$$S(\%) = 0.05\ C\ (\%) + 0.86$$

ACKNOWLEDGMENTS

The authors wish to thank the Compañia Sevillana de Electricidad S.A., for their kind permission to publish this study and gratefully acknowledge E. Catalá, J. M. Sosa, A. Lara and J. Fazio for their assistance

The contributions of F. Bernier and personnel of the Department of Chemical Engineering are also acknowledged.

LITERATURE CITED

1. Beachler, D. S. and G. T. Joseph, "Emission Regulations and Air Pollution Control Equipment for Industrial and Utility Boilers," *Envir. Prog.*, **3**, No. 1, 44 (1984).
2. Henry, W. M., "Methods for Analyzing Inorganic Compounds in Particles Emitted from Stationary Sources." EPA report 600/7-79-206, Sept. 1979.
3. Henry, W. M. and K. T. Knapp, "Compound Forms of Fossil Fuel Fly Ash Emissions." *Envir. Scien. Tech.*, **4**, 450 (1980).
4. Miller, S. M., "Particulate Characterization," DOE report FE/60181-1642, August 1984.
5. Sakai, T. and S. Sugiyama, "Residual Carbon Particles yielded by Combustion of Atomized Heavy-fuel-oil Droplets." *J. Inst. Fuel.*, **43**, 295 (1970).
6. Cheng, R. M. *et al.*, "Characterization of Particulates from Power Plants." *J. Air Poll. Const. Ass.*, **26**, 787 (1976).
7. Goldstein, H. L. and C. W. Siegmund, "Particulate Emissions from Residual Fuel Fired Boilers: Influence of Combustion Modification." *J. Eng. Power*, 371, July, 1977.

TABLE 5. RATIO C/ INSOLUBLE SULPHUR ON PARTICULATES

Case	1	2	3	4	5	6	7	8
F. O. type	A_1	A_2	A_2	A_2	B	B	C_1	C_2
Oxygen, % vol.	1.5	1	1	1.5	1.5	1.5	1.5	1.5
Additive, Kg/h	20	20	—	—	—	53	53	—
C/S, W/W	14.3	15.9	15.6	14.8	16.0	15.9	16.3	15.8

8. Bennett, R. L. and K. T. Knapp, "Particulate Sulfur and Trace Metals Emissions from Oil Fired Power Plants." *AIChE Symp. Series*, No. 188, 75, 174, 1979.
9. Goldstein, H. L. and C. W. Siegmund, "Influence of Heavy Fuel Oil Composition and Boiler Combustion Conditions on Particulate Emissions." *Envir. Scien. Tech.*, **10,** 1109 (1976).
10. Bachman, K. C. and C. W. Siegmund, "The Effect of Fuel Oil Composition on Particulate Emission." IFRE. Doc. Nr. F 23/ea/3, Sept. 1979.
11. Bocca, P. *et al.*, "Chemical Factors Influencing Particulate Emissions from Fuel Oil." *Riv. dei Combusti. III*, 239 (1976).
12. Dietz, R. N., Private communication and BNL-30155 report.

Luis A. Salvador is Professor of Chemical Engineering at the Department of Chemical and Process Engineering, University of Seville, Spain. He has been working as a Chemical Engineer with Union Explosivos Rio Tinto, for several years, and is a Consultant Engineer in the field of Environmental Engineering.

V. Cortés-Galeano is an Associate Professor in the Chemical Engineering Department of the Seville University, Spain. He holds a PhD degree in Chemical Engineering from the same University and is an active consultant on environmental problems derived from fossil fuels combustion.

Eduardo J. Sánchez Peña is an associate professor of chemical engineering at the University of Seville, Spain. Professor Sánchez Peña has a doctorate in chemical engineering from the same University. He is a registered professional engineer in Seville, and is a member of Spanish Nuclear Society.

P. Garcia-Caballero is Assistant Professor for the Chemical Engineering Dept.-Sevilla University, Spain. He holds several years experience on fertilizers and petrochemicals industries and he has been actively involved in the area of "Residual oil combustion problems and its control through magnesium based additives" for the last four years.

Health Risk Comparison Between Groundwater Transport Models and Field Data

The potential of ground water contamination is one of the major concerns over land disposal of hazardous waste. Risk assessment requires information on groundwater concentrations of contaminants at the exposure location. Results are presented of case studies comparing health risk assessment and plume delineation based on state-of-the-modeling and monitoring data.

Seong T. Hwang, Office of Research and Development, U.S. EPA, Washington, D.C. 20460

Proper management of solid and hazardous waste should provide acceptable levels of human exposure to toxic waste constituents released from disposal, treatment and storage facilities into ground water. Frequent findings of ground water contamination underscore the ability to conduct an adequate assessment of migration potentials of contaminants as well as their harmful effects on human health as a consequence of drinking the contaminated water. To overcome the weakness in the present state-of-the-art technique for conducting such assessment, current regulatory approaches to waste management tend to emphasize control technology for waste containment, monitoring to detect contamination, and the alternate method of setting contaminant limitations based on consideration of short and long-term human health effects. There is a more recent Congressional mandate (such as 1984 reauthorization of the Resource Conservation and Recovery Act) totally devoted to waste characterization for the purpose of banning toxic waste from disposal.

Despite these different conceptual approaches to waste management, the basic need for predicting contaminant migration has not diminished, but seems to be ever growing. This is because exposure to contaminants that have migrated or have potential to migrate needs to be assessed for sound risk assessment, regardless of the conceptual approaches used.

This paper will present the methodologies that have been used in conducting exposure assessments for sites where ground water monitoring data show contamination, and also where no field data are available. Ground water monitoring data and transport models were used to determine the levels of contaminant concentrations in ground water. Models used range from computerized models to simple analytical models [*3, 4, 6, 7, 8, 9, 11, 13*]. The paper also presents the results of health risk assessment for protection of human health from carcinogenic and noncarcinogenic effects based on the exposure assessments.

GENERAL METHODOLOGY

Assessing exposure to contaminants in ground water impacted by waste facilities is a stepwise process which may involve the following steps: (1) site characterization for collecting relevant site-specific information, (2) collection of available monitoring data, and (3) estimating concentrations at the points of exposure.

Monitoring data from the point of exposure should be used wherever available for estimating the potential intakes of waste constituents. Since the concentrations in the plume will be steadily changing, the concentrations monitored at a well location are transient in nature. If the site is releasing contaminants continuously, the plume dimensions will grow, thereby increasing the concentrations at the exposure point until steady-state concentrations are attained.

Since monitoring data could be a measurement of dynamically changing plume dimensions, it is appropriate to ascertain that the data represent steady state conditions at the time of sampling. Unacceptable exposures, as indicated by the monitoring data, should trigger further investigation or some sort of corrective action for steadily growing plumes, unless remedial measures have been completed at the site. The monitored concentrations below an acceptable exposure level do not always guarantee future safety in protecting public health and the environment from exposure to contaminants being released, until no further growth in plume dimensions can be ascertained.

Monitoring data obtained from a facility operating over an extended period of time may correspond to steady-state concentrations. In such cases, any significant increase in concentration in the future may be unlikely. Models can be used to simulate the conditions existing in the ground water environment, estimating transient and steady state concentrations which may be attained.

The concentration at an exposure point determined from monitoring data, or calculated from transport modeling can be used to estimate the health effects on a short- or long-term basis. A compilation of health effect data is available which are derived from the weight of evidence on carcinogenic effects, and short-term and chronic noncarcinogenic effects.

One type of health effect model expresses the carcinogenic effect as a linear relationship between dose and effect, called the potency factor K(mg/kg · day)$^{-1}$, while noncarcinogenic effect data are used to derive acceptable daily intake (ADI, mg/day) dose below which no adverse noncarcinogenic health effects can be observed. Because of difference in body weight between an adult

and a child, a 70 kg adult will require a higher ADI than a 10 kg child.

The risk(R) associated with the intake of contaminants in normal 2 L/day of drinking water over a lifetime can be obtained by

$$R = 1 - e^{-KD}$$

where D is the daily intake of a contaminant present in drinking water per unit weight of human body (mg/kg · day). When the cancer risk is less than 10^{-3}, this formula can be approximated by $R = K \cdot D$.

ASSESSMENT USING MONITORING DATA

The data obtained from ground water monitoring wells can be effectively used to conduct health risk assessment. The concentration level will be different depending upon the location of monitoring wells in relation to waste treatment, storage and disposal facilities where contaminant migration occurs. The concentration should be evaluated to determine if the level is acceptable to prevent the carcinogenic and noncarcinogenic health effects.

As indicated previously, the concentration variation is a dynamic process being affected by hydrogeologic conditions under which contaminant transport occurs, and chemical and physical properties of the contaminants. The concentrations are also changing in time and space unless steady state conditions are reached. This consideration should be important in making conclusions on health effect consequences based on monitoring data. The results based on transport modeling will be helpful in determining the degree of variation in health risk assessment over a time period of interest.

ASSESSMENT USING MATHEMATICAL MODELING

Although the usefulness of mathematical modeling as an important tool in predicting contaminant migration in ground water has long been recognized, reluctance on its use relates to the depth of understanding of fundamental processes that control fate and transport, and legimate confusion stemming from "too many" available models that can be found in the literature.

Before resorting to mathematical modeling, it is critical to define the objective of using it. This process is important in selecting appropriate models among various models available in the literature, as well as in defining the significance of assigned values for chemical, physical and hydrogeologic parameters that affect transport processes. The objective could be one or more of the following:

1. To compare monitoring data with calculated results.
2. To estimate the dynamic nature of monitored plumes.
3. To estimate concentration levels in the absence of monitoring data.
4. To compare the results of different models.
5. To compare the results based on different parameter values.

Whatever the resulting solutions of the models may be, the starting equation describing the fate and transport of contaminant in ground water is obtained by writing a material balance around an infinitesimal flow element in the aquifer. For steady flow through a uniform aquifer medium, the partial differential equation takes the form

$$R_d \frac{\partial C}{\partial t} = D_x \frac{\partial^2 C}{\partial x^2} + D_y \frac{\partial^2 C}{\partial y^2} + D_z \frac{\partial^2 C}{\partial z^2} - V \frac{\partial C}{\partial x} - kR_dC \quad (1)$$

where C = concentration of a contaminant at a ground water location x(cm), y(cm) and z(cm), g/cm^3; V = seepage velocity, cm/s, which can be obtained by dividing Darcy's velocity by porosity ϵ; R_d = retardation factor: D_x, D_y, D_z = effective diffusion coefficients in x, y and z directions, respectively, cm^2/s, which are normally expressed by the relationships $D_x = \alpha_x V$, $D_y = \alpha_y V$ and $D_z = \alpha_z V$, where α represents dispersivity in the respective direction; t = time in sec., and k = biodegradation constant, 1/s.

Different models result not only because Equation (1) is solved analytically or numerically, but also because it is solved under the assumption of one, two or three dimensional transport problems depending upon the simplication needed. There are also numerous computer codes, some being proprietary, simulating ground water transport by numerically solving Equation (1) coupled with flow equations and appropriate boundary conditions [6, 7, 9]. A computer code in the public domain makes use of a technique tracking particles initially placed in grid cells [9]. Also many of the analytical solutions have been documented [4, 8, 13, 15].

Since one or two dimensional solutions are often unrealistic for three dimensional aquifer problems, a few three dimensional solutions which can be easily used in exposure assessment are presented herein. Because of space limitation, the technique of numerical solution is not explained in this paper.

The analytical solution to the three dimensional transport model Equation (1) under the condition of a continuous point source discharge is taken from Turner's solution [12], and takes the following form:

$$C(x,y,z,t) = \frac{C_o Q}{4\pi\epsilon R\sqrt{D_y D_z}} e^{\frac{Vx}{2D_x}} \left\{ e^{\frac{UR}{2D_x}} \operatorname{erfc}\left(\frac{Ut + R_dR}{\sqrt{4R_dR_dt}} \right) + e^{-\frac{UR}{2D_x}} \operatorname{erfc}\left(\frac{R_dR - Ut}{\sqrt{4R_dD_xt}} \right) \right\} \quad (2)$$

where

$$R^2 = x^2 + \frac{D_x}{D_y} y^2 + \frac{D_x}{D_z} z^2;\ U = V\left(1 + \frac{4D_xR_dk}{V^2} \right)^{1/2}$$

The expression for steady state concentration can be easily obtained from Equation (2) by letting $t \to \infty$, and using erf (0) = 0.

The release from land disposal facilities does not in general approximate the point source assumption, unless it occurs in a form of leakage through a punctured hole in containing liners. Leakage from underground storage tanks may often resemble point source release. Since the release from land disposal facilities impacts ground water from an area on the top of flowing water rather than in a form of point source release, Equation (1) can be solved with the following boundary and initial conditions:

1. $C = C_b$ (background concentration) at $t = 0$, $z > 0$, and all x and y

2. $\dfrac{\partial C}{\partial z} = 0$ at $z = H$

3. $VC - \epsilon Dz \dfrac{\partial C}{\partial z} = M$ at $z = 0$,

$$-\frac{A}{2} \leq x \leq \frac{A}{2},\ -\frac{B}{2} \leq y \leq \frac{B}{2}$$

where H = aquifer depth, M = rate of contaminant release per unit area, g/cm^2 · s, and A and B are the dimensions of a disposal facility in the direction and cross-direction of ground water flow. See Figure 1 for an idealized sketch showing a plane source on the groundwater surface, and waste cells from which leakage occurs.

The solution to Equation (1) with the three boundary and initial conditions given above are

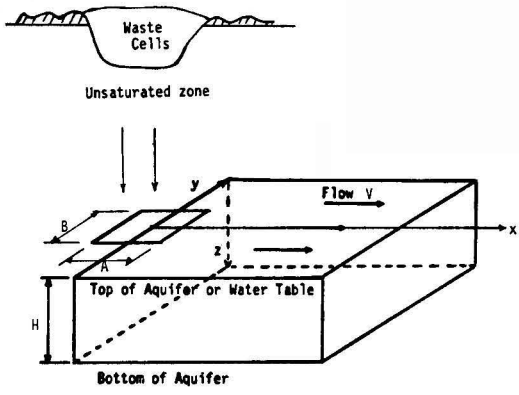

Figure 1. Idealized sketch of a horizontal plane source and waste cell arrangement approximating the source.

$$C(x,y,z,t) = \frac{C_o Q}{4\epsilon R_d A \cdot B} \int_{t'=0}^{t'=t_d} \frac{1}{\sqrt{\pi D_z (t-t')}\,\mathrm{erf}\left(\frac{H}{\sqrt{4D_z^*(t-t')}}\right)} \exp\left[-\frac{z^2}{4D_z^*(t-t')} - k(t-t')\right] \cdot F\, dt' \quad (3)$$

where

$$F = \left[\mathrm{erf}\left(\frac{x - V^*(t-t') + A/2}{\sqrt{4D_x^*(t-t')}}\right) - \mathrm{erf}\left(\frac{x - V^*(t-t') - A/2}{\sqrt{4D_x^*(t-t')}}\right)\right] \left[\mathrm{erf}\left(\frac{y + B/2}{\sqrt{4Dy^*(t-t')}}\right) - \mathrm{erf}\left(\frac{y - B/2}{\sqrt{4Dy^*(t-t')}}\right)\right]$$

$V^* = V/R_d$; $D_x^* = D_x/R_d$; $D_y^*, D_z^* = D_z/R_d$; t_d = length of source discharge time in seconds; H = depth of aquifer in cm; and the other symbols have the same meaning as in Equation (1). Equation (3) can also be integrated over the aquifer depth to obtain the vertically averaged concentrations in the aquifer over its depth.

The integration in Equation (3) with respect to release time t_d is necessary because contaminants being released are assumed to reach ground water continuously. The integration should be performed numerically from the start to cessation of contaminant release to ground water because no closed form integration is possible.

The analytical or numerical solutions can be used to estimate the concentration level at the point of exposure or to establish plume isopleths under dynamic or steady state conditions. Health risk assessment can be performed based on the calculated results or monitoring data.

EXAMPLE ASSESSMENT

Use of Monitoring Data

After an extensive search for candidate sites with good plume delineation, five sites were selected for health risk assessment evaluation. The criteria for selection included the analysis of ground water contaminants for which applicable unit risk (UCR) and ADI values were available. The sites selected after this initial screening were also subjected to modeling if adequate site characterization data were available for determination of transient behavior of the plume and steady-state concentrations. The concentration values were determined in the immediate vicinity of the facility and at a distance away from the source, within the property boundary.

The sites extensively monitored by the U.S. Geological Survey (USGS) were also investigated for possible use in the health risk assessment. Out of about seven sites investigated, only two sites have been selected for evaluation. This determination was made because the other sites either do not have ground water contaminants for which the UCR or ADI values have been determined, or the plume delineation is not adequate.

Table 1 summarizes an evaluation of exposure to contaminants monitored at the waste boundary and approximately 100 feet away from the migration side of the waste boundary. Alternate waste management boundaries other than the 100 feet distance or the waste boundary can be chosen as favored by the availability of monitoring data. EPA's UCR values given in units of $(mg/kg \cdot day)^{-1}$ are obtained mostly from the animal dose-response experiments that are used in determining the risks associated with ex-

TABLE 1. SUMMARY OF HEALTH RISK EVALUATION FOR SITES WITH GOOD MONITORING DATA

Site No.	Contaminants	Concentration (ug/L) at 100 ft from Waste Boundary	Concentration (ug/L) at Waste Boundary	UCR[e] $(mg/kg \cdot day)^{-1}$	ADI[f] (mg/day)	Upper Bound Cancer Risk at 100 ft from Waste Boundary	Exposure Ratio for Noncarcinogens (Exposure/ADI) 100 ft from Waste Boundary	Exposure Ratio for Noncarcinogens (Exposure/ADI) at Waste Boundary
1[a]	Naphthalene	650	1630		18		0.07	0.18
	PHA	1170	1800		18		0.13	0.2
2[b]	Chromium (Hexavalent	24		41		0.028		
	Cadmium	6900		7.8		0.785[c]		
3	Arsenic	623000		15		1		
	Phenol		60		7			
4	1,2-Dichlorobenzene		16000		6.3			5.1[d]
	Chlorobenzene		1100		1			2.2
	Toluene		2300		30			0.15
	Xylene		1900		160			0.02
5.	Phenol	8	28		7		0.002	0.008
	Pentachlorophenol	57	3400		2.1		0.054	3.2

a: Data from Reference 1 and private communication with Bedient.
b: Data from South Farmingdale-Massapequa, N.Y. are used for evaluation (10).
c: The risk calculated by $R = 1 - \exp(-7.8(6900/1000)(2)(1/70)) = 0.785$ where a daily water intake rate of 2 L/day, and the weight of a human body of 70 kg are assumed.
d: Exposure/ADI = (16 mg/L · 2 L/day)/6.3 mg/day = 5.1
e: The source of data is Reference (16).
f: The source of data is Reference (17).

posure to carcinogenic contaminants. There is a column in the table, showing the estimated carcinogenic risk for drinking 2 L/day of water contaminated at the corresponding concentrations. According to the definition of UCR, the risk level shown represents the upper bound estimate. An upper bound estimate of risk of 0.028, for example, means that upon lifetime exposure to 2 liters of water per day, a person experiences an increased maximum risk of developing cancer in a probability of 28 in 1000. This level of risk used in this example represents very unacceptable risk, considering that current EPA's strategy is more in line with keeping the risk level at in between $10^{-4} - 10^{-7}$ with a particular level to be based on site-specific characteristics including population distribution.

Use of Mathematical Models

Three sites with partially documented and undocumented contaminant plumes were selected for modeling. The movement of a contaminant plume was simulated with a two-dimensional finite element code. The three dimensional analytical models are also employed for comparison purposes. The comparison will be presented later. For the example simulation, the amount of leachate entering ground water was set at 1.0 mg/L of a contaminant, which forms one of the boundary conditions. Site characterization data were collected for the three sites. One of the criteria for selection was the presence of tight geologic formations affecting leachate and ground water flow. This is because geologic formations of the sites with monitoring data showing contamination are relatively all loose with high values of hydraulic conductivity.

Site 6 is a landfill located in northeast glaciated terrain. The cross-section of the site shows fill, silt, clay, loam, and dolomite materials in layers. The simulation for this site was performed for both high- and low-permeability scenarios. Site 7 is a landfill covering approximately 300 acres, which has been in operation since 1977. The facility is underlain by chalk. Two types of clay were identified at the site. Site 8 is located in the Basin and Range physiographic province, and is characterized by a thick, unsaturated layer and infrequent precipitation. Although the site appears to be in a zero recharge zone, the ground water generally flows at the rate of 2 to 4 ft/day within the aquifer.

The principal model input parameters in this simulation were hydraulic conductivity (or seepage velocity), size of the facility, and duration of the facility's operation. Additional information was obtained from the water table contour maps and from characterization data relating to the geologic setting of the sites.

Table 2 is a summary of some of the results obtained from the numerical modeling of the three sites. The hydraulic conductivity rate used for site 6 was obtained from existing data, and ranges from 10^{-5} to 8.5 ft/day. The hydraulic conductivity for site 7 ranges from 1.7×10^{-4} to 1.7×10^{-5} ft/day; and that for site 8 is 8.7 ft/day. The longitudinal dispersivity values used for Sites 6, 7, and 8 are 300 cm, 450 cm, and 75 cm, respectively. The results shown in Table 2 are based on the lateral dispersivity, which is 1/10 of the longitudinal dispersivity. The retardation factor used is 2 for all sites. Grid spacing was used to divide the study area into 288, 462, and 1000 elements, respectively.

Sites 7 and 8 were selected from the facilities for which site characterization information was sufficient for numerical modeling, and which also had low hydraulic conductivity. For this reason, the time-of-travel, defined as the time required for water to travel the 100-ft distance from the edge of the waste discharge area along a ground water flowline, is very large for the sites represented in Table 2. The results indicate that for site 6, the plume at the 100-ft distance closely approximates the steady state concentrations in about 100 years, but for sites 7 and 8, the concentrations are seen to be far from reaching steady-state values in 100 years.

The last column in Table 2 tabulates the risks associated with drinking ground water containing the contaminant at a 100-ft distance under steady state conditions. The table indicates that, when the conditions are such that steady-state is very slowly reached, the exposure assessment based on estimation or monitoring data in the early stage of plume development will lead to an inadequate assessment for the purposes of protecting public health in the future. In computing the upper bound estimates of risk from the data in Table 2, a UCR value of 0.052 $(mg/kg \cdot day)^{-1}$, which is a value for benzene, was used.

Additional computer runs were made for Site 7 using longitudinal dispersivity values of 150 cm and 1,500 cm, and the transverse dispersivities at 10% of the longitudinal dispersivity as some have suggested. The results showed that higher longitudinal dispersivities resulted in higher concentrations at each point during unsteady-state plume development. The simulation was run for up to 10,000 years. The trend indicates that the steady state concentrations increase at greater longitudinal dispersivities.

LIMITATIONS OF ASSESSMENT METHODS

The use of monitoring data would render the results of health risk assessment more factual than the use of mathematical modeling because actual data would be less subject to uncertainty normally considered present in the estimation. However, the drawbacks associated with the use of monitoring include: 1) Protection of future health risks can not be ascertained if the assessment is solely based on monitoring data, since the plume behavior is a dynamic process until it reaches a steady state condition; 2) The wide-ranging variability in ground water monitoring data may result in a large confidence interval, making it difficult to distinguish the increase in concentration from the background, and hence to determine the extent of contamination; and 3) Extensive monitoring is costly compared with the effective use of modeling technique in combination with monitoring effort.

The uncertainty problem associated with the use of monitoring data is not necessarily resolved by the use of modeling. This is not only because models have variations in describing the fate and transport process, but also because there are a number of chemical and physical parameters needed in the modeling process, that are poorly

TABLE 2. RESULTS OF NUMERICAL MODELING FOR PARTIALLY DOCUMENTED AND UNDOCUMENTED PLUMES

	Concentrations (mg/L) at 100 ft			Time (yrs)		Risks for steady concentrations
	at 20 yrs	at 100 yrs	steady-state	to reach steady-state	of travel	
Site 6	0.38	0.5	0.53	1,200	1-10	8×10^{-4}
Site 7		0.023	0.69	>10,000	1,200	1.0×10^{-3}
Site 8		1.5×10^{-10}	1	>14,000	7,000	1.5×10^{-3}

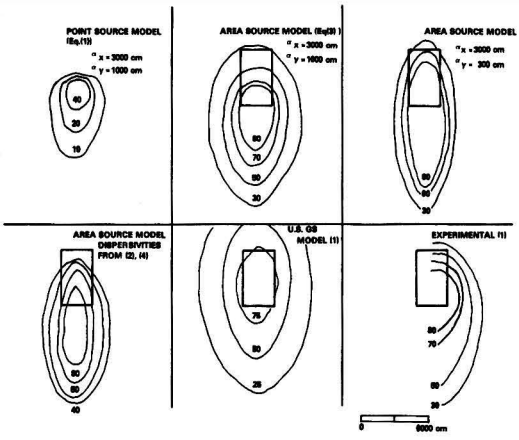

Figure 2. Comparison of plume concentrations (mg/l).

defined. To illustrate the point, analytical and numerical solutions are applied to draw plume isopleths for the identical transport problem. The numerical model used is the computer code developed by the U.S. Geological Survey (USGS), which is available for use to the public [9] Figure 2 compares their results obtained using different dispersivity correlations reported in the literature [*2, 5, 11, 14*] with plume data as found for a creosote disposal site in Conroe, Texas [*1*].

The principal parameter values used in the simulation were as follows: the average seepage velocity at 9.5×10^{-6} cm/s; the source width and length at 3,048 cm and 6,098 cm, respectively, lasting for 7,300 days (1952-1972) with the concentration evaluated at t = 10,950 days (1952-1982); aquifer depth at 300 cm; the contaminant concentration $C = 7.5 \times 10^{-5}$ g/cm^3 in leachate flowing at a rate of 28.9° cm^3/s; and dispersivities. Since the dispersivity values were the most elusive of all of the input parameters, several dispersivity correlations were tried. These included both fixed values and scale-dependent values which become asymtotic at great distances from the source [*1, 2, 8*]. The lateral dispersivity calculated at 1/10 and 1/3 of the longitudinal value was tried.

In this particular example, the use of $\alpha_x = 3000$ and $\alpha_T = 1{,}000$ most closely matches the experimental data. The lateral dispersivity at 1/10 of longitudinal dispersivity was used in the USGS model. The use of the same ratio (1/10) for lateral dispersivity in the area source analytical model [Equation (3)] results in plumes that are somewhat more elongated. The reason for this discrepancy cannot be explained at this time. The use of scale-dependent dispersivities in the area source model results in plume isopleths showing higher concentrations at the location immediately downstream from the source than in the groundwater directly below the source. The concentrations shown for the point source model are those at a depth of 100 cm below the water table. Applicability of the dispersivity ratio used for this example to other hydrogeologic settings is not known.

Correlations for dispersivity by Guven et al., Gelhar et al., Yeh, and Hamilton et al. were applied for comparative purposes [*2, 5, 11, 13*]. As can be noted, difficulty in defining dispersivities makes the sophisticated mathematical exercise often than not fruitless in obtaining reliable estimated results.

CONCLUSIONS

Techniques of performing assessments of health risk from intake of ground water impacted by waste disposal facilities are presented. The assessment consists of using monitored plume data, fate and transport modeling, or combination of both for exposure assessment, and of using health effect data for carcinogens and noncarcinogens for health risk assessment.

Despite uncertain parameters, particularly values for dispersivities, the fate and transport models are an important tool in supporting the health risk assessment which is based on monitoring data or conducted in the absence of such data. Though there are many analytical and numerical simulation techniques available at present, the reliability of such models cannot be adequately tested because of the inability to define the dispersion parameter for model validation.

LITERATURE CITED

1. Bedient, P. B., A. C. Rodgers, T. C. Bouvette, M. B. Tomson, and T. M. Wang, "Ground water quality at a creosote waste site," *Ground Water*, **22**, 318 (1984).
2. Guven, O., F. J. Molz, and J. G. Melville, "An analysis of dispersion in a stratified aquifer," *Water Resources Research*, **200**, 1337 (1984).
3. Codell, R. B., K. T. Kay, and G. Whelan, A collection of mathematical models for dispersion in surface water and ground water, NUREG-0868, Washington, D.C., Nuclear Regulatory Commission (1982).
4. Domenico, P. A. and V. V. Palciauskas, "Alternate Boundaries in Solid Waste Management," *Ground Water*, **13**, No. 3, 303 (1982).
5. Gelhar, L. W. and C. L. Axness, "Three-dimensional stochastic analysis of macrodispersion in aquifers," *Water Resources Research*, **19**, 161 (1983).
6. Geotrans, Inc., SATURN: A Finite Element Model for Simulating Saturated-Unsaturated Flow and Radionuclide Transport, August 1983.
7. Geraghty & Miller, Inc., Analysis of Surface Impoundment Discharge of Contaminants to Ground Water and Surface Water Bodies, Annapolis, Maryland, March 1984.
8. Javandel, I., C. Doughty, and C. E. Tsang, "Groundwater Transport: Handbook of Mathematical Models," American Geophysical Union, Washington, D.C.
9. Konikow, L. F. and J. D. Brendehoeft, "Computer Model of Two-Dimensional Solute Transport and Dispersion in Ground Water," U.S.G.S., 1978.
10. Ku, H. F. H., B. G. Katz, D. J. Sulam, and R. K. Krulikas, "Scavenging of chromium and cadmium by aquifer material, South Farmingdale-Massapequa area, Long Island, New York, *Ground Water*, **16**, 112 (1978).
11. Hamilton, D. A., D. C. Wiggert, and S. J. Wright, "Field comparison of three mass transport models," *J. Hydraulic Eng.*, **3**, 1 (1985).
12. Turner, Heat and concentration waves, New York, Prentice-Hall, 1972.
13. Yeh, G. T. AT123D: Analytical transient one-, two-, and three-dimensional simulation of waste transport in the aquifer system, ORNL-5602, Oak Ridge, TN, Oak Ridge National Laboratory, 1981.
14. Perlmutter, N. M. and M. Lieger, "Disposal of plating wastes and sewage contaminants in ground water and surface water, South Farmingdale-Massapequa area, Nassau County, New York, U.S. Geological Survey, Reston, VA 1970.
15. Wilson, J. L. and P. J. Miller, "Two-Dimensional Plume in Uniform Ground-Water Flow," *J. of the Hydraulics Div.*, HY4:503, 1878.
16. U.S. EPA, (August 1985) Health Assessment Document for Polychlorinated Dibenzo-Dioxins, EPA-600/8-84-014F, Environmental Criteria and Assessment Office, Cincinnati, Ohio.
17. U.S. EPA, (May 1984) Summary of Current Oral Acceptable Daily Intakes (ADIs) for Systemic Toxicants, Environmental Criteria and Assessment Office, Cincinnati, Ohio. (The document cautions not be cited or quoted. Hence, not all of the ADI values may reflect current EPA policy.)

Seong T. Hwang received his B.S., M.S., and Ph.D. in chemical engineering from the University of Michigan, and is currently with U.S. EPA, Washington, D.C.

Three Mile Island Cleanup

Experiences, Waste Disposal, And Environmental Impact

Lester J. King and James H. Opelka, Editors

"The papers included in this book deal with the experiences and problems in cleaning up Three Mile Island Unit-2 (TMI-2) following the accident . . . and the waste disposal and environmental impacts of the cleanup.

The material damages and losses resulting from the accident are very high. Cleanup will take many years and . . . costs will certainly be somewhere near $1 billion" (from the foreword).

Contents:

Material presented was selected from papers presented at AIChE's National Meeting in Detroit, Michigan, August 16-19, 1981.

Pub. #S-213

AIChE Members $19.50; Others $37.00

Send orders to:

Publications Sales, Dept. E
American Institute of Chemical Engineers
345 East 47 Street
New York, NY 10017

Pub. #S-213. THREE MILE ISLAND CLEANUP.

No. of copies_____ $_____

Membership No._____

Amount enclosed $_____

Name _____

Address _____

City _____ State_____ ZIP_____

Please be sure to include check or money order in U.S. dollars. U.S. postage is prepaid. Please add $2.00 per book to cover postage on foreign orders. Members must include Membership No. in order to qualify for member price, and may order only one copy of each title at the member price. *Prices are subject to change.*

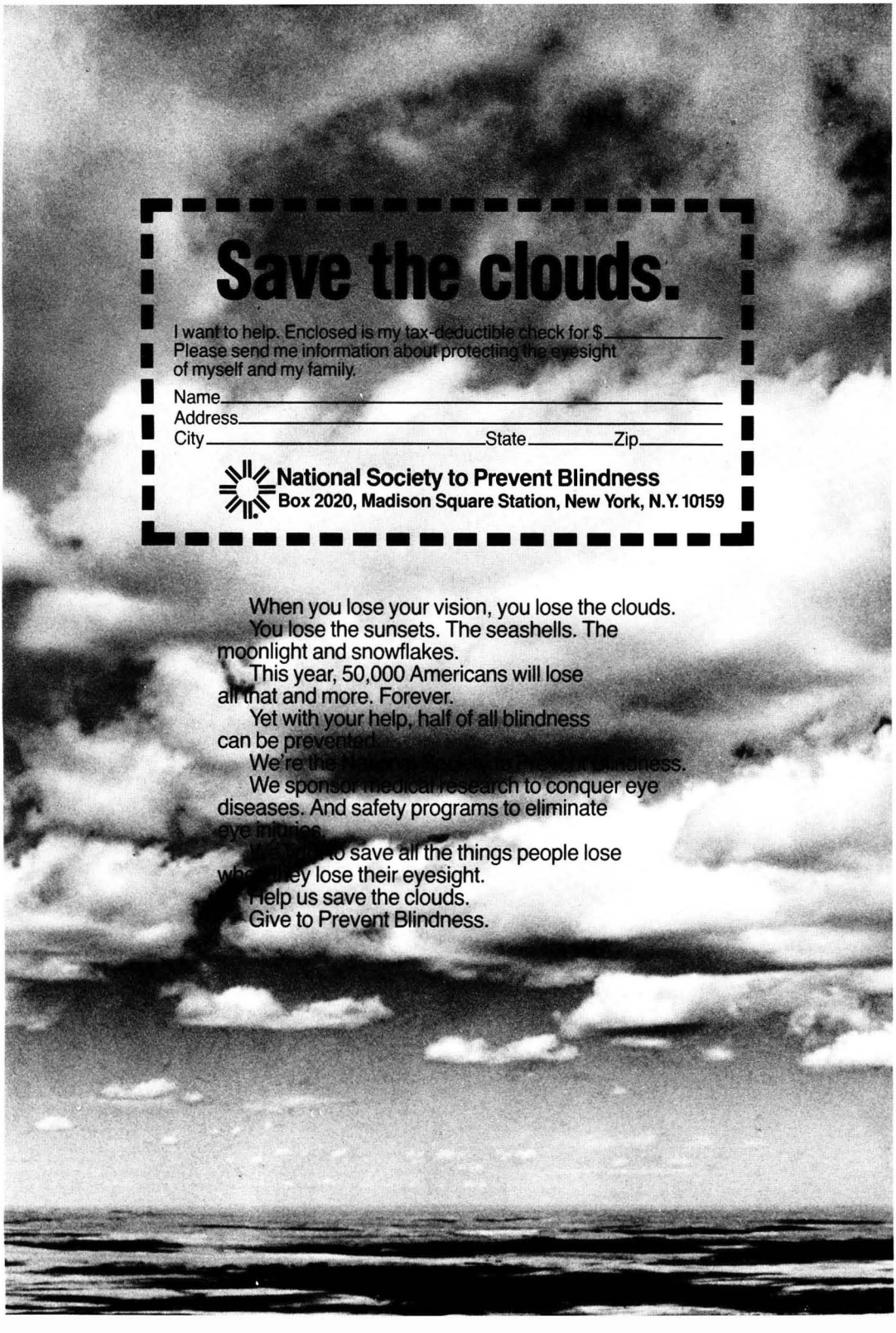
Save the clouds.
I want to help. Enclosed is my tax-deductible check for $_____
Please send me information about protecting the eyesight
of myself and my family.
Name_____
Address_____
City_____State_____Zip_____
National Society to Prevent Blindness
Box 2020, Madison Square Station, New York, N.Y. 10159
When you lose your vision, you lose the clouds.
You lose the sunsets. The seashells. The
moonlight and snowflakes.
This year, 50,000 Americans will lose
all that and more. Forever.
Yet with your help, half of all blindness
can be prevented.
We're the
We sponsor medical research to conquer eye
diseases. And safety programs to eliminate
eye injuries.
save all the things people lose
ey lose their eyesight.
Help us save the clouds.
Give to Prevent Blindness.